University of Alberta

The Role of Intracellular Bile Acid Binding Proteins in Bile Acid Transport and Cytoprotection

by

Enrique C. Torchia ©

A thesis submitted to the Faculty of Graduate Studies and Research in partial fulfillment of the requirements for the degree of Doctor of Philosophy

Department of Biochemistry

Edmonton, Alberta

Spring 2001

National Library
of Canada

Acquisitions and
Bibliographic Services

395 Wellington Street
Ottawa ON K1A 0N4
Canada

Bibliothèque nationale
du Canada

Acquisitions et
services bibliographiques

395, rue Wellington
Ottawa ON K1A 0N4
Canada

Your file Votre référence

Our file Notre référence

The author has granted a non-exclusive licence allowing the National Library of Canada to reproduce, loan, distribute or sell copies of this thesis in microform, paper or electronic formats.

L'auteur a accordé une licence non exclusive permettant à la Bibliothèque nationale du Canada de reproduire, prêter, distribuer ou vendre des copies de cette thèse sous la forme de microfiche/film, de reproduction sur papier ou sur format électronique.

The author retains ownership of the copyright in this thesis. Neither the thesis nor substantial extracts from it may be printed or otherwise reproduced without the author's permission.

L'auteur conserve la propriété du droit d'auteur qui protège cette thèse. Ni la thèse ni des extraits substantiels de celle-ci ne doivent être imprimés ou autrement reproduits sans son autorisation.

0-612-60354-7

Canada

University of Alberta

Library Release Form

Name of Author: Enrique C. Torchia

Title of Thesis: The Role of Intracellular Bile Acid Binding Proteins in Bile Acid Transport and Cytoprotection

Degree: Doctor of Philosophy

Year this Degree Granted: 2001

Permission is hereby granted to the University of Alberta Library to reproduce single copies of this thesis and to lend or sell such copies for private, scholarly or scientific research purposes only.

The author reserves all other publication and other rights in association with the copyright in the thesis, and except as herein before provided, neither the thesis nor any substantial portion thereof may be printed or otherwise reproduced in any material form whatever without the author's prior written permission.

402N, 9909-104 Street
Edmonton, Alberta
Canada, T5K 2G5

Date: Dec 19, 2000

University of Alberta

Faculty of Graduate Studies and Research

The undersigned certify that they have read, and recommend to the Faculty of Graduate Studies and Research for acceptance, a thesis entitled The Role of Intracellular Bile Acid Binding Proteins in Bile Acid Transport and Cytoprotection submitted by Enrique C. Torchia in partial fulfillment of the requirements for the degree of Doctor of Philosophy.

Luis B. Agellon, Supervisor

Allan W. Wolkoff, External Examiner

Carol Cass

Carol Cass

Warren Gallin

Warren Gallin

R. Lehner

Richard Lehner

Date: November 17, 2000

Abstract

Bile acids are cholesterol derivatives synthesized exclusively by the liver. These natural detergents are necessary for the absorption and digestion of lipophilic nutrients in the gut. Their levels in the enterohepatic circulation (EHC) are tightly conserved by efficient hepatic and ileal recovery systems that are mediated by the sodium/taurocholate cotransporting polypeptide (ntcp) and the apical sodium bile acid transporter (asbt), respectively.

Intracellular proteins such as the human bile acid binding protein (HBAB) and ileal lipid binding protein (ilbp) may protect against toxic bile acids and are implicated in cytosolic trafficking of bile acids. However, the precise function of this class of proteins remains unknown. The overall goal of this thesis was to define the role of HBAB and ilbp in cellular bile acid transport and protection against toxic bile acids. McArdle RH-7777 cells were engineered to take up bile acids from the culture medium by stable expression of ntcp. These cells, termed McNtcp, showed differential sensitivity to different species of bile acids. In particular, taurine-conjugated bile acids were well tolerated, while glycine-conjugated bile acids were extremely cytotoxic. Expression of HBAB in McNtcp cells was unable to protect against glycine-conjugated bile acids or modulate ability of these cells to take up or secrete bile acids.

To define the role of ilbp in the conservation of bile acids in the EHC, I undertook the targeted gene disruption of the murine *ilbp* gene. Murine embryonic stem cells with a mutation in the *ilbp* locus were isolated and used to construct a mouse

strain with a disrupted *ilbp* gene. Ilbp null mice did not express ilbp, but were clearly viable and indistinguishable from wild type mice. More importantly, they had a normal spectrum and size of bile acids in EHC in comparison to wild type mice. These findings indicated that ilbp expression is not crucial for the conservation of bile acids, and suggested that ilbp is not a critical component of the ileal recovery system. In conclusion, the class of proteins represented by HBAB and ilbp may play a subtle role in cellular bile acid transport and protection against bile acid toxicity.

Contents

Chapter 1: Introduction 1

1.0 Introduction 2

1.1 Bile acid biosynthesis 2

1.2 Enterohepatic circulation of bile acids 6

1.2.1 Bile secretion and physiological function in the intestine 6

1.2.2 Intestinal conservation of bile acids 7

1.2.3 Hepatic transport of bile acids 9

1.2.3.1 Hepatic uptake of bile acids 9

1.2.4 Enterohepatic circulation 11

1.3. Intracellular bile acid transport 12

1.3.1. Intracellular transport in hepatocytes 14

1.3.1.1 Role of Glutathione S-transferases and Liver fatty acid binding protein in bile acid intracellular transport 14

1.3.1.2 Role of 3α-hydroxysteroid dehydrogenase in bile acid transport 16

1.3.1.3 Role of the human bile acid binder in bile acid transport 17

1.3.2. Intracellular bile acid transport in ileocytes 17

1.4 Bile acids as regulators of cellular function 22

1.5 Thesis question 25

1.5.1 Objectives of the thesis 26

Objective i: Create a model system to test the role of HBAB 26

Objective ii: Characterization of McNtcp.24 cells 26

Objective iii: Determine if expression of HBAB in bile acid transport competent cells has an impact on cellular bile acid transport and cytotoxicity 27
Objective iv: Disruption of the murine ilbp gene 27
1.6 REFERENCES 29
Chapter 2: General Methods 47
2.1 Chemicals 48
2.2 Cell culture 48
2.3 Molecular biology 49
2.4 RNA blot analysis 49
2.5 DNA blot analysis 50
2.6 Bile acid uptake assays 51
2.7 Immunoblot analysis 52
2.8 Lactate dehydrogenase (LDH) assays 52
2.9 Transfection experiments 53
2.10 Plotting and Statistics 53
2.11 REFERENCES 54
Chapter 3: Reconstitution of Bile Acid Transport in the Rat Hepatoma McArdle RH-7777 Cell Line 56
3.1 Introduction 57
3.2 Methods 58
3.2.1 Stable expression of Ntcp in McArdle RH-7777 cells 58
3.2.2 Primary culture of hepatocytes 58
3.2.3 Bile acid uptake assays 59
3.3 RESULTS 60
3.3.1 Expression of Ntcp in McArdle RH-7777 cells 60
3.3.2 Characterization of McNtcp clones 63

- 3.4 DISCUSSION 73
- 3.5 REFERENCES 76

Chapter 4: Bile acid-induced morphological changes in McNtcp.24 cells . 81

- 4.1 INTRODUCTION 82
- 4.2 METHODS 83
  - 4.2.1 Culture conditions 83
  - 4.2.2 Light microscopy 83
  - 4.2.3 Electron microscopy 84
  - 4.2.4 Labeling of the intracellular bile acid pool. 85
  - 4.2.5 Measurement of fatty acid oxidation rate 85
  - 4.2.6 Measurement of glycolytic rate 85
  - 4.2.7 Lipid analysis 86
- 4.3 RESULTS 87
  - 4.3.1 Effect of bile acid treatment on McNtcp.24 cell ultrastructure. . 87
  - 4.3.2 Electron microscopic analysis 89
  - 4.3.3 Analysis of fatty acid oxidation and glycolytic rates 92
  - 4.3.4 Cytological staining of lipid in McNtcp.24 cells 94
  - 4.3.5 Metabolic labeling of the intracellular bile acid pool. 97
  - 4.3.6 Localization of microvilli-lined vesicles 97
- 4.4 DISCUSSION 103
- 4.6 REFERENCES 106

Chapter 5: Cytotoxicity of bile acids in cells of hepatic and non-hepatic origin 111

- 5.1 INTRODUCTION 112
- 5.2 METHODS 114
  - 5.2.1 Cell lines 114
  - 5.2.2 Immunoblot analysis 114

5.2.3 Visualization of Genomic DNA fragmentation 115

5.2.4 Caspase activity assays 115

5.2.5 Phosphatidylinositol 3-kinase assays 116

5.3 RESULTS 117

5.3.1 Bile acid uptake in CHO.asbt cells 117

5.3.2 Cytotoxic potential of bile acid in CHO.asbt.35 cells 117

5.3.3 Mechanism of bile acid-mediated cell death 123

5.3.4 Differential sensitivity 130

5.3.5 Cytotoxic Potential of bile acids in HBAB-expressing McNtcp.24 cells 133

5.4 DISCUSSION 138

5.5 REFERENCES 143

Chapter 6: Disruption of the murine ilbp gene 149

6.1 INTRODUCTION 150

6.2 METHODS 151

6.2.1 Construction of targeting vector for the ilbp gene 151

6.2.2 Disruption of the ilbp gene in R1 ES cells 152

6.2.3 Production of germ line-competent chimeras and genotyping of germline progeny. 153

6.2.4 Bile acid analysis 154

6.3 RESULTS 156

6.3.1 Targeted gene disruption of the ilbp locus in ES cells 156

6.3.2 Creation of ilbp-deficient mice 160

6.3.3 Characterization of disrupted ilbp mice. 164

6.4 DISCUSSION 172

Chapter 7: Summary and Conclusion 180

Appendix I: Composition of commonly used buffers 187

Appendix II : Additional data for Chapter 6 189

Figures

Chapter 1:

Fig. 1-1 Schema of the bile acid biosynthetic pathways in the liver 3

Fig. 1-2 Chemical structures of the major bile acid species in humans 4

Fig. 1-3 Schema of the enterohepatic circulation of bile acids 13

Fig. 1-4 Depiction of proteins implicated in cellular bile acid transport 15

Fig. 1-5 Distribution of cytosolic lipid binding proteins and asbt in the small intestine 19

Fig. 1-6 Regulation of mouse ilbp and asbt mRNA abundance 21

Chapter 3:

Fig. 3-1 Uptake of TCA from the culture medium by McNtcp clones, hepatoma cells and primary hepatocytes 61

Fig. 3-2. Detection of the native and recombinant Ntcp mRNA in hepatocytes, McArdle RH-7777 cells and McNtcp cells 62

Fig. 3-3 Concentration dependent uptake of TCA 64

Fig. 3-4. Detection of Ntcp in membrane extracts from McNtcp cells 65

Fig. 3-5. Detection of the Ntcp transgene in genomic DNA from McNtcp and McArdle RH-7777 cells 66

Fig. 3-6. Accumulation of TCA in McNtcp cells and primary hepatocytes .. 67

Fig. 3-7. Efflux of TCA from hepatocytes and McNtcp cells 69

Fig. 3-8. Detection of BSEP/spgp in McNtcp cells 70

Fig. 3-9. Inhibition of TCA uptake in McNtcp cells by different bile acids ... 72

Chapter 4:

Fig. 4-1. Phase contrast photomicrographs of untreated and TCA-treated McNtcp.24 cells 88

Fig. 4-2. Inhibition of TCA uptake by various bile acids 90

Fig. 4-3. Electron micrograph of McNtcp.24 cells 91

FIG. 4-4 ^3H_2O production from exogenous [^{3}H]-palmitate or [^{3}H]-glucose by McNtcp.24 cells 93

Fig. 4-5 Photomicrographs of TCA-treated McNtcp.24 cells stained with Oil-red-O and filipin 96

Fig. 4-6. Cell associated [^{3}H]-TCA in McNtcp.24 and McArdle cells 98

Fig. 4-7 Localization of microvilli-lined vesicles in McNtcp.24 cells 100

Fig. 4-8 Cellular localization of CgamF in untreated McNtcp.24 cells....... 101

Fig. 4-9. Cellular localization of CgamF in TCA-treated McNtcp.24 cells . 102

Chapter 5:

Fig 5-1 Functional expression of asbt in CHO.asbt cells 118

Fig 5-2 Detection of LDH activity in the medium of bile acid-treated cells 120

Fig 5-3 LDH activity in medium of bile acid-treated CHO.asbt.35 cells 121

Fig 5-4 Genomic DNA fragmentation in bile acid-treated CHO.asbt.35 and McNtcp.24 cells 122

Fig 5-5 Activation of caspase 8 in bile acid-treated cells 124

Fig 5-6 Caspase 8 activity in CHO.asbt.35 cells treated with unconjugated bile acids 126

Fig 5-7 Time dependent activation of caspase 8 in bile acid-treated CHO.asbt.35 and McNtcp.24 cells 127

Fig 5-8 Caspase 8 activity in McArdle RH-7777 cells expressing asbt and treated with bile acids 128

Fig 5-9 Caspase 3 activity in bile acid-treated cells 129

Fig 5-10 Caspase 8 activity in bile acid-treated McNtcp.24 cells after pretreatment with LY-294002 131

Fig 5-11 PI3K activity in bile acid-treated cells 132

Fig 5-12 Stable expression of HBAB in McNtcp.24 cells 134

Fig 5-13 TCA uptake and efflux in BN and McNtcp.24 cells 135

Fig 5-14 Cytotoxic potential of GCDCA in BN and McNtcp.24 cells 137

Chapter 6:

Fig 6-1 Strategy for disrupting the murine ilbp locus 157

Fig 6-2 Screening of ES cell DNA for presence of a disrupted ilbp allele . 159

Fig 6-3 Protocol and approximate time line for generating ES cells with a single disrupted ilbp allele 161

Fig 6-4 Karyotype of positive ES cell lines 162

Fig 6-5 A germline chimera and one of its progeny 163

Fig 6-6 Representative genotyping of ilbp null mice 166

Fig 6-7 Detection of ilbp gene expression in ileal sections of ilbp$^{+/+}$, ilbp$^{+/-}$, and ilbp$^{-/-}$ mice 167

Fig. 6-8 Speciation of bile acids isolated from ilbp$^{+/+}$ and ilbp$^{-/-}$ mice 171

Chapter 7:

Fig. 7-1 Schema depicting the molecular events that occur once bile acids are internalized by cells 185

Appendix II:

Fig. 1 Detection of ilbp expression in protein extracts from transfected cells and mouse intestinal sections 190

Tables

Chapter 4

Table 4-1. Lipid composition of McNtcp.24 cells 95

Chapter 6:

Table 6-1 Summary of blastocyst injection and chimera production. 165

Table 6-2 Body weights of 77 day old ilbp$^{+/+}$, ilbp$^{+/-}$, and ilbp$^{-/-}$ mice. 169

Table 6-3 Determination of the size of the bile acid pool in ilbp$^{+/+}$, ilbp$^{+/-}$, and ilbp$^{-/-}$ mice. 170

Abbreviations

3HSD	3α-hydroxysteroid dehydrogenase
ATP	Adenosine 5'-triphosphate
BA	Bile acids
BAC	Bacterial artificial chromosome
BSA	Bovine serum albumin
BSEP	Bile acid export pump
CA	Cholic acid
CBATP	Canalicular bile acid transporter/Ecto-ATPase
CDCA	Chenodeoxycholic acid
cDNA	complementary DNA
CgamF	Cholylglycylamidofluorescein
CHAPS	3-[(3-Cholamidopropyl) dimethylammonio]-1-propanesulfonate
CHO	Chinese hamster ovary
CS	Calf serum
CYP27b	Cholesterol 27α-hydroxylase
CYP7a	Cholesterol 7α-hydroxylase
CYP7b	Oxysterol 7α-hydroxylase
DAPI	4',6-diamidino-2-phenylindole, dihydrochloride
DCA	Deoxycholic acid
dCTP	Deoxycytidine 5'-triphosphate
DMEM	Dulbecco's modified Eagle's medium
DMSO	Dimethyl sulfoxide
DNA	Deoxynucleic acid
EDTA	Ethylenediaminetetraacetic acid
EHC	Enterohepatic circulation

E.R.	Endoplasmic reticulum
ES	Embryonic stem
FA	Fatty acids
FABP-i	intestinal fatty acid binding protein
FBS	Fetal bovine serum
FDA	Fluorescein diacetate
FIAU	[1-(2'-deoxy-2'-flouro-b-D-arabinofuranosyl)-5-iodouracil]
FITC	Fluorescein Iso-thiocyanate
FXR	Farnesoid x receptor
G3PDH	Glyceraldehyde-3-phosphate dehydrogenase
GCA	Glycocholic acid
GCDCA	Glychenodeoxycholic acid
GDCA	Glycodeoxycholic acid
GST	Glutathione S-transferases
HBAB	Human bile acid binder
HPTLC	High performance TLC
HS	Horse serum
I-BABP	Intestinal bile acid binding protein
ilbp	ileal lipid binding protein
Kb	Kilobase
kDa	Kilodalton
K_m	Michaelis-Menten constant
LBP	lipid binding protein
LDH	Lactate dehydrogenase
L-FABP	Liver fatty acid binding protein
LN	Natural log
LST	Liver specific transporter

mEH	microsomal Epoxide hydroxylase
MOPS	3-(N-Morpholino)propanesulfonic acid
mRNA	messenger Ribonucleic acid
NA	No addition
Neo^r	Neomycin resistance
NTCP	Sodium/bile acid transporting polypeptide
OATP	Organic anion transporting polypeptide
PAGE	Polyacrylamide gel electrophoresis
pASBT	Asbt-expression plasmid
PBS	Phosphate-buffered saline
PI3K	Phosphatidylinositol 3-kinase
PIPES	Piperazine-N,N'-bis(2-ethanesulfonic acid)
RT	Room temperature
SDS	Sodium dodecyl sulfate
SPGP	Sister of p-glycoprotein
t-ASBT	truncated Apical sodium/bile acid transporter
TBS	Tris-buffered saline
TCA	Taurocholic acid
TCDCA	Taurochenodeoxycholic acid
TDCA	Taurodeoxycholic acid
TLC	Thin layer chromatography
TUDCA	Tauroursodeoxycholic acid
UDCA	Ursodeoxycholic acid
U.V.	Ultraviolet
v	Volume
V_{max}	Maximum velocity
wt	weight

Acknowledgements

I would like thank my supervisor, Dr. L. B. Agellon, and the other members of my supervisory committee, Drs. Warren Gallin and Carol Cass, for their guidance and patience throughout my studies.

I would like to thank Dr. Sukhinder Kaur for the many scientific discussions that inspired me think critically. I am also very grateful for her unwavering friendship and support during difficult times.

I would like to acknowledge Debbie Merriam for her encouragement and friendship over the years.

I would like to thank the past and present members of the Agellon Lab, Dr. Jean Shapiro, Dr. Liqing Yu, Darren Cikaluk, Vic Drover, Eric Huang, and Eric LaBonte, who remain more than just colleagues.

Special thanks to Jody Aldrich for her excellent and professional help with the ilbp knockout mice, Dr. Lopaschuck and Rick Barr for their help on measuring cellular glucose and fatty acid utilization rates, Dr. G. Scraba and Roger Bradley for their assistance with electron microscopy, and Dr. Derrick Rancourt and Eileen Rattner for their assistance with embryonic stem cell cultures and ilbp knockout mice.

Finally, I would like to thank the Alberta Heritage Foundation for Medical Research for granting me a studentship award.

Chapter 1: Introduction

1.0 Introduction

Bile acids are cholesterol derivatives that are fundamental to the acquisition of lipophilic nutrients from the environment. The liver and small intestine play pivotal roles in the metabolism of bile acids. In turn, bile acids may play an important role in the regulation of cellular function in these organ systems. Below is an overview of bile acid biosynthesis, the enterohepatic circulation of bile acids, cellular bile acid transport, the putative regulatory role of bile acids in cellular function, and the objectives of this thesis.

1.1 Bile acid biosynthesis

Bile acid biosynthesis occurs exclusively in the liver by two well-characterized pathways (Fig 1-1). In the classical or neutral pathway, cholesterol is hydroxylated in the 7th position of the steroid ring by the microsomal cholesterol 7α-hydroxylase (cyp7a) (Russell *et al.* 1992). Subsequent enzymatic steps result in the epimerization of the 3β-hydroxyl group and the possible addition of a 12α-hydroxyl group (Russell *et al.* 1992). Following cleavage of the cholesterol side chain, hepatic bile acid CoA:amino acid N-acyltransferase conjugates bile acids with either taurine or glycine (Falany *et al.* 1994). The major or primary bile acids produced in humans are amino acid conjugates of cholic acid (CA) and chenodeoxycholic acid (CDCA) (Fig 1-2) (Russell *et al.* 1992). Secondary bile acids such as deoxycholic (DCA) and lithocholic acid (LCA) are derived from the removal of hydroxyl groups at position 7 or 12 of the bile acid moiety by intestinal bacteria. The liver also conjugates these bile acids after they are reclaimed from the intestine and returned to the liver.

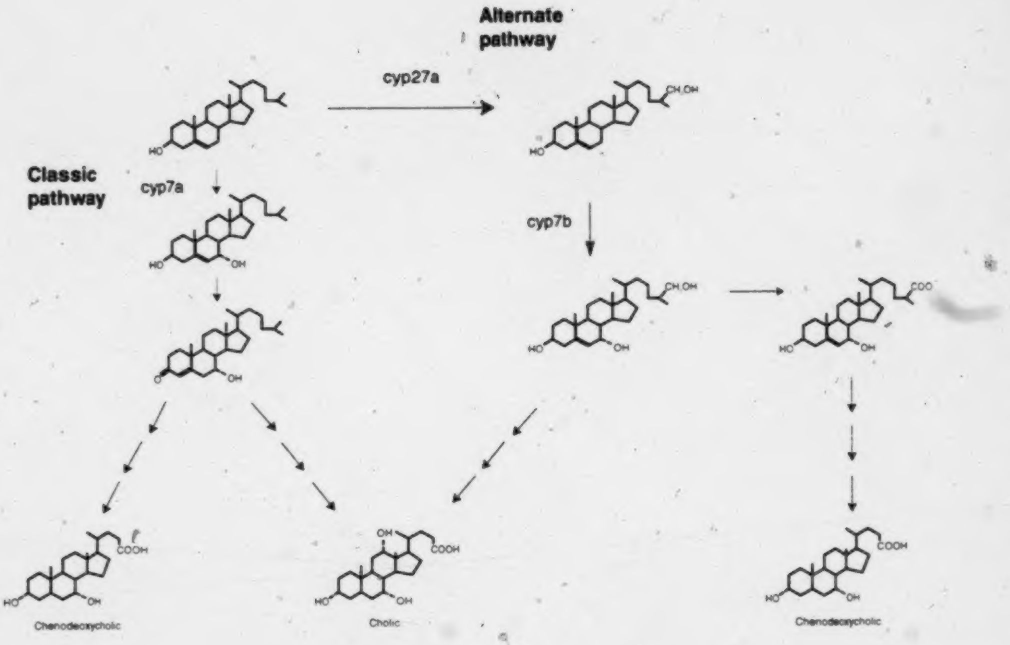

Fig. 1-1 Schema of the bile acid biosynthetic pathways in the liver. The classical or neutral pathway begins with the 7α-hydroxylation of cholesterol. This reaction is catalyzed by the rate-limiting enzyme of this pathway, cholesterol 7α-hydroxylase (cyp7α). Through several subsequent enzymatic steps, 7α–hydroxy cholesterol is converted into the primary bile acids, chenodeoxycholic and cholic acids. The alternate or acidic pathway begins with 27α-hydroxylation of cholesterol by 27α-hydroxylase (cyp27a). Oxysterol 7α-hydroxylase (cyp7b) converts subsequent intermediaries of cyp27a to a dihydroxycholesterol, which can then enter the later steps of the neutral pathway.

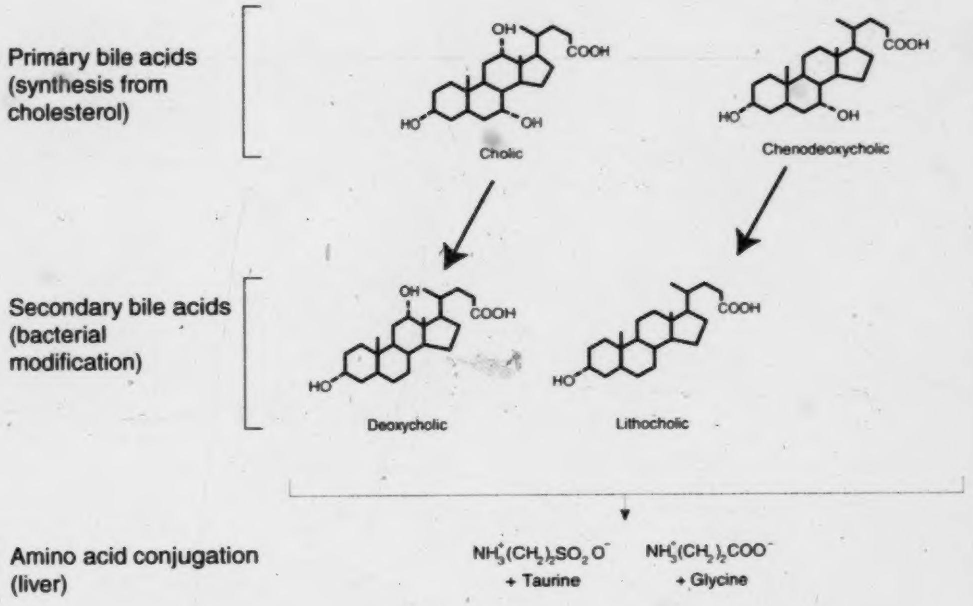

Fig. 1-2 Chemical structures of the major bile acid species in humans. The primary bile acids cholic and chenodeoxycholic acid are synthesized from cholesterol by the liver. Bacterial modification of primary bile acids in the intestine gives rise to secondary bile acids such as lithocholic and deoxycholic acid. Secondary bile acids undergo further modification in the liver to form tertiary bile acids. Sulfolithocholic acid and ursodeoxycholic acid are examples of tertiary bile acids. Free bile acids are conjugated by the liver with the amino acids taurine or glycine. Figure adapted from Carey *et. al.*, 1994.

Cyp7a is the rate limiting enzyme of the neutral pathway and has a central role in the regulation of overall hepatic bile acid production (Agellon *et al.* 2000). The targeted disruption of the murine *Cyp7a* gene illustrates the importance of this pathway in bile acid production. *Cyp7a* null mice have a dramatic postnatal deficiency in bile acid production that disrupts bile acid function in the gut (Schwarz *et al.* 1996). Consequently, cyp7a null mice show a drastic decrease in post-natal survival that can be improved by inclusion of vitamins in the drinking water of the mothers, and CA in the chow of the offspring (Ishibashi *et al.* 1996).

The alternate or acidic pathway begins with the hydroxylation of cholesterol on the side chain that is catalyzed by cholesterol 27α-hydroxylase (cyp27a) (Fig 1-1). Oxysterol 7α-hydroxylase (cyp7b) further modifies the product of cyp27a to form 7α, 27-dihydroxycholesterol (Schwarz *et al.* 1997). This intermediate subsequently enters the later steps of the neutral pathway allowing its conversion into bile acids. Both cyp27a and cyp7b are expressed in non-hepatic tissues (Schwarz *et al.* 1997; Rosen *et al.* 1998), and oxysterols made in peripheral tissue are converted into bile acids by the liver. In healthy humans, the contribution of the alternate pathway to overall hepatic bile acid biosynthesis is considered small (Duane *et. al* 1999 ; Vlahcevic *et al.* 1999; Li-Hawkins *et al.* 2000]. Although a reduction in hepatic bile acid formation is observed in mice with a disrupted *Cyp27a* gene, there is no apparent effect on survival or intestinal absorption of lipovitamins in these mice (Rosen *et al.* 1998). Therefore, it is likely that the alternate pathway plays an important role in the catabolism of cholesterol in peripheral tissues and conditions where cyp7a enzymatic activity is impaired (Schwarz *et al.* 1996).

1.2 Enterohepatic circulation of bile acids

1.2.1 Bile secretion and physiological function in the intestine

Hepatic bile acid secretion provides the main driving force for bile formation (Nathanson *et al.* 1991), and is mediated by an integral ATP-dependent transporter on the canalicular membranes of hepatocytes (see Section 1.2.3.2). Biliary bile acids promote the extraction of phospholipids, mainly phosphatidylcholine, from the luminal face of the canalicular membrane (Meier *et al.* 2000). Bile acids and phospholipids form mixed vesicles and micelles that solubilize cholesterol and other exogenous lipophilic compounds, and provide protection to biliary epithelia from bile acid-mediated damage (Kuipers *et al.* 1997; Meier *et al.* 2000). Secretion of glutathione drives bile acid-independent bile flow, but constitutes a small fraction of overall bile formation (Kuipers *et al.* 1997). Hepatic secretion of free cholesterol and bile acids, as the end-product of cholesterol catabolism, represents the major disposal route for cholesterol in the body (Dietschy 1997).

Bile acids are concentrated in the gall bladder interdigestively. When a meal is eaten, the gall bladder contracts and releases bile into the duodenum in response to signaling from the hormone cholecystokinin (Carey *et al.* 1994). In the lumen of the proximal intestine bile acids play a fundamental role in digestion and absorption of lipophilic nutrients by forming mixed micelles with cholesterol, phospholipids, and other dietary lipids. Solubilization of fats in mixed micelles makes them accessible to secreted pancreatic lipases and facilitates their absorption by intestinal cells (Hofmann 1999). As illustrated in Section 1.2, deficiencies in bile acid production can lead to impaired absorption of lipovitamins and other lipophilic nutrients. Bile acids may also affect gastrointestinal motility and mucin secretion (Hofmann 1999).

1.2.2 Intestinal conservation of bile acids

Intestinal conservation of bile acids in humans is very efficient. Greater than 95% of secreted primary bile acids are reclaimed from the intestine (Carey *et al.* 1994). Recovery of bile acids is passive along the axis of the intestine and active in the terminal ileum (Dawson 1999). The efficiency of bile acid absorption largely depends on the conjugation and hydroxylation state of the particular bile acid (Carey *et al.* 1994). For example, unconjugated and protonated bile acids are easily absorbed by passive diffusion (Carey *et al.* 1994). In contrast, conjugated primary and secondary bile acids do not readily cross biological membranes and depend protein mediated transport for their entry into cells (Hofmann 1999).

Using a photoactive bile acid probe, Kramer and coworkers identified an integral 93-kDa and a cytosolic 14-kDa protein whose expression correlates with the site of active taurocholic acid (TCA) uptake in the rabbit intestine (Kramer *et al.* 1993). They also identified an 87-kDa protein expressed throughout the axis of the rabbit small intestine that may be responsible for facilitative intestinal bile acid recovery (Kramer *et al.* 1993). Dawson and co-workers later cloned the putative ileal bile acid transporter using expression-cloning techniques (Wong *et al.* 1994). The apical sodium bile acid transporter (asbt) is a 348 amino acid integral transporter that forms oligomeric complexes (Kramer *et al.* 1995; Kramer *et al.* 1997) on the brush border membranes of ileocytes (Shneider *et al.* 1995). The ontogeny of asbt coincides with the onset of ileal active bile acid uptake in rats (Shneider *et al.* 1995) and mutations in the human asbt gene can result in primary bile acid malabsorption (Oelkers *et al.* 1997). These observations suggest that asbt mediates ileal sodium dependent bile acid transport. Asbt is also expressed on the apical membranes of renal proximal convoluted tubule cells (Christie *et al.* 1996) and on cholangiocytes that line the biliary epithelia (Alpini *et al.* 1997). Expression of asbt in the kidneys is consistent with the active reclamation of bile acids that escape hepatic recovery and spill over into arterial circulation. Cholangiocytes appear to be part of an intra-hepatic shunt that allows bile acids to bypass the intestine and return to the liver. The physiological significance of this intra-hepatic shunt remains to be elucidated. Asbt preferentially transports conjugated primary bile acids (Kramer *et al.* 1999), and this narrow substrate specificity is consistent with its role in bile acid recovery in the small intestine.

The jejunum may also play an important role in the recovery of di-hydroxy bile acids from the gut. In support of this idea, an anion-exchange transport system for bile acids has been identified in the jejunal brush border membranes prepared from rats (Amelsberg *et al.* 1999). However, there is a substantial body of evidence to suggest that ileal recovery of bile acids is critical for efficient reclamation of bile acid from the gut. For example, re-sectioning of ¼ or more of the human ileum results in both bile acid and fatty acid malabsorption with severe diarrhea and steatorrhea (Shearman *et al.* 1989). In addition, asbt inhibitors mimic the activity of cholestyramine, a bile acid sequestrant, in reducing bile acid recovery in the intestine (Lewis *et al.* 1995; Root *et al.* 1995). The targeted disruption of the murine *asbt* gene could help to determine the relative importance of the jejunum to overall bile acid recovery in the gut.

Photoaffinity labelling experiments using ileal basolateral membrane preparations identified a 54-kDa integral protein that is thought to mediate efflux of bile acids from rat enterocytes (Lin *et al.* 1988). This protein has remained uncharacterized, but is believed to be an anion exchanger (Weinberg *et al.* 1986; Lin *et al.* 1988). Recently, an alternate spliced form of asbt, designated t-asbt, was identified in the rat that conferred bile acid secretion activity in Xenopus oocytes made to express the protein (Lazaridis et al. 2000). T-asbt is 19-KDa polypeptide expressed in cholangiocytes, ileum, and kidney and is confined to the basolateral membrane of cholangiocytes (Lazaridis *et al.* 2000). The role of t-asbt in bile acid efflux from cholangiocytes, ileocytes, and renal tubular epithelia remains unknown.

1.2.3 Hepatic transport of bile acids

1.2.3.1 Hepatic uptake of bile acids

Absorbed bile acids return to the liver via portal circulation, mostly bound by lipoproteins and albumin (Carey *et al.* 1994). The liver efficiently extracts bile acids from circulation by carrier-mediated mechanisms and passive diffusion. The concentration of bile acids in portal circulation varies in different species, and can range between 50 to 170 μM in rats (Carey *et al.* 1994). Well-characterized Na^+-dependent and -independent bile acid transport systems exist on the basolateral (sinusoidal) surface of hepatocytes, and are responsible for uptake of the majority of bile acids from circulation (Bahar *et al.* 1999). The Na^+ taurocholate co-transporting polypeptide (ntcp), a 362 amino acid integral protein in rats, has been shown to account for the essential features of hepatic Na^+-dependent conjugated bile acid uptake in health and disease (Hagenbuch *et al.* 1991; Hagenbuch 1997; Love *et al.* 1998). The rat ntcp and hamster asbt share a 38% identity and constitute a new family of Na^+ dependent transporters (Dawson 1999). Although ntcp prefers conjugated bile acids as substrate (Schroeder *et al.* 1998), it can also transport a variety of organic anions (Kouzuki *et al.* 1998; Kramer *et al.* 1999). With its broad substrate specificity compared to asbt, ntcp contributes to hepatic clearance of xenobiotics and other organic compounds from circulation for disposal into bile (Meier *et al.* 1997). A second Na^+-dependent bile acid transporter, microsomal epoxide hydroxylase (mEH), is expressed on the sinusoidal membranes of hepatocytes (Von Dippe *et al.* 1993). However, mEH is also expressed in hepatocyte smooth endoplasmic reticulum (ER) membranes in two topological orientations as shown by a study using monoclonal antibodies directed to mEH (Alves *et al.* 1993). Smooth ER vesicles take up bile acids with transport characteristics that differ significantly in comparison to sinusoidal derived vesicles (Alves *et al.* 1993). The physiological significance of the different forms of mEH expressed intracellularly remains unknown. The contribution of mEH to overall hepatic recovery of conjugated bile acids is considered small (Hagenbuch *et al.* 1996b; Kouzuki *et al.* 1998). However, mEH may be quantitatively important for the reclamation of unconjugated bile acids from portal circulation (Von Dippe *et al.* 1996), or serve in a yet unknown role in the intracellular trafficking of bile acids.

Na^+-independent bile acid transport can account for most of the uptake of unconjugated bile acids by the liver (Hagenbuch *et al.* 1996a). The organic anion-transporting polypeptides (oatps) are one of two families of organic transporters that mediate the Na^+-independent bile acid transport on the sinusoidal membranes of hepatocytes. Oatps are multispecific organic anion integral-membrane proteins that transport both conjugated and free bile acids (Kullak-Ublick *et al.* 1995; Noé *et al.* 1997; Abe *et al.* 1998; Eckhardt *et al.* 1999). The expression of these proteins in rat is not restricted to the liver, underscoring the importance of oatps in the cellular transport of non-bile acid organic anions (Jacquemin *et al.* 1994; Angeletti *et al.* 1997); Noé *et al.* 1997; Abe *et al.* 1998). However, the recently cloned liver specific organic anion transporter (LST) in humans and rats may be more physiologically relevant to bile acid transport in hepatocytes than the oatps (Abe *et al.* 1999; Hsiang *et al.* 1999; Kakyo *et al.* 1999; Konig *et al.* 2000). Unfortunately, understanding the relative importance of oatps and LST to hepatic conservation of bile acids in both health and disease must await further studies.

1.2.3.2 Hepatic bile acid secretion

Hepatocytes do not accumulate bile acids and efficiently translocate them from the basolateral to the apical or canalicular membrane for secretion into bile (Carey *et al.* 1994). In non-pathological conditions, bile acid concentration in hepatocytes is considered to be very low (<1 μM) (Setchell *et al.* 1997; Hofmann, 1999). Canalicular secretion of bile acids is largely dependent on members of two subfamilies of the ATP binding cassette protein superfamily (Agellon *et al.* 2000). The bile acid export pump (BSEP) is an ~160-kDa integral protein belonging to the p-glycoprotein subfamily that was initially identified in pig liver as sister of p-glycoprotein (spgp) (Childs *et al.* 1995). BSEP/spgp accepts monovalent taurine- and glycine-conjugated bile acids with a substrate preference that is similar to ATP-dependent bile acid transport observed in canalicular membrane preparations (Gerloff *et al.* 1998). Mutations in the BSEP/spgp gene in humans appear to be associated with subtype II familial progressive familial intrahepatic cholestasis (Strautnieks *et al.* 1998). Given these observations, BSEP/spgp is considered the major bile acid export protein in hepatocytes (Gerloff *et al.* 1998). MRP2/cMoat belongs to the multidrug resistant protein (MRP) subfamily and transports sulfated and glucuronidated bile acids (Agellon *et al.* 2000). Other proteins expressed in hepatocytes such as the MRP3 and the ecto ATPase have been implicated in canalicular bile acid export (Sippel *et al.* 1993; Sippel *et al.* 1997; Ortiz *et al.* 1999). However, the role of these proteins in hepatic bile acid secretion remains controversial and unproven (Agellon *et al.* 2000).

1.2.4 Enterohepatic circulation

The cycling of bile acids between the liver, gall bladder, intestine, and portal circulation constitutes the enterohepatic circulation (EHC) of bile acids (Fig. 1-3). The liver and ileum are important regulatory sites of the EHC, which has important implications for the metabolism of bile acids in both health and disease. The bile acid pool is regulated by a variety of parameters, including gastrointestinal motility, gall bladder contractility, cycling rate, the rate of bile acid biosynthesis, and efficiency of bile acid recovery (Carey *et. al* 1994). Disruptions in bile acid metabolism in either the liver or ileum will have a negative and dramatic impact on the trafficking of bile acids in the EHC. As discussed in Section 1.2.2, disruption of bile acid recovery in ileal resected patients compromises the effective concentration of bile acids in the proximal intestine, resulting in poor fat absorption. If the impairment in ileal bile acid recovery is small (e.g., resectioning < 1/4 of the ileum), then the bile acid production in the liver increases to maintain the size of the pool in the EHC (Hofman, 1999). Numerous studies have shown that impairment or cessation of hepatic bile secretion causes cholestatic liver disease (Koopen et al. 1998). Bile acids do not transit the EHC in cholestasis, but accumulate in liver and plasma along with other biliary constituents (Koopen *et al.* 1998; Chisolm *et al.* 1999). Cholestatic liver patients suffer from malabsorption of fat soluble nutrients, and these patients go on to develop permanent liver damage if the disease is left untreated. Bile acids are suspected to mediate liver damage observed in cholestatic disease, presumably because of their detergent properties (Hofmann 1999).

1.3. Intracellular bile acid transport

Cells that transport bile acids must have mechanisms to sequester these potentially harmful molecules and shuttle them from the cellular sites of uptake to the sites of secretion. Therefore, the cellular transport and trafficking of potentially

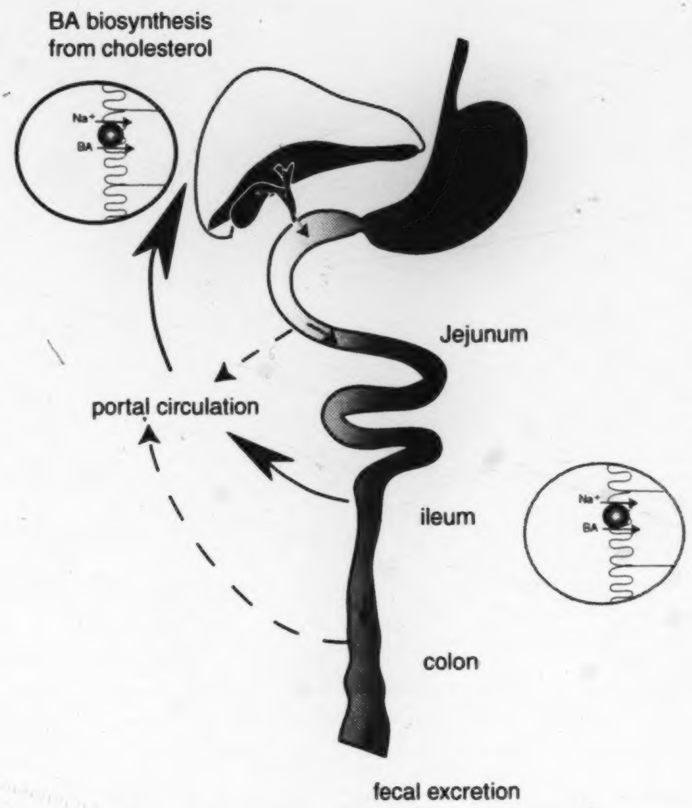

Fig. 1-3 Schema of the enterohepatic circulation (EHC) of bile acids. Bile acids (BA) are stored in the gall bladder interdigestively and are secreted into the duodenum when a meal is ingested. In the lumen of the small intestine, BA aid the digestion and absorption of lipophilic nutrients. They are recovered passively along the axis of the intestine (dashed arrows), but actively in the ileum (solid arrow). The liver absorbs BA from portal circulation and re-secretes them into bile. Ileocytes and hepatocytes are important sites for the conservation of BA in the EHC. In these cells, BA are predominantly taken up by secondary active transport systems that are sodium-dependent (left and right insets). Although conservation of BA in the EHC is very efficient, small amount of bile acids are lost from the EHC in feces. These losses are recompensed by daily bile acid biosynthesis in the liver. This figure was adapted from Carey *et al.* 1994.

toxic bile acids would appear to depend on the precise orchestration of both membrane bound and cytosolic proteins. Because hepatocytes and ileocytes play an integral role in the trafficking of bile acids within the EHC (Fig 1-3), these cells have been focus of intense research. However, despite numerous studies, the intracellular trafficking of bile acids remains an area that is poorly understood (Agellon *et al.* 2000). Several studies have shown that bile acids may interact with intracellular organelles. As mentioned in Section 1.2.3.1, mEH is expressed in smooth ER membranes in two topological orientations. The significance of its intracellular and topological expression pattern with respect to bile acid trafficking remains unknown. Based on electron microscopy and immunofluorescence evidence, bile acids have been shown to associate with Golgi membranes and pericanalicular vesicles (Erlinger 1996). Currently, it seems unlikely that intracellular organelles are involved in the translocation of bile acids from the basolateral to the apical poles of hepatocytes (Agellon *et al.* 2000). The prevalent thought is that bile acids are bound to intracellular proteins and then translocate from the sinusoidal to canalicular membrane for secretion (Agellon *et al.* 2000). Fig. 1-4 summarizes the molecules implicated in bile acid transport in hepatocytes and ileocytes. In addition, TCA has been shown to activate signal transduction pathways leading to the recruitment of canalicular transporters to the canaliculus, thereby increasing the capacity of liver to secrete bile acids and other lipophilic compounds (Misra *et al.* 1998; Misra *et al.* 1999).

1.3.1. Intracellular transport in hepatocytes

1.3.1.1 Role of Glutathione S-transferases and Liver fatty acid binding protein in bile acid intracellular transport

Three types of proteins in rat hepatic cytosol bind bile acids *in vitro*. The first of

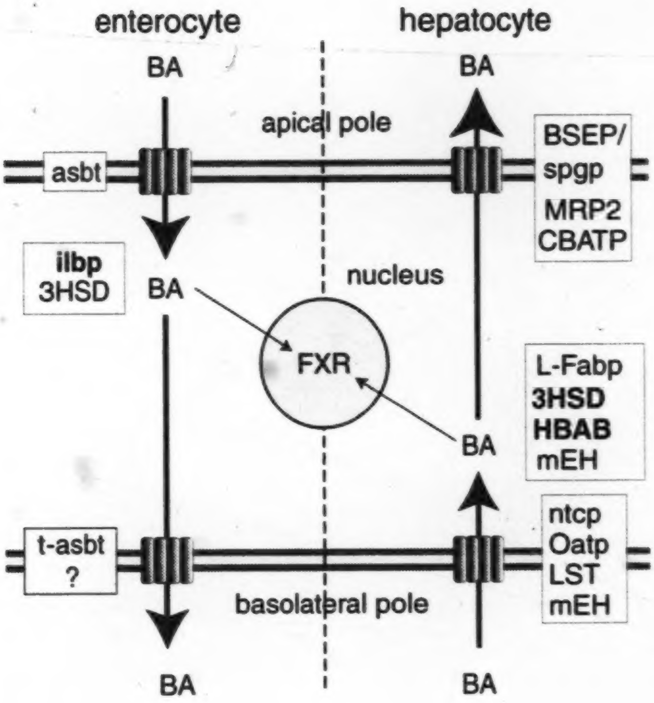

Fig. 1-4 Depiction of proteins implicated in cellular bile acid transport. Bile acids (BA) are taken up by integral membrane transporters (cylinders). Cellular binding proteins (boxes) presumably translocate BA to the opposite pole of the cell for secretion. Ilbp and HBAB/3HSD (in bold) have been proposed to be the major bile acid binding protein in the cytosol of ileocytes and hepatocytes, respectively. BA may interact with other intracellular proteins to modulate cell function (e.g. interaction with the nuclear receptor farnesoid-X-receptor, FXR). Asbt, apical sodium bile acid transporter; ilbp, ileal lipid binding protein; 3HSD, 3α-hydroxysteroid dehydrogenase; t-asbt, truncated asbt; BSEP, bile acid export pump; spgp, sister of p-glycoprotein; MRP2, multidrug resistance protein 2; CBATP, canalicular bile acid transporter/ecto-ATPase; L-Fabp, Liver fatty acid binding protein; HBAB, human bile acid binder; ntcp, sodium bile acid co-transporting polypeptide; Oatp, organic anion transporting polypeptide; LST, liver specific transporter; mEH, microsomal epoxide hydrolase; "?", unidentified protein. For explanation of each molecule and its respective function, please see text. This figure was modified from Agellon *et al.*, 2000.

these are the glutathione S-transferases (GSTs) (Stolz *et al.* 1989). GSTs normally function in the detoxification of xenobiotics by catalyzing the formation of thioesters of glutathione (Jakoby 1994). Rat GSTs also bind a variety of lipophilic compounds including LCA with high affinity (Stolz *et al.* 1989; Jakoby 1994). Because GSTs are abundantly expressed in hepatocytes (5% of total cellular protein in rat) (Jakoby 1994), GSTs could function in the sequestration of hydrophobic bile acids in hepatocytes. However, GSTs are not labeled with photolabile bile acid probes in intact cells, and human GSTs do not appear to bind bile acids (Stolz *et al.* 1989). These observations suggest that GSTs are not involved in intracellular bile acid transport, at least in humans. The second class of bile acid binding proteins belongs to the small cytosolic lipid binding protein (lbp) gene family (Bernlohr *et al.* 1997). The liver fatty acid binding protein (L-fabp) has been shown to weakly bind bile acids (Stolz *et al.* 1989), but has much higher binding affinity for fatty acids (FA) (Bernlohr *et al.* 1997). L-fabp is considered important in FA metabolism in both the liver and intestine (Van Nieuwenhoven *et al.* 1996; (Storch *et al.* 2000).

1.3.1.2 Role of 3α-hydroxysteroid dehydrogenase in bile acid transport

Stolz and coworkers identified 3α-hydroxysteroid dehydrogenase (3HSD) as the major bile acid binder in rat hepatic cytosol (Stolz *et al.* 1987). 3HSD is a member of the aldo-keto reductase supergene family and plays a crucial role in the bile acid biosynthetic pathway (Bahar *et al.* 1999). During bile acid biosynthesis, 3HSD reduces the oxo-bile acid precursor before it undergoes side chain cleavage (Russell *et al.* 1992). This enzyme is expressed in a variety of extrahepatic tissues including brain, ovaries and intestine (Stolz *et al.* 1991). Indirect evidence exists to support the involvement of 3HSD in bile acid intracellular transport. Using indomethacin to inhibit bile acid binding, Stolz and co-workers saw increased cellular displacement of radiolabeled bile acids from primary culture of hepatocytes (Stolz *et al.* 1989). In liver perfusion experiments, indomethacin decreased the excretion of bile acids into bile as compared to control livers (Bahar *et al.* 1999). Interestingly, the levels of 3HSD mRNA and protein decreased in rats made cholestatic by ligation of the common bile duct (Gartung *et al.* 1996). Concomitant decreases were also observed in ntcp mRNA and protein in this model. The decrease in ntcp activity is consistent with the notion that hepatocytes may decrease the recovery of potentially toxic bile acids under cholestatic conditions. However, the decrease in 3HSD is inconsistent with its proposed role in bile acid transport.

1.3.1.3 Role of the human bile acid binder in bile acid transport

Stolz and co-workers have identified a 36-kDa protein from human liver which displays this protein possess high bile acid binding affinity (K_d ~10 to 20 nM) similar to the rat 3HSD (Stolz *et al.* 1993). This protein, termed the human bile acid binder (HBAB), is not a true homologue to 3HSD because it lacks appreciable 3α-hydroxysteroid dehydrogenase activity (Takikawa *et al.* 1990), although it does posses dihydrodiol dehydrogenase activity for polycyclic aromatic hydrocarbons (Stolz *et al.* 1993). Because HBAB is similar to 3SHD and binds bile acids with high affinity, it is thought that HBAB may be involved in the intracellular transport of bile acid in human hepatocytes. However, the precise role of 3HSD and HBAB in bile acid intracellular transport remains unknown.

1.3.2. Intracellular bile acid transport in ileocytes

Intracellular transport of bile acids in the gut is less well understood than in the liver. Using a photolabile derivative of TCA, Wilson and co-workers identified a 14-

kDa protein in rat ileocytes as the major cytosolic bile acid binding protein (Lin *et al.* 1990; Lin *et al.* 1991). This protein, termed the intestinal bile acid binding protein (I-BABP), was previously identified as gastrotropin, a hormone thought to be involved in gastric secretion (Gantz *et al.* 1989; Gong *et al.* 1994). When gastrotropin was isolated and purified, it failed to elicit gastric secretion in rats or cultured gastric cells (Gantz *et al.* 1989). I-BABP is also known as the ileal lipid binding protein (ilbp) after it was characterized in mouse (Sacchettini *et al.* 1990). I-BABP/ilbp belongs to the lbp gene family (Bernlohr *et al.* 1997) and binds both bile acids and fatty acids *in vitro* (Sacchettini *et al.* 1990; Gong *et al.* 1994; Fujita *et al.* 1995). Because of its dual binding characteristics, ilbp is a much better name for this protein and will be used in the rest of this thesis. Fig. 1-5 shows the distribution of ilbp and other lbp members in mouse intestinal sections. As in humans, the expression of ilbp appears to be restricted to ileum (Oelkers *et al.* 1995; Watanabe *et al.* 1995) and coincides with the expression of asbt (Fig. 1-5). Ilbp is distinct from both the L-fabp and intestinal fatty acid binding protein, which are also expressed in the intestine (Bernlohr *et al.* 1997). In rats, ilbp is expressed abundantly in the ileum and somewhat less in cholangiocytes, ovaries, and adrenal gland (Iseki *et al.* 1993; Gong *et al.* 1994; Sato *et al.* 1995; Alpini *et al.* 1997). The expression of ilbp in the ovaries and adrenal in rat is rather perplexing, because it is not consistent with the putative role of ilbp in intracellular bile acid transport. Like 3HSD and HBAB in the liver, the precise role of ilbp in bile acid transport remains unproven.

The best evidence supporting a role for ilbp in ileal bile acid transport comes from studies done in rabbits by Kramer and co-workers (Kramer *et al.* 1993; Kramer *et al.* 1995; Kramer *et al.* 1997; Kramer *et al.* 1998; Kramer *et al.* 1999). Using radiation-inactivation analysis, they determined that ilbp is intimately associated with asbt in large homotetrameric complexes composed of four asbt/ilbp pairs (Kramer *et al.* 1995). The interaction between asbt and ilbp was later confirmed by

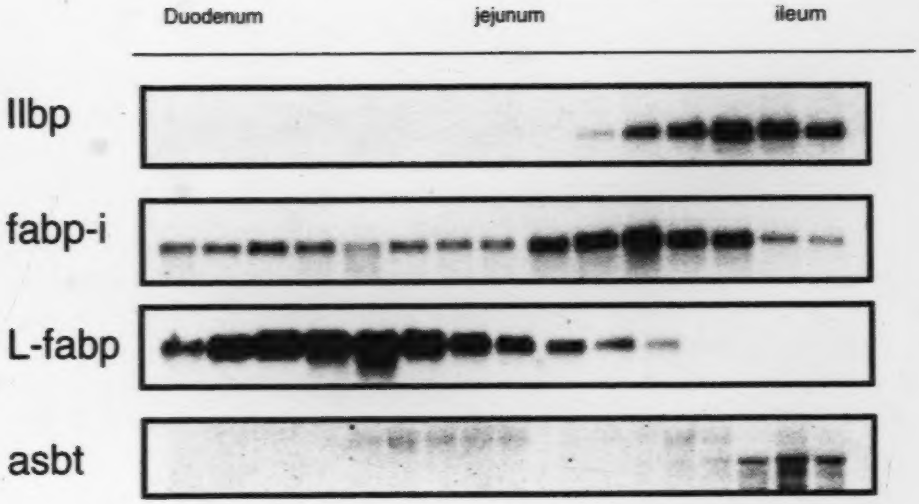

Fig. 1-5 Distribution of cytosolic lipid binding proteins (lbp) and asbt in the small intestine. Expression of lbp was analyzed by RNA blot analysis as detailed in Chapter 2 using radiolabeled cDNA probes for each of the lbps and asbt. Expression of ilbp is restricted to the ileum in the small intestine and coincides with expression of the asbt. L-fabp and fabp-i gene expression can be detected along the gastrocolic axis. L-fabp is maximally expressed in duodemun, while fabp-i is maximal expressed at the jejunal/ileal borders. Ten micrograms of total RNA was loaded in each well.

6

using specific "photolabile-dimeric" bile salt transport inhibitors (photoblockers) (Kramer *et al.* 1997). These photoblockers are not transported by asbt or able to span the bilayer, but were able to specifically label ilbp on the cytoplasmic side of ileocytes (Kramer *et al.* 1997). In other studies, the binding of bile acids to the ileal transport complex appears to increase the affinity of ilbp for bile acids (Kramer *et al.* 1998). These observations would strongly suggest that ilbp modulates ileal bile acid transport function and acts as an acceptor for bile acids as they enter ileocytes. Ilbp would presumably translocate bile acids from the apical to the basolateral membrane for secretion out of the cell (Fig. 1-4).

The evidence against the involvement of ilbp in ileal bile acid transport comes from several avenues of research. Firstly, ilbp is not necessary for asbt function as expression of recombinant asbt confers saturable Na^+-dependent bile acid transport in various tissue culture cell models (Wong *et al.* 1994; Craddock *et al.* 1998). Secondly, several groups have failed to detect ilbp expression in the kidney, where asbt has been shown to function in the recovery of bile acid in renal tubules (Christie *et al.* 1996; Craddock *et al.* 1998). Consistent with these observations, ileal bile acid transport in fetal rats is concomitant with expression of asbt, but not with ilbp (Shneider *et al.* 1997). Ilbp is not detected in the ileum of rats until post-natal day 17 (Gong *et al.* 1996). Thirdly, ilbp gene expression does not appear to be regulated by changes in the bile acid pool of the EHC. As shown in figure 1-6A, feeding of C57BL/6 mice with dietary supplements that alter the size of the bile acid pool induced dramatic changes in the level of asbt gene expression. However, there was no significant change in ilbp mRNA abundance under identical dietary conditions (Fig 1-6B, Torchia *et al.* 1996). Similar lack of responsiveness in ilbp gene expression has been observed in rats after bile acid feeding, ligation of the common bile duct, and intestinal sequestration of bile acids (Arrese *et al.* 1998; Coppola *et al.* 1998). In addition, supplementation of cholesterol to the diet of rabbits does

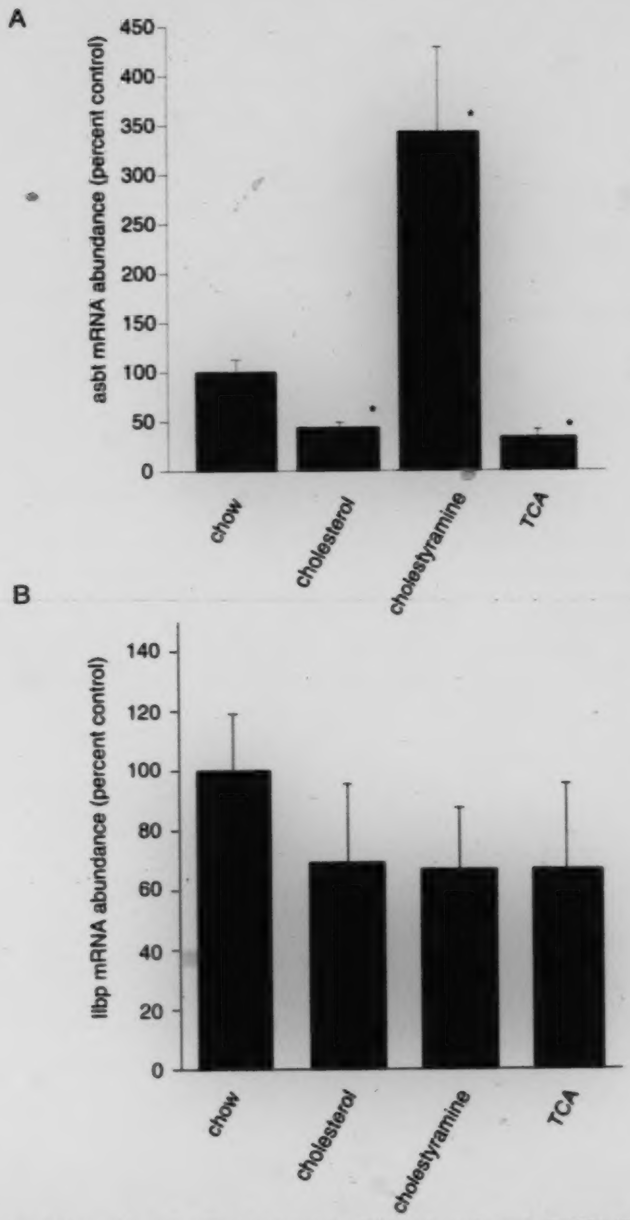

Fig. 1-6 Regulation of mouse ilbp and asbt mRNA abundance. C57BL/6 female mice were fed a chow diet or the chow diet supplemented with 1% cholesterol, 2% cholestyramine or 0.5% taurocholate. After two weeks on the diet, total RNA isolated from the liver and ileum were analyzed for ilbp and asbt mRNA abundance as described in Torchia *et al.*, 1996. Panel A, asbt mRNA abundance. Panel B, ilbp mRNA abundance. The mean ± S.E. are indicated. Differences in ilbp and asbt abundance in the absence (chow) or presence of supplements were evaluated using Student's t test. * denotes significant difference in comparison to the chow group ($P<0.05$).

not result in changes in ilbp protein or mRNA abundance (Xu *et al.* 2000). These studies notwithstanding, expression of ilbp has been shown to up-regulate in response to bile acids in Swiss male mice and Caco-2 cells (Kanda *et al.* 1996; Grober *et al.* 1999). The apparent differences observed in ilbp gene expression in these studies remain unexplained. However, there is precedence for significant variation in the responsiveness of genes involved in lipid metabolism between different genders and species. For example, susceptibility to formation of cholesterol gallstones and hypercholesterolemia varies between different strains of mice challenged with lipid rich diets (Albers *et al.* 1999; Mu *et al.* 1999; Wang *et al.* 1999c). In addition, Simon and co-workers documented gender differences with respect to hepatic taurocholate uptake in Sprague-Dawley rats that may depend on the responsiveness of the ntcp promoter to sex hormone levels (Simon *et al.* 1999).

1.4 Bile acids as regulators of cellular function

In addition to the importance of bile acids in the digestion and absorption of lipophilic nutrients in the gut, the last few years have shown that bile acids may play fundamental roles in the regulation cellular function in both enterocytes and hepatocytes. There is a body of evidence demonstrating the involvement of bile acids in regulation of lipoprotein metabolism and expression of liver specific genes. For many years, it has been known that bile acids can downregulate the expression of cyp7a, illustrating feedback regulation to the bile acid biosynthetic pathway (Vlahcevic *et al.* 1999). Bile acids regulate cyp7a gene expression transcriptionally (Vlahcevic *et al.* 1999) and post-transcriptionally by destabilizing its mRNA (Agellon *et al.* 1997). In animal studies, TCA feeding can suppress both the mRNA abundance and enzyme activity of the rate-limiting enzyme of the cholesterol biosynthetic pathway, 3-

hydroxy-3-methylglutaryl CoA reductase (Shefer *et al.* 1992). In primary culture of hepatocytes, bile acids inhibit the secretion of apolipoprotein B secretion (Lin *et al.* 1996a; Lin *et al.* 1996b). In swine intestinal epithelial cells, TCA appears to increase the secretion of apolipoprotein AI from the basolateral side of the cells (Wang *et al.* 1999b). Bile acids also have been shown to activate signal transduction pathways in hepatocytes that affect bile acid transport across both the basolateral and apical membranes (Bouscarel *et al.* 1999). As mentioned in section 1.2.5, toxic bile acids may mediate liver damage in observed in cholestatic diseases. In support of this notion, glycine conjugates of CDCA (GCDCA) and DCA (GDCA) have been shown by Gores and co-workers to induce apoptosis in primary cultures of hepatocytes (Spivey *et al.* 1993; Patel *et al.* 1994; Kwo *et al.* 1995). The concentration at which GCDCA and DCA can induce apoptosis is far below the concentration needed to form mixed micelles with cholesterol and phospholipids (Spivey *et al.* 1993; Patel *et al.* 1994). Despite numerous studies on the subject of bile acid-mediated apoptosis, the precise molecular mechanism underlying this phenomenon remains poorly understood.

The recent discovery that bile acids are the natural ligands for the transcription factor farnesoid x receptor (FXR;NR1H4) has ushered a new era in the understanding of how bile acids regulate gene expression (Makishima *et al.* 1999; Parks *et al.* 1999; Wang *et al.* 1999a). Evidence exists for the involvement of FXR in the regulation of ilbp and cyp7a gene expression (Grober *et al.* 1999; Chiang *et al.* 2000). However, it is unproven that changes in the levels of ilbp gene expression modulate asbt function or the ability of the ileum to reclaim bile acids. As discussed in Section 1.3.2, the responsiveness of ilbp gene expression to bile acids in different experimental models shows great variation (Torchia *et al.* 1996; Arrese *et al.* 1998; Coppola *et al.* 1998; Grober *et al.* 1999; Xu *et al.* 2000). The basis for these differences may lie in the differential ability of FXR to interact with the ilbp promoters in different species and sub-species of animals used to study the problem. FXR is expressed in a variety of tissues including liver, kidney, adrenal glands, and the small intestine (Forman *et al.* 1995). Its expression along the axis of the small intestine (Forman *et al.* 1995) suggests that FXR may regulate enterocyte gene expression along the gastro-cecal axis in response to bile acids. The functional relationship between putative bile acid binding proteins of the liver and intestine (eg. 3HSD/HBAB, ilbp) and FXR is not known. Cytosolic bile acid binding proteins may well function to regulate the substrate pool for FXR that would in turn regulate their own expression. Further studies are needed to elucidate the molecular mechanisms of FXR-mediated gene regulation.

One of the major obstacles to the study of bile acid transport and the role of bile acids in the regulation of cellular function has been the paucity of suitable *in vitro* models. Primary cultures of hepatocytes have been extensively used to study hepatic bile acid transport function. However, primary cultures quickly become dedifferentiated and lose the expression of liver-specific genes. For example, mouse albumin gene transcription falls dramatically within 24 h of isolation and culturing of hepatocytes (Clayton *et al.* 1983). The ability to express cyp7a mRNA and its corresponding activity is markedly reduced in 72 h old rat cultures of hepatocytes (Hylemon *et al.* 1992). Great efforts have been made to extend the differentiated phenotype of hepatocytes in culture, but these methods require extensive manipulations. Hepatoma cell lines resemble undifferentiated hepatocytes with respect to the number of liver-specific enzymes that they express. For example, although the Morris McArdle RH-7777 hepatoma cell line (McArdle RH-7777) has been routinely used to study the secretion and assembly of apolipoprotein B containing particles (Boren *et al.* 1994; Cavallo *et al.* 1998; Xiao *et al.* 2000), these cells do not express cyp7a (Labonte *et al.* 2000). The cloning of asbt, ntcp, 3HSD, and ilbp has made it possible to express these recombinant proteins in tissue culture models and examine their role in bile acid metabolism.

1.5 Thesis question

As outlined in section 1.3, ilbp and HBAB have been proposed to act as mediators of intracellular bile acid transport in the cytosol of ileocytes and hepatocytes, respectively. However, the precise role of these proteins in bile acid transport remains unknown. Because certain bile acids have the potential to be cytotoxic, sequestration and transport by cytosolic bile acid binders may be required for cell survival. To date, the role of intracellular bile acid binders in cytoprotection against toxic bile acids has not been addressed. The paucity of convenient tissue culture models is one reason for the lack of study in this area. **The overall goal of the work described in this thesis was to define the roles of ilbp and HBAB in cellular bile acid transport and cytoprotection from toxic bile acids.**

1.5.1 Objectives of the thesis

Objective i: Create a model system to test the role of HBAB

Primary cultures of hepatocytes have been used previously to study cellular bile acid transport. However, as mentioned in Section 1.4, cultured hepatocytes quickly lose characteristics of hepatocytes in the liver. Commonly used liver-derived cells do not exhibit appreciable bile acid uptake activity. Therefore, given the lack of convenient and useful tissue culture models in which to study bile acid intracellular transport, my first objective was to create such a model. Chapter 3 details the establishment of active bile acid transport in McArdle RH-7777 cells by the stable expression of recombinant rat ntcp. This cell line was selected because of its availability, ease of culturing, and the facility of doing DNA transfection experiments. In addition, this liver-derived cell line has been characterized extensively in the study of liver function (e.g. apolipoprotein secretion). Cells expressing ntcp, termed McNtcp, were evaluated for bile acid uptake and secretion.

Objective ii: Characterization of McNtcp.24 cells

As detailed in Section 1.4, toxic bile acids may mediate liver damage observed in cholestatic disease. In addition, certain kinds of bile acids have been shown to induce cell death in primary culture of hepatocytes. Before I could address the role of HBAB, I had to determine the cytotoxic potential of bile acids in McNtcp cells. Chapter 4 and 5 details these experiments. I also compared the cytotoxic potential of bile acids in McNtcp.24 cells with a non-liver derived cell line made to take up bile acids. Chapter 5 details these experiments.

***Objective iii*: Determine if expression of HBAB in bile acid transport competent cells has an impact on cellular bile acid transport and cytotoxicity**

Having characterized the model system, I created cell lines that stably co-expressed HBAB and ntcp in the McArdle RH-7777 background. As discussed in Section 1.3, HBAB is a high affinity bile acid binding protein that may protect cells by sequestering potentially toxic bile acids. I tested the hypothesis that expression of HBAB could protect the cells from toxic bile acids or overtly affect the ability of cells to take up or secrete bile acids. Chapter 5 details these experiments.

***Objective iv:* Disruption of the murine ilbp gene**

Insights obtained from tissue culture models into the molecular working of biological systems must be verified ultimately with *in vivo* data. I undertook the disruption of the murine ilbp gene to define its role in the conservation of bile acids in the EHC. Unlike the human bile acid binder, ilbp is a suitable candidate for a "knock-out" experiment. It is a small gene (4 exons) that is present as a single copy gene on chromosome 11 in the mouse genome (Crossman *et al.* 1994). It is distinct from the other members of the lbp gene family and is not linked to any known gene involved in the metabolism of fatty acids or bile acids (Bernlohr *et al.* 1997). In the mouse, its expression is limited to ileum, and is easily detectable in the ileum after birth (Sacchettini *et al.* 1990). As outlined in section 1.2.2, mutations in the asbt gene can cause bile acid malabsorption in humans. If ilbp is critical for ileal active bile acid transport, then its gene disruption should have an obvious effect on the conservation of bile acid in the gut and the bile acid pool of the EHC. If the ilbp is moderately important for ileal bile acid transport, then ilbp null mice may be able to compensate for a small disruption in intestinal bile acid recovery. This scenario would be similar to cyp27 null mice (see section 1.1), which have a reduced bile acid pool, but digest and absorb lipophilic nutrients normally. Ilbp is abundantly expressed in the ileum (see Fig. 1-5), and ilbp may cytoprotect ileocytes from exposure to high flux of potentially toxic bile acids. Because the size of the bile acid pool does not reach adult levels until the suckling/weaning transition, expression of ilbp may not be necessary for protection of ileocytes until after this period, when mice have a fully functional EHC. This alternate hypothesis could account for the lack of expression of ilbp in fetal life of the rat (see section 1.3.2). The last possibility is that ilbp does not play any role in ileal bile acid transport. In this case, ilbp null mice would not display an obvious phenotype. Chapter 6 details the creation and early characterization of ilbp knockout mice.

1.6 REFERENCES

Abe, T., M. Kakyo, H. Sakagami, T. Tokui, T. Nishio, *et al.* (1998). Molecular characterization and tissue distribution of a new organic anion transporter subtype (oatp3) that transports thyroid hormones and taurocholate and comparison with oatp2. *J. Biol. Chem.* 273: 22395-22401.

Abe, T., M. Kakyo, T. Tokui, R. Nakagomi, T. Nishio, *et al.* (1999). Identification of a novel gene family encoding human liver-specific organic anion transporter LST-1. *J. Biol. Chem.* 274: 17159-17163.

Agellon, L. and S. Cheema (1997). The 3'-untranslated region of the mouse cholesterol 7alpha-hydroxylase mRNA contains elements responsive to post-transcriptional regulation by bile acids. *Biochem. J.* 328: 393-399.

Agellon, L.B. and E.C. Torchia (2000). Intracellular transport of bile acids. *Bioch. Biophys. Acta* 1486: 198-209.

Albers, J.J., W. Pitman, G. Wolfbauer, M.C. Cheung, H. Kennedy, *et al.* (1999). Relationship between phospholipid transfer protein activity and HDL level and size among inbred mouse strains. *J. Lipid Res.* 40: 295-301.

Alpini, G., S.S. Glaser, R. Rodgers, J.L. Phinizy, W.E. Robertson, *et al.* (1997). Functional expression of the apical Na+-Dependent bile acid transporter in Large but not small rat cholangiocytes. *Gastroenterology* 113: 1734-1740.

Alves, C., P. Von Dippe, M. Amoui and D. Levy (1993). Bile acid transport into hepatocyte smooth endoplasmic reticulum vesicles is mediated by microsomal epoxide hydrolase, a membrane protein exhibiting two distinct topological orientations. *J. Biol. Chem.* 268: 20148-20155.

Amelsberg, A., C. Jochims, C.P. Richter, R. Nitsche and U.R. Folsch (1999). Evidence for an anion exchange mechanism for uptake of conjugated bile acid from the rat jejunum. *Am. J. Physiol.* 276: G737-G742.

Angeletti, R.H., P.M. Novikoff, S.R. Juvvadi, J.M. Fritschy, P.J. Meier, *et al.* (1997). The choroid plexus epithelium is the site of the organic anion transport protein in the brain. *Proc. Natl. Acad. Sci. U.S.A.* 94: 283-286.

Arrese, M., M. Trauner, R.J. Sacchiero, M.W. Crossman and B.L. Shneider (1998). Neither intestinal sequestration of bile acids nor common bile duct ligation modulate the expression and function of the rat ileal bile acid transporter. *Hepatology* 28: 1081-1087.

Bahar, R.J. and A. Stolz (1999). Bile acid transport. *Gastroenterology Clin. North Am.* 28(1): 27-58.

Bernlohr, D.A., M.A. Simpson, A. Vogel Hertzel and L.J. Bamaszak (1997). Intracellular lipid binding proteins and their genes. *Annu. Rev. Nutr.* 17: 277-303.

Boren, J., S. Rustaeus and S.-O. Olofsson (1994). Studies on the assembly of apolipoprotein B-100 and B-48 very low density lipoproteins in McA-RH7777 cells. *J. Biol. Chem.* 269: 25879-25888.

Bouscarel, B., S.D. Kroll and H. Fromm (1999). Signal transduction and hepatocellular bile acid transport: cross talk between bile acids and second messengers. *Gastroenterology* 117: 433-452.

Carey, M.C. and W.C. Duane (1994). Enterohepatic circulation. in The liver biology and pathobiology, third edition. A. I. M, J. L. Boyer and D. A. Shafriz. New York 1994, Raven Press, Ltd.: 719-767.

Cavallo, D., R.S. McLeod, D. Rudy, A. Aiton, Z. Yao, *et al.* (1998). Intracellular translocation and stability of apolipoprotein B are inversely proportional to the length of the nascent polypeptide. *J. Biol. Chem.* 273(50): 33397–33405.

Chiang, J.Y.L., R. Kimmel, C. Wienberger and D. Stroup (2000). Farnesoid X receptor responds to bile acids and repressed 7 alpha-hydroxylase gene (cyp7a1) transcription. *J. Biol. Chem.* 275: 10918-10924.

Childs, S., R.L. Yeh, E. Georges and V. Ling (1995). Identification of a sister gene to P-glycoprotein. *Cancer Res.* 55: 2029-2034.

Chisolm, J.W., P. Nation, P.J. Dolphin and L.B. Agellon (1999). High plasma cholesterol in drug-induced cholestasis is associated with enhanced hepatic cholesterol synthesis. *Am. J. Physiol.* 276: G1165-G1173.

Christie, D.M., P.A. Dawson, S. Thevananther and B.L. Shneider (1996). Comparative analysis of the ontogeny of a sodium dependent bile acid transporter in rat kidney and ileum. *Am. J. Physiol.* 271(34): G377-G385.

Clayton, D.F. and J.E. Darnell (1983). Changes in liver-specific compared to common gene transcription during primary culture of mouse hepatocytes. *Mol. Cell. Biol.* 3(9): 1552-61.

Coppola, C.P., J.R. Gosche, M. Arrese, B. Ancowitz, J. Madsen, *et al.* (1998). Molecular analysis of the adaptive response of intestinal bile acid transport after ileal resection in the rat. *Gastroenterology* 115: 1172-1178.

Craddock, A.L., M.W. Love, R.W. Daniel, L.C. Kirby, H.C. Walters, *et al.* (1998). Expression and transport properties of the human ileal and renal sodium-dependent bile acid transporter. *Am. J. Physiol* 274(37): G157-G169.

Crossman, M.W., S.M. Hauft and J.I. Gordon (1994). The mouse Ileal Lipid-binding Protein gene: a model for studying axial patterning during gut morphogenesis. *J. Cell Biol.* 126: 1547-1564.

Dawson, P.A. (1999). Intestinal bile acid transport. Falk symposium: Bile Acids and Cholestasis (Titisee, Germany). G. Paumgartner, A. Stiehl, W. Gerok, D. Keppler and U. Leuschner, Kluwer Academic Publishers, Lancaster. 108: 1-28.

Dietschy, J.M. (1997). Theoretical consideration of what regulates low-density-lipoprotein and high-density-lipoprotein cholesterol. *Am. J. Clin. Nutr.* 65: 1581S-1589S.

Duane, W.C. and N.B. Javitt (1999). 27-hydroxycholesterol: production rates in normal human subjects. *J. Lipid Res.* 40: 1194-1199.

Eckhardt, U., A. Schroeder, B. Stieger, M. Hochli, L. Landmann, *et al.* (1999). Polyspecific substrate uptake by the haptic organic anion transporter Oatp1 in stably transfected CHO cells. *Am. J. Physiol.* 276: G1037-G1042.

Erlinger, S. (1996). Do intracellular organelles have any role in transport of bile acids by hepatocytes. *J. Hepatology* 24 (suppl. 1): 88-93.

Falany, C.N., M.R. Johnson, S. Barnes and R.B. Diasio (1994). Glycine and taurine conjugation of bile acids by a single enzyme. Molecular cloning and expression of human liver bile acid CoA:amino acid N-acyltransferase. *J. Biol. Chem.* Vol. 269(30): 19375-19379.

Forman, B.M., E. Goode, J. Chen, A.E. Oro, D.J. Bradley, *et al.* (1995). Identification of a nuclear receptor that is activated by Farnesol metabolites. *Cell* 81: 687-693.

Fujita, M., H. Fujii, T. Kanda, R. Sato, K. Hatakeyama, *et al.* (1995). Molecular cloning, expression, and characterization of a human intestinal 15-kDa protein. *Eur. J. Biochem.* 233: 406-413.

Gantz, I., S.F. Nothwehr, M. Lucey, J.C. Sacchettini, J. DelValle, *et al.* (1989). Gastrotropin: Not an enterooxyntin but a member of a family of cytoplasmic hydrophobic ligand binding protein. *J. Biol. Chem.* 264: 20248-20254.

Gartung, C., M. Ananthanarayanan, M.A. Rahman, S. Schuele, S. Nundy, *et al.* (1996). Down-regulation of expression and function of the liver Na+/bile acid cotransporter in extrahepatic cholestasis. *Gastroenterology* 110: 199-209.

Gerloff, T., B. Stieger, B. Hagenbuch, J. Madon, L. Landmann, *et al.* (1998). The sister of p-glycoprotein represents the canalicular bile salt export pump of mammalian liver. *J. Biol. Chem.* 273: 10046-10050.

Gong, Y.Z., E.T. Everet, D.A. Schwartz, J.S. Norris and F.A. Wilson (1994). Molecular cloning, tissue distribution, and expression of a 14-kDa bile acid-binding protein from rat ileal cytosol. *Proc. Natl. Acad. Sci USA* 91: 4741-4745.

Gong, Y.Z., T. Kato, D.A. Schwartz, J.S. Norris and F.A. Wilson (1996). Ontogenic and glucocorticoid-accelerated expression of rat 14-kDa bile acid-binding protein. *Anat. Record* 245: 532-538.

Grober, J., I. Zaghini, H. Fujii, S.A. Jones, S.A. Kliewer, *et al.* (1999). Identification of a bile acid-responsive element in the human ileal bile acid binding protein gene. *J. Biol. Chem.* 274: 29749-29754.

Hagenbuch, B. (1997). Molecular properties of hepatic uptake systems for bile acids and organic anions. *J. Membrane Biol.* 160: 1-8.

Hagenbuch, B. and P.J. Meier (1996a). Sinusoidal (basolateral) bile salt uptake systems of hepatocytes. *Sem. Liver Dis.* 16: 129-135.

Hagenbuch, B., B.F. Scharschmidt and P.J. Meier (1996b). Effect of antisense oligonucleotides on the expression of hepatocellular bile acid and organic anion uptake systems in Xenopus laevis oocytes. *Biochem. J.* 316: 901-904.

Hagenbuch, B., B. Stieger, M. Foguet, H. Lubbert and P.J. Meier (1991). Functional expression cloning and characterization of hepatocyte Na+/bile acid cotransport system. *Proc. Natl. Acad. Sci U.S.A.* 88: 10629-10633.

Hofmann, A.F. (1999). The continuing importance of bile acids in liver and intestinal disease. *Arch. Intern. Med.* 159: 2647-2658.

Hsiang, B., Y. Zhu, [illegible] Wang, Y. Wu, V. Sasseville, *et al.* (1999). A novel human hepatic organic anion transporting polypeptide (OATP2). *J. Biol. Chem.* 274: 37161-37168.

Hylemon, P.B., E.C. Gurley, R.T. Stravitz, J.S. Litz, W.M. Pandak, *et al.* (1992). Hormonal regulation of cholesterol 7α-hydroxylase mRNA levels and transcriptional activity in primary rat hepatocyte cultures. *J. Biol. Chem.* 267(24): 16866-71.

Iseki, S., O. Amano, T. Kanda, H. Fujii and T. Ono (1993). Expression and localization of intestinal 15-kDa protein in the rat. *Mol. Cell. Biochem.* 123: 113-120.

Ishibashi, S., M. Schwarz, P.K. Frykman, J. Herz and D.W. Russell (1996). Disruption of cholesterol 7α-hydroxylase gene in mice: i. postnatal lethality reversed by bile acid and vitamin supplementation. *J. Biol. Chem.* 271: 18017-18023.

Jacquemin, E., B. Hagenbuch, B. Stieger, A.W. Wolkoff and P.J. Meier (1994). Expression cloning of a rat liver Na(+)-independent organic anion transporter. *Proc. Natl. Acad. Sci. USA* 91: 133-137.

Jakoby, W.B. (1994). Detoxication: Conjugation and Hydrolysis. in The liver biology and pathobiology, third edition. A. I. M, J. L. Boyer and D. A. Shafriz. New York 1994, Raven Press, Ltd.: 429-442

Kanda, T., I. Niot, L. Foucaud, H. Fuji, A. Bernard, *et al.* (1996). Effect of bile on the intestinal bile-acid binding protein (I-BABP) expression. In vitro and in vivo studies. *FEBS Let.* 384: 131-134.

Kakyo, M., M. Unno, T. Tokui, R. Nakagomi, T. Nishio, *et al.* (1999). Molecular characterization and functional regulation of a novel rat liver specific organic anion transporter rlst-1. *Gastroenterology* 117: 770-775.

Konig, J., Y. Cui, A. Nies and D. Keppler (2000). A novel human organic anion transporting polypeptide localized to the basolateral hepatocyte membrane. *Am. J. Physiol.* 278: G156-G164.

Koopen, N.R., M. Muller, R.J. Vonk, P. Zimniak and F. Kuipers (1998). Molecular mechanisms of cholestasis: causes and consequences of impaired bile formation. *Bioch. Biophys. Acta* 1408: 1-17.

Kouzuki, H., H. Suzuki, K. Ito, R. Ohashi and Y. Sugiyama (1998). Contribution of sodium taurocholate co-transporting polypeptide to the uptake of its possible substrates into rat hepatocytes. *J. Pharma. Exp. Therap.* 286: 1043-1050.

Kramer, W., D. Corsiero, M. Friedrich, F. Girbig, S. Stengelin, *et al.* (1998). Intestinal absorption of bile acids: paradoxical behavior of the 14-kDa ileal lipid-binding protein in differential photoaffinity labelling. *Biochem J.* 333: 335-341.

Kramer, W., F. Girbig, U. Gutjahr and S. Kowalewski (1995). Radiation-inactivation analysis of the Na+/bile acid co-transport system from rabbit ileum. *Biochem. J.* 306: 241-246.

Kramer, W., F. Girbig, U. Gutjahr, S. Kowlewski, K. Jouvenal, *et al.* (1993). Intestinal bile acid absorption. *J. Biol. Chem.* 268: 18035-18046.

Kramer, W., S. Stengelin, K. Baringhaus, A. Enhsen, H. Heuer, *et al.* (1999). Substrate specificity of the ileal and the hepatic Na+/bile acid cotransporters of the rabbit. I. transport studies with membrane vesicles and cell lines expressing the cloned transporters. *J. Lipid Res.* 40: 1604-1617.

Kramer, W., G. Wess, U. Bewersdorf, D. Corsiero, F. Girbig, *et al.* (1997). Topological photaffinity labeling of the rabbit ileal Na+/bile-salt-cotransport system. *Eur. J. Biochem.* 249: 456-464.

Kuipers, F., R.P.J.O. Elferink, H.J. Verkade and A.K. Groen (1997). Mechanisms and (patho)physiological significance of biliary cholesterol secretion. In Subcellular biochemistry: volume 28: Cholesterol: Its functions and metabolism in biology and disease, edited by R. Bittman, Plenum, New York, 1997.

Kullak-Ublick, G.A., B. Hagenbuch, B. Stieger, C.D. Schteingart, A.F. Hofmann, *et al.* (1995). Molecular and functional characterization of an organic anion transporting polypeptide cloned from human liver. *Gastroenterology* 109: 1274-1282.

Kwo, P., T. Patel, S.F. Bronk and G.J. Gores (1995). Nuclear serine protease activity contributes to bile acid-induced apoptosis in hepatocytes. *Am. J. Physiol.* 268: G613-G21.

Labonte, E.D., Q. Li and L.B. Agellon (2000). Expression bile cholesterol 7α-hydroxylase restores bile acid synthesis in McArdle RH7777 cells. *Arch. Biochem. Biophys. in press.*

Lazaridis, K.N., P. Tietz, T. Wu, S. Kip, P. A. Dawson, and N. F. Larusso. Alternative splicing of the rat sodium bile acid transporter changes its cellular localization and transport properties. *Proc. Natl. Acad. Sci. USA* 97: 11092-11097

Lewis, M.C., L.E. Brieaddy and C. Root (1995). Effects of 2164U90 on ileal bile acid absorption and serum cholesterol in rats and mice. *J. Lipid Res.* 36: 1098-1105.

Li-Hawkins, J., E.G. Lund, S.T. Turley and D.E. Russell (2000). Disruption of the oxysterol 7α-hydroxylase Gene in Mice. *J. Biol. Chem.* 275 (22): 16536-16542.

Lin, M.C., Y. Gong, K.F. Geoghegan and F.A. Wilson (1991). Characterization of a novel 14-kDa bile acid-binding protein from rat ileal cytosol. *Bioch. Biophys. Acta.* 1078: 329-335.

Lin, M.C., W. Kramer and F.A. Wilson (1990). Identification of cytosolic and microsomal bile acid-binding proteins in rat ileal enterocytes. *J. Biol. Chem.* 265: 14986-14995.

Lin, W.C., S.L. Weinberg, W. Kramer, G. Burckhardt and F.A. Wilson (1988). Identification and comparison of bile acid-binding polypeptide in ileal basolateral membrane. *J. Membrane Biol.* 106: 1-11.

Lin, Y., R. Havinga, I.J. Schippers, H.J. Verkade, R.J. Vonk, *et al.* (1996a). Characterization of the inhibitory effects of bile acids on very-low-density lipoprotein secretion by rat hepatocytes in primary culture. *Biochem. J.* 316: 531-538.

Lin, Y., R. Havinga, H.J. Verkade, H. Moshage, M.J. Slooff, *et al.* (1996b). Bile acids suppress the secretion of very-low density lipoprotein by human hepatocytes in primary cultures. *Hepatology* 23: 218-28.

Love, M.W. and P.A. Dawson (1998). New insights into bile acid transport. *Curr. Opin. Lipidol.* 9: 225-229.

Makishima, M., A.Y. Okamoto, J.J. Repa, H. Tu, R.M. Learned, *et al.* (1999). Identification of a nuclear receptor for bile acids. *Science* 248(5418): 1362-1365.

Meier, P.J., U. Eckhardt, A. Schroeder, B. Hagenbuch and B. Stieger (1997). Substrate specificity of sinusoidal bile acid and organic anion uptake systems in rat and human liver. *Hepatology* 26: 1667-1677.

Meier, P. and B. Stieger (2000). Molecular mechanisms in bile formation. *News Physiol. Sci.* 15: 89-93.

Misra, S., P. Ujhazy, Z. Gatmaitan, L. Varticovski and I.M. Arias (1998). The role of phosphoinositide 3-kinase in taurocholate-induced trafficking of ATP-dependent canalicular transporters in rat liver. *J. Biol. Chem.* 273(41): 26638-26644.

Misra, S., P. Ujhazy, L. Varticovski and I.M. Arias (1999). Phosphoinositide 3-kinase lipid products regulate ATP-dependent transport by sister of P-glycoprotein and multidrug resistance associated protein 2 in bile canalicular membrane vesicles. *Proc. Natl. Acad. Sci. U.S.A.* 96: 5814-5819.

Mu, J., J.K. Naggert, K.L. Svenson, G.B. Collin, J. Han Kim, *et al.* (1999). Quantitative trait loci analysis for the differences in susceptibility to atherosclerosis and diabetes between inbred mouse strains C57BL/6J and C57 BLKS/J. *J. Lipid Res.* 40: 1328-1335.

Nathanson, N.H. and J.L. Boyer (1991). Mechanisms and regulation of bile secretion. *Hepatology* 14: 551-566.

Noé, B., B. Hagenbuch, Stieger B and M. PJ (1997). Isolation of a multispecific organic anion and cardiac glycoside transporter from rat brain. *Proc. Natl. Acad. Sci. U.S.A.* 94: 10346–10350.

Oelkers, P. and P.A. Dawson (1995). Cloning and chromosomal localization of the human ileal lipid-binding protein. *Bioch. Biophys. Acta* 1257: 199-202.

Oelkers, P., L.C. Kirby, J.E. Heubi and P.A. Dawson (1997). Primary bile acid malabsorption caused by mutation in the ileal sodium-dependent bile acid transporter gene (SLC10A2). *J. Clin. Invest.* (99): 1880-1887.

Ortiz, D.F., S. Li, R. Iyer, X. Zhang, P. Novikoff, *et al.* (1999). MRP3, a new ATP-binding cassette protein localized to the canalicular domain of the hepatocyte. *Am. J. Physiol.* 276: G1493-G1500.

Parks, D.J., S.G. Blanchard, R.K. Bledsoe, G. Chandra, T.G. Consler, *et al.* (1999). Bile acids: natural ligands for an orphan nuclear receptor. *Science* 284(5418): 1365-1368.

Patel, T., S.F. Bronk and G.J. Gores (1994). Increases of intracellular magnesium promote glycodeoxycholate-induced apoptosis in rat hepatocytes. *J. Clin. Invest.* 94: 2183-2192.

Root, C., C.D. Smith, L.E. Brieaddy and M.C. Lewis (1995). Inhibition of ileal sodium-dependent bile acid transport by 2164U90. *J. Lipid. Res.* 36: 1106-1115.

Rosen, H., A. Reshef, N. Maeda, A. Lippoldt, S. Shpizen, *et al.* (1998). Markedly reduced bile acid synthesis but maintained levels of cholesterol and vitamin D metabolites in mice with disrupted sterol 27-hydroxylase gene. *J. Biol. Chem.* 273: 14805-14812.

Russell, D.W. and D.R. Setchell (1992). Bile acid biosynthesis. *Biochemistry* 31(20): 4737-4749.

Sacchettini, J.C., S.M. Hauft, S.L. Van Camp, D.P. Cistola and J.I. Gordon (1990). Developmental and structural studies of an intracellular lipid binding protein expressed in the ileal epithelium. *J. Biol. Chem.* 265: 19199-19207.

Sato, E., H. Fujii, M. Fujita, T. Kanda, S. Iseki, *et al.* (1995). Tissue-specific regulation of the expression of rat intestinal bile acid-binding protein. *FEBS let.* 374: 184-186.

Schroeder, A., U. Eckhardt, B. Stieger, R. Tynes, C.D. Schteingart, *et al.* (1998). Substrate specificity of the rat liver Na+ - bile salt cotransporter in Xenopus laevis oocytes and in CHO cells. *Am. J. Physl.* 274(37): G370-G375.

Schwarz, M., E.G. Lund, R. Lathe, I. Bjorkhem and D.W. Russell (1997). Identification and characterization of a mouse oxysterol 7α-hydroxylase cDNA. *J. Biol. Chem.* 272: 23995-24001.

Schwarz, M., E.G. Lund, K.D.R. Setchell, H.J. Kayden, J.E. Zerwekh, *et al.* (1996). Disruption of cholesterol 7α-hydroxylase gene in mice: ii bile acid deficiency is overcome by induction of oxysterol 7α-hydroxylase. *J. Biol Chem* 271: 18024-18031.

Setchell, K.D.R., C.M.P. Rodriguez, C. Clerici, A. Solinas, A. Morelli, *et al.* (1997). Bile acid concentrations in human and rat liver tissue and in hepatocyte nuclei. *Gastroenterology* 117: 226-235.

Shefer, S., L.B. Nguyen, G. Salen, G.C. Ness, I.R. Chowdhary, *et al.* (1992). Differing effects of cholesterol and taurocholate on steady state hepatic HMG-CoA reductase and cholesterol 7α-hydroxylase activities and mRNA levels in the rat. *J. Lipid Res.* 33: 1193-1200.

Shearman, D.J.C. and N.D.C. Finlayson (1989). Diseases of the gastrointestinal tract and liver, Edinburgh ; New York : Churchill Livingstone, 1989: 459-466.

Shneider, B.L., P.A. Dawson, D.M. Christie, W. Hardikar, M.H. Wong, *et al.* (1995). Cloning and molecular characterization of the ontogeny of a rat ileal sodium-dependent bile acid transporter. *J. Clin. Invest.* 95: 745-754.

Shneider, B.L., K.D.R. Setchell and M. Crossman (1997). Fetal and Neonatal expression of the apical sodium-dependent bile acid transporter in the rat ileum and Kidney. *Pediatric Res.* 42: 189-194.

Simon, F.R., J. Fortune, M. Iwashi, S. Bowman, A. Wolkoff, *et al.* (1999). Characterization of the mechanism involved in the gender differences in hepatic taurocholate uptake. *Am. J. Physiol.* 276: G556-G565.

Sippel, C.J., P.A. Dawson, T. Shen and D.H. Perlmutter (1997). Reconstitution of bile acid transport in a heterologous cell by co-transfection of transporter for bile acid uptake and efflux. *J. Biol. Chem.* 272: 18290-18297.

Sippel, C.J., F.J. Suchy, M. Anathanarayanan and D.H. Perlmutter (1993). The rat liver ecto-ATPase is also a canalicular bile acid transport protein. *J. Biol. Chem.* 268: 2083-2091.

Spivey, J.R., S.F. Bronk and G.J. Gores (1993). Glycochenodeoxycholate-induced lethal hepatocellular injury in rat hepatocytes. *J. Clin. Invest.* 92: 17-24.

Stolz, A., L. Hammond, H. Lou, H. Takikawa, M. Ronk, *et al.* (1993). cDNA cloning and expression of the human hepatic bile acid-binding protein. *J. Biol. Chem.* 268: 10448-10457.

Stolz, A., M. Rahimi-Kiani, D. Ameis, E. Chan, M. Ronk, *et al.* (1991). Molecular structure of rat hepatic 3 alpha-hydroxysteroid dehydrogenase. *J. Biol. Chem.* 266: 15253-15257.

Stolz, A., H. Takikawa, M. Ookhtens and N. Kaplowitz (1989). The role of cytoplasmic proteins in hepatic bile acid transport. *Ann. Rev. Physiol.* 51: 161-76.

Stolz, A., H. Takikawa, Y. Sugiyama, J. Kuhlenkamp and N. Kaplowitz (1987). 3 alpha-hydroxysteroid dehydrogenase activity of the Y' bile acid binders in rat liver cytosol. Identification, kinetics, and physiologic significance. *J. Clin. Invest.* 79: 427-434.

Storch, J. and A.E.A. Thumser (2000). The fatty acid transport function of fatty acid-binding proteins. *Bioch. Biophys. Acta* 1486: 28-44.

Strautnieks, S.S., L.N. Bull, A.S. Knisely, S.A. Kocoshis, N. Dahl, *et al.* (1998). A gene encoding a liver-specific ABC transporter is mutated in progressive familial intrahepatic cholestasis. *Nat. Genetics* 20: 233-238.

Takikawa, H., A. Stolz, Y. Sugiyama, H. Yoshida, M. Yamanaka, *et al.* (1990). Relationship between the newly identified bile acid binder and bile acid oxidoreductases in human liver. *J. Biol. Chem.* 265: 2132-2136.

Torchia, E.C., S.K. Cheema and L.B. Agellon (1996). Co-ordinate regulation of bile acid biosynthetic and recovery pathways. *Bioch. Biophys. Res. Com.* 225: 128-133.

Van Nieuwenhoven, F.A., G.J. Van der Vusse and J.F.C. Glatz (1996). Membrane-associated and cytoplasmic fatty acid-binding proteins. *Lipids* 31: S223-S227.

Vlahcevic, Z.R., W.M. Pandak and R.T. Stravitz (1999). Regulation of bile acid biosynthesis. *Gastroenterology Clin. North. Am.* 28: 1-24.

Von Dippe, P., M. Amoui, A. C and D. Levy (1993). Na(+)-dependent bile acid transport by hepatocytes is mediated by a protein similar to microsomal epoxide hydrolase. *Am. J. Physiol.* 264: G528-G534.

Von Dippe, P., M. Amoui, R.H. Stellwagen and D. Levy (1996). The functional expression of sodium-dependent bile acid transport in Madin-Darby Canine kidney cells transfected with the cDNA for microsomal epoxide hydrolase. *J. Biol. Chem.* 271: 18176-18180.

Wang, H., J. Chen, K. Hollister, L.C. Sowers and B.M. Forman (1999a). Endogenous bile acids are ligands for the nuclear receptor FXR/BAR. *Mol. Cell* 3: 543-553.

Wang, H., R. Roberson, J. Du, J.K. Eshun, H.M. Berschneider, *et al.* (1999b). Regulation of apolipoprotein secretion by biliary lipids in newborn swine intestinal epithelial cells. *Am. J. Physiol.* 276: G353-G362.

Wang, D.Q., F. Lammert, B. Paigen and M.C. Carey (1999c). Phenotypic characterization of Lith genes that determine susceptibility to cholesterol cholelithiasis in inbred mice: pathophysiology of biliary lipid secretion. *J. Lipid Res.* 40: 2066-2079.

Watanabe, K., N. Hoshi, Y. Tsuura, T. Kanda, M. Fujita, *et al.* (1995). Immunohistochemical distribution of intestinal 15-kDa protein in human tissues. *Arch. Hist. Cyt.* 58: 303-306.

Weinberg, S.L., G. Burckhardt and F.A. Wilson (1986). Taurocholate transport by rat intestinal basolateral membrane vesicles. *J. Clin. Invest.* 78: 44-50.

Wong, M.H., P. Oelkers, A.L. Craddock and P.A. Dawson (1994). Expression cloning and characterization of the hamster ileal sodium-dependent bile acid transporter. *J. Biol. Chem.* 269: 1340-1347.

Xiao, Q., J. Elovson and V.N. Schumaker (2000). Rat McA-RH7777 cells efficiently assemble rat apolipoprotein B-48 or larger fragments into VLDL but not human apolipoprotein B of any size. *J. Lipid Res.* 241: 116-125.

Xu, G., B.L. Shneider, S. Shefer, L.B. Nguyen, A.K. Batta, *et al.* (2000). Ileal bile acid transport regulates bile acid pool, synthesis, and plasma cholesterol levels differently in cholesterol-fed rats and rabbits. *J. Lipid Res.* 41: 298-304.

Chapter 2: General Methods

2.1 Chemicals

[^{3}H]-taurocholic acid (2.6 Ci/mmol), [^{32}P]-α-dCTP (3000 Ci/mmol), and [^{32}P]-γ-ATP (3000 Ci/mmol) were purchased from Amersham Corporation (Baie d'Urfé, PQ). Cell culture media, fetal bovine serum (FBS), horse serum (HS), calf serum (CS) and other media supplements were obtained from Life Technologies (Burlington, ON). Bile acids were obtained from Sigma-Aldrich Chemical Co (St. Louis, MO) and Calbiochem (San Diego, CA). Other chemicals used were of analytical grade and obtained from various commercial sources. For composition of commonly used buffers, please refer to Appendix I.

2.2 Cell culture

The permanent mammalian cell lines used in this thesis were maintained using standard tissue culture techniques (Freshney 1994). All cell lines were adherent and were cultured in tissue culture dishes of different sizes (35 to 100 mm). Cells were maintained at 37 °C and 5% CO_2 and routinely passaged every second day. Cells were passaged by washing with PBS, treating briefly with a 0.25% trypsin solution (Life Technologies, Burlington, ON) and pipetting up/down several times in culture medium containing serum. Cell number was determined by use of a hemocytometer and approximately 5×10^5 cells were plated in 100 mm dishes. The rat hepatoma cell line McArdle RH-7777 and its derivatives were cultured in Dulbecco's modified Eagle's medium (DMEM) containing 4500 mg/L glucose, 10% FBS, 10% CS or 10% HS, without sodium pyruvate. Chinese hamster ovary (CHO) cells and derivatives of this cell line were cultured in Ham's F12 media containing 10% FBS. For frozen storage, cells were collected and resuspended in medium containing

10% FBS and 10% DMSO. Cells were aliquoted into 1.5 ml cryovials and placed at -70 °C in an isopropanol cooler (Stratagene, La Jolla, CA). After 16 h, vials were transferred to liquid nitrogen for long term storage.

R1 embryonic stem (ES) cells (Nagy *et al.* 1993) were routinely cultured in DMEM containing 4500 mg/L glucose, 2 mM glutamine, 15% FCS, 100 µM β-mercaptoethanol, and 1000 U/ml of leukemia inhibitory factor, 1 mM sodium pyruvate and 0.1 mM non-essential amino acids (Life Technologies, Burlington, ON) and plated on γ-irradiated Neo^r primary murine embryonic fibroblasts (Thomas *et al.* 1987). For frozen storage, ES cells were collected and resuspended in ES medium containing 20% FCS and 10% DMSO. Cells were aliquoted into 1.5 ml cryovials and placed at -70 °C in an isopropanol cooler (Stratagene, La Jolla, CA). After 16 h, vials were transferred to liquid nitrogen for long term storage.

2.3 Molecular biology

Standard molecular biology techniques were used for DNA transformation of bacteria, isolation of plasmid DNA from bacteria, endonuclease digestion of plasmid DNA, ligation of plasmid constructs, DNA amplification, and for generation of radiolabeled DNA probes (Maniatis *et al.* 1989; Ausubel *et al.* 1989).

2.4 RNA blot analysis

Total RNA was isolated using a one step guanidinium thiocynate method (Chomczynski *et al.* 1987) and separated by electrophoresis on a 1% agarose-formaldehyde gel (Maniatis *et al.* 1989). The RNA was transferred onto a Hybond-N nylon membrane, cross-linked using a Stratalinker device (Stratagene, La Jolla, Ca.) and probed with a radiolabeled cDNA probe. The probe was hybridized in buffer containing 0.25 M sodium phosphate (pH 7.2), 7% SDS, 0.1% sodium pyrophosphate and 2 mM EDTA for 16 h at 60°C. Membranes were washed twice with 2X SSC containing 0.1% SDS for 15 min each at room temperature (RT), twice with 1X SSC/0.1% SDS for 15 min each at RT, and once with 0.5 X SSC/ 0.1% SDS for 15 min at 60°C. Membranes were then exposed to x-ray film or a phospho-imaging screen. Phospho-imaging screens were scanned in a Fuji-X Bas 1000 phosphorimager. For re-probing, membranes were stripped of bound probe by incubating membranes in boiling water containing in 0.1% SDS until the solution cooled to RT.

2.5 DNA blot analysis

Tissue culture cells were grown to 80% confluency for isolation of genomic DNA. Cells were washed once with PBS and lysed directly in TBS containing 0.5% sarkosyl and 1 mg/ml proteinase K. For preparation of genomic DNA from tail biopsies, small pieces of mouse tails (0.5 to 1 cm) were incubated in 100 mM NaCl, 20 mM Tris (pH 7.5), 50 mM EDTA, 0.5% SDS and 1 mg/ml proteinase K. After digestion (~16 h) of cellular proteins at 55 °C, DNA was sequentially extracted with an equal volume of buffered-saturated phenol, phenol/chloroform (1:1, v/v), and chloroform. The DNA was precipitated with either 1 vol of isopropanol or 2 vol of 100% ethanol with 0.3 M sodium acetate. After a 70% ethanol wash, the DNA was resuspended in 200 µl of TE buffer. Typically, 5 to 10 µg of genomic DNA were digested for 16 h at 37 °C with appropriate restriction endonucleases. Digested DNA was precipitated, washed with 70% ethanol, resuspended in TE, electrophoresed in a 0.8% agarose gel, and transferred onto a Hybond-N membrane (Amersham Corp., Baie d'Urfé, PQ) using standard techniques (Maniatis *et al.* 1989). DNA membranes were hybridized with radiolabeled cDNA probes as detailed for RNA membranes (see Section 2.3)

2.6 Bile acid uptake assays

Cells were grown on 35 mm tissue culture plates to approximately 70% confluency for bile acid uptake assays. The cell culture medium was removed and replaced with 1 ml of DMEM containing 0.2% bovine serum albumin (BSA), 5 nM of [^{3}H]-Taurocholic acid (TCA) (2.6 mCi/mmol), and unlabeled TCA. The total concentration of TCA used depended on the type of assay (concentration dependence, 0-400 μM; all other assays, 25 μM). Cells were incubated at 37 °C and then the assay was terminated by aspirating the assay medium. Cells were immediately washed four times with ice cold PBS containing 0.2% BSA and 1 mM unlabeled TCA, and then rinsed once with cold PBS. Cells were dried and dissolved in 1 ml of 0.1 N NaOH solution. The amount of radioactivity in half of the sample was determined by liquid scintillation spectrometry and the amount of protein in the remaining half was determined using the Bradford method (Bradford 1976). All activity assay measurements were done in triplicate and repeated at least twice. In time course assays, the amount of radioactivity associated with the cells at time zero was measured by adding the assay solution and immediately removing it by aspiration. The amount of radioactivity incorporated by these cells was subtracted from that determined for other time intervals. For bile acid efflux assays, the intracellular pool of bile acids was labeled with [^{3}H]-TCA for 20 - 30 min. The cells were washed as above and then incubated at 37°C with DMEM containing 0.2% BSA, and 1 mM unlabeled TCA.

2.7 Immunoblot analysis

In preparation for immunoblotting of proteins, cells or tissues were processed as detailed in individual chapters. Protein concentration was determined by the method Bradford (Bradford 1976) using BSA as standard. Protein samples were then resolved by SDS polyacrylamide gel electrophoresis (PAGE) by the method of Laemmeli (Laemmeli 1970) and transferred onto a PVDF (Millipore Ltd., Nepean, ON) membrane by electroblotting. Membranes were typically blocked 1 to 16 h with 5% skimmed milk powder in PBS containing 0.5% Tween 20 (PBS-T), washed several times with PBS-T, and incubated for 1 h with diluted primary antiserum in PBS-T with 5% skimmed milk powder. Following primary antibody incubation, membranes were washed again with PBS-T and incubated with appropriate horseradish peroxidase-conjugated secondary antiserum for 1 h. Membranes were extensively washed with PBS-T before chemiluminescent detection using the ECL detection system (Amersham Corp., Baie d'Urfé, PQ)

2.8 Lactate dehydrogenase (LDH) assays

To determine the amount of LDH released from cells treated with bile acids, Cells (10^4 per well) were plated on 24 well multiwell plate 16 h prior to the addition of bile acids. The cells were washed with PBS and then incubated in medium (Ham's F12 or DMEM) containing 100 μM bile acids. The media was collected and adjusted to 0.1% Triton X-100. Cells left on the dish were then dissolved in medium (Ham's F12 or DMEM) containing 0.1% Triton X-100. LDH activities in both the cell lysates and media were measured as described by Berstein and Everse (Berstein *et al.* 1975).

2.9 Transfection experiments

Cells were grown to 60% confluency prior to commencement of DNA transfection experiments. DNA was transfected into cells using either calcium phosphate/DNA co-precipitation, lipofectamine reagent (Life Technologies, Burlington, ON), or electroporation. Please refer to individual chapters for the experimental details of each of these methods. To generate stable transfectants, cells were allowed to recover for 24 h before beginning selection with antibiotics for an additional 10 days. For transient transfections, cells were harvested after 48 h post-transfection.

2.10 Plotting and Statistics

Excel 97 (Microsoft Corp.) was used for basic statistical analysis. Student's t- and F-test were used for comparison of data from different experimental conditions (Armitage *et al.* 1994). P values of < 0.05 were judged to be significant. SigmaPlot v. 5 (SPSS Inc.) was employed to generate linear regression lines and other plots.

2.11 REFERENCES

Armitage, P. and G.E. Berry (1994). Statistical methods in Medical research. *Blackwell Scientific publications, Oxford* .

Ausubel, F. M., R. B. Robert, E. Kingston, D. D. Moore, G. Seidman, K. Struhl, and J.A. Smith (1989). Current protocols in molecular biology, red book, Wiley & Sons.

Berstein, L. and J. Everse (1975). Determination of the isozyme levels of lactate dehydrogenase. *Methods Enzymol.* 41: 47-53.

Bradford, M. (1976). A rapid and sensitive method for the quantitation of microgram quantities of protein utilizing the principle of protein dye binding. *Anal. Biochem.* 72: 1248-254.

Chomczynski, P. and N. Sacchi (1987). Single-step method of RNA isolation by acid guanidinium thiocyanate-phenol-chloroform extraction. *Anal. Biochem.* 162: 156-159.

Freshney, R.I. (1994) Culture of animal cells : a manual of basic technique (3rd ed.). *New York : Wiley-Liss.*

Laemmeli, U. (1970). Cleavage of structural proteins during the assembly of the head of bacteriophage T4. *Nature* 227: 680-685.

Nagy, A., J. Rossant, R. Nagy, W. Abramow-Newerly and J.C. Roder (1993). Derivation of completely cell culture-derived mice from early-passage embryonic stem cells. *Proc. Natl. Acad. Sci. USA* 90: 8424-8428.

Maniatis, T., E. Fitch and J. Sambrook (1989). Molecular cloning, a laboratory manual. *Cold Spring Harbor, New York: Cold Spring Harbor Laboratory Press.*

Thomas, K.R. and M.R. Capecchi (1987). Site-directed mutagenesis by gene targeting in mouse embryo-derived stem cells. *Cell* 51(3): 503-12.

Chapter 3: Reconstitution of Bile Acid Transport in the Rat Hepatoma McArdle RH-7777 Cell Line

A version of this chapter has been published in Hepatology (1996) 24, 201-206.

3.1 Introduction

As detailed in Section 1.2.3.1 of this thesis, the liver reclaims bile acids from portal circulation by sodium-dependent and -independent bile acid transport systems. Hepatocellular membrane vesicles and isolated hepatocytes have been used to characterize hepatic basolateral bile acid transport (Schwarz *et al.* 1975; Van Dyke *et al.* 1982; Meier *et al.* 1984). In primary hepatocytes, active bile acid transport activity is quickly lost and is associated with an overall decline of liver specific functions (Follman *et al.* 1990). In liver-derived cell lines such as the rat and human hepatoma cell lines (e.g. McArdle RH-7777 and HepG2, respectively), active bile acid transport activity is not detectable (Von Dippe *et al.* 1983; Von Dippe *et al.* 1990; Marchegiano *et al.* 1992). Thus, these hepatoma cell lines are not appropriate models to study bile acid transport or the effects of bile acids on hepatocyte function. When the experiments presented in this chapter were carried out, the exact contribution of each sinusoidal transport protein (e.g. Ntcp, oatp, LST-1, mEH) to the overall hepatic recovery of bile acids was unclear. However, it is now generally accepted that sodium-dependent uptake constitutes the primary mechanism of bile acid recovery from plasma (Frimmer *et al.* 1982; Hagenbuch 1997). In the present chapter, I describe experiments to re-establish active bile acid transport in the hepatoma cell line McArdle RH-7777.

3.2 METHODS

3.2.1 Stable expression of Ntcp in McArdle RH-7777 cells

Dr. Jean Shapiro (University of British Columbia, Vancouver, BC) constructed a pCMV-Ntcp expression vector while on sabbatical in Dr. L. Agellon's laboratory. The cDNA encoding full length rat Ntcp was a kind gift of Dr. P. Meier (University Hospital, Zürich, Switzerland). The pCMV-Ntcp was co-transfected with pWLneo, which confers neomycin resistance, into the rat hepatoma McArdle RH-7777 cell line using DNA: calcium phosphate co-precipitation (Graham *et al.* 1973). This cell line was ideal for the stable expression of Ntcp because of its ease of handling, liver origin, and several liver-like characteristics (Becker *et al.* 1976; Tanabe *et al.* 1989). After 48 h, the medium was replaced with medium containing the antibiotic G418 (400 μg/ml) to generate stable transfectants. Surviving colonies were expanded and screened for incorporation of the Ntcp expression plasmid by *in vitro* DNA amplification using primers directed to amplify a 344 bp fragment of the 3' translated region of the Ntcp cDNA. Clones which produced the expected 344 bp fragment were assayed for the ability to incorporate radiolabelled TCA from the culture media.

3.2.2 Primary culture of hepatocytes

Rat hepatocytes were isolated by perfusion with collagenase IV and trypsin inhibitor as previously described (Houweling *et al.* 1994). Viability of isolated hepatocytes was greater than 90% as determined by trypan blue exclusion. Single cells were suspended in DMEM with 10% FBS, 100 μg/ml streptomycin, 100 U/ml penicillin, and in the presence or absence of 0.1 μM each of insulin and dexamethasone, and plated on 35 mm gelatin coated tissue culture plates. Tissue culture plates (35 mm) were coated with gelatin by applying 1 ml of a sterile 0.1% gelatin for 5 min, and then rinsed with PBS. The hepatocytes were plated immediately after isolation and Ntcp activity was assayed 4 h and 24 h after plating (see below). Cell culture media was replaced every second day. Cells were grown on 35 mm tissue culture plates to approximately 70% confluency for Ntcp assays.

3.2.3 Bile acid uptake assays.

Please refer to Chapter 2 for general methodologies including bile acid uptake assays (Section 2.6) and culturing of various cell lines.

3.3 RESULTS

3.3.1 Expression of Ntcp in McArdle RH-7777 cells

The Ntcp expression vector was constructed by inserting a *Sal* I fragment of the cDNA containing the entire Ntcp translated region downstream of the human cytomegalovirus (CMV) promoter and upstream of the 3' region of the human growth hormone gene. The CMV promoter was selected for its high activity in mammalian cells (Anderson *et al.* 1988). The expected size of the recombinant Ntcp message encoded by the vector is ≈1.6 kb. This size is clearly distinguishable from that of the native rat Ntcp mRNA whose size is ≈1.7 kb (Hagenbuch *et al.* 1991).

Of the 48 colonies initially isolated as G418 resistant, 15 clones incorporated the pCMV-Ntcp expression vector. These clones were assayed for TCA uptake activity and clones expressing Ntcp activity were selected. These clones, designated McNtcp.1, McNtcp.18, and McNtcp.24, showed low, intermediate, and high levels, respectively, of taurocholic acid transport activity. To determine the extent of the reconstituted bile acid transport activity in McNtcp clones, [^{3}H]-TCA uptake was compared to the parental McArdle RH-7777 cells, isolated hepatocytes, and other permanent cell lines. As shown in Fig. 3-1, transport activity in parental cells or HepG2 did not differ significantly compared to CHO cells, which has no active capacity to take up bile acids. This observation confirmed the loss of active bile acid transport activity in the hepatoma cell lines. On the other hand, selected clones showed activities ranging from 26 to 117% of that observed in primary hepatocytes (Fig. 3-1). RNA blot analysis of total RNA isolated from McNtcp clones confirmed the existence of the recombinant Ntcp mRNA (Fig. 3-2). The recombinant Ntcp message produced in McNtcp corresponded to the predicted size and was slightly smaller than the native Ntcp message (lanes 1 and 3, Fig. 3-2). The

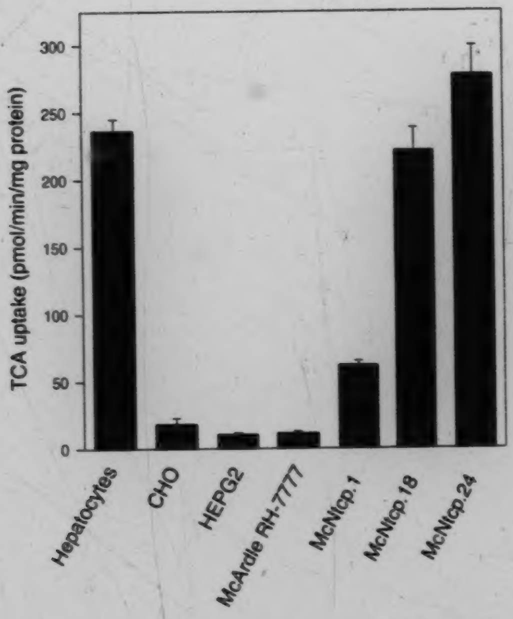

Fig. 3-1 Uptake of TCA from the culture media by McNtcp clones, hepatoma cells and primary hepatocytes (4 h after plating). Cells were incubated in assay solution containing 25 µM TCA for 20 min. Values shown are mean ± S.E. (n=3). Human hepatoma HepG2 cells were cultivated in DMEM with 10% FBS, 1 mM sodium pyruvate, 100 µg/ml streptomycin, 100 U/ml penicillin.

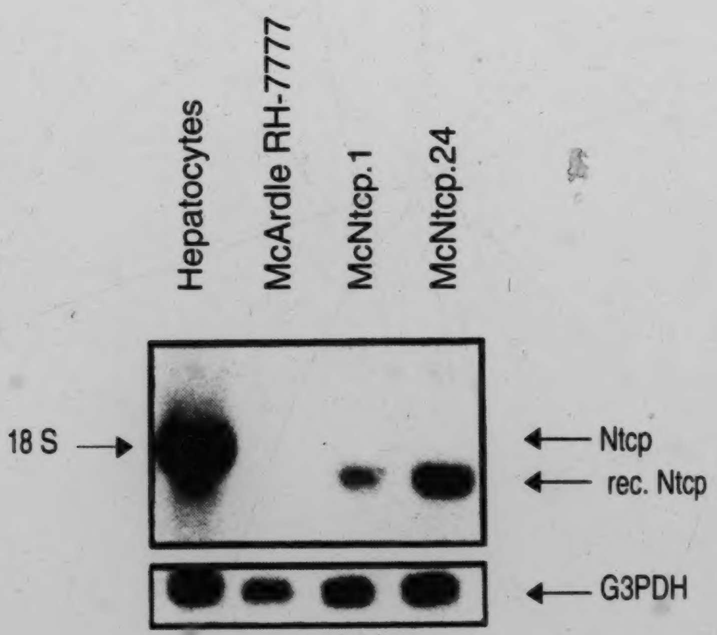

Fig. 3-2. Detection of the native and recombinant Ntcp mRNA in hepatocytes, McArdle RH-7777 cells and McNtcp cells. RNA blot analysis was done on total RNA preparations using a rat Ntcp cDNA probe. The native and recombinant Ntcp mRNA are approximately 1.7 kb and 1.6 kb, respectively. The blot was stripped and re-probed with a mouse G3PDH cDNA (bottom panel). The position of the 18S ribosomal RNA is indicated on the left hand side (arrow).

lack of any detectable Ntcp message in untransfected cells most likely accounts for the absence of active bile acid uptake in the parental line. The detection of glyceraldehyde-3-phosphate dehydrogenase (G3PDH) message in total RNA of these cells indicated that the RNA preparations were intact (Fig. 3-2).

3.3.2 Characterization of McNtcp clones.

Concentration-dependent uptake of TCA was determined in McNtcp clones and primary hepatocytes. In McNtcp clones, bile acid transport was saturated at 25 μM, similar to that observed in primary hepatocytes. The apparent K_m of TCA transport into isolated hepatocytes and the McNtcp clones are also in agreement within experimental error (Fig. 3-3). The V_{max} of bile acid transport varied among clones and is correlated with the abundance of recombinant Ntcp mRNA and the level of the expressed protein (Fig. 3-4). The recombinant Ntcp mRNA abundance is most likely determined by the copy number of the integrated transgene (see Fig. 3-5). Insulin and glucocorticoids are commonly used in primary cultures of hepatocytes to suppress the loss of liver specific function (Laishes *et al.* 1976a; Laishes *et al.* 1976b). Ntcp function in primary hepatocytes cultured in the presence or absence of these hormones was investigated by measuring TCA uptake activity. The presence of these hormones in the culture media of primary cells had no appreciable effect on the apparent K_m of Ntcp, although the V_{max} was higher by 178% in isolated hepatocytes (Fig. 3-3). The time course of bile acid accumulation in McNtcp cells was also compared with primary hepatocytes under the same assay conditions. Uptake of TCA in isolated rat hepatocytes was rapid and reached equilibrium within 20 min (Fig. 3-6). However, the activity decreased significantly (73%) after 24 h of plating. The loss of transport activity was paralleled by the decay of Ntcp mRNA abundance (Fig. 3-6A, inset) (Liang *et al.* 1993). Therefore,

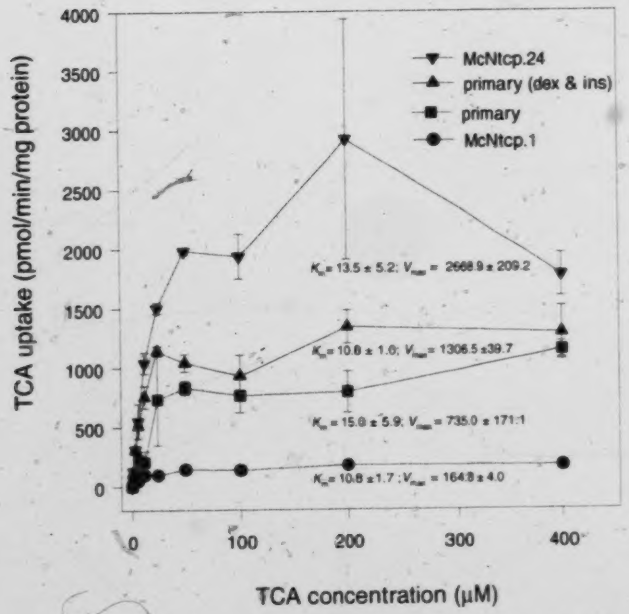

Fig. 3-3 Concentration dependent uptake of TCA. McNtcp cells and primary hepatocytes (4 h after plating) were cultivated in the presence or absence of 0.1 µM dexamethasone and insulin. Uptake velocities were determined at 4 min, in the linear portion of the uptake curve. Values shown are mean ± S.E. (n=3). Kinetic parameters (K_m [µmol/L]; V_{max} [pmol/min/ mg protein]) shown are the average of values calculated using the Lineweaver-Burk, Woolf, and Eidee-Hofstee equations.

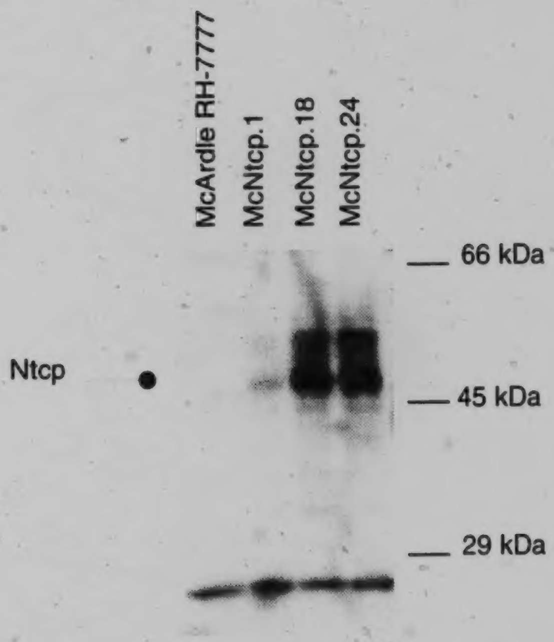

Fig. 3-4. Detection of Ntcp in membrane extracts from McNtcp cells. Membrane extracts were prepared as described in Cheema *et al.* 1997, fractionated by SDS PAGE, and transferred to a PVDF membrane. An approximately 48-kDa band (depicted by the bolt) is detectable using Ntcp antiserum in extracts from McNtcp cells. This band is absent in extracts from McArdle RH-7777 cells.

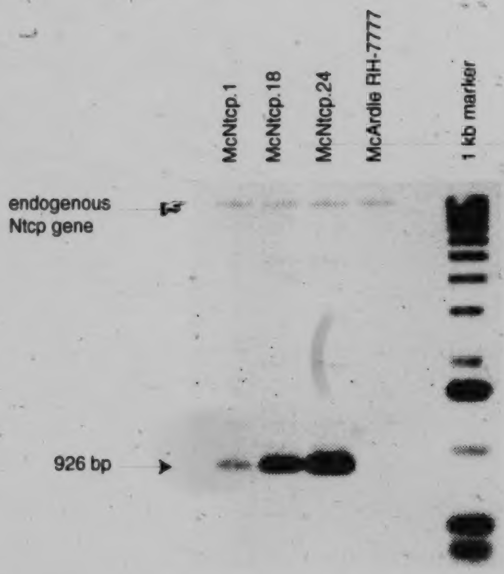

Fig. 3-5. Detection of the Ntcp transgene in genomic DNA from McNtcp and McArdle RH-7777 cells. Genomic DNA (10 µg) was digested with *Eco RI*, fractionated by agarose gel electrophoresis, blotted onto a nylon filter and hybridized with an Ntcp cDNA probe. A 0.9 kb fragment (depicted by the arrow) corresponding to the Ntcp transgene can be easily detectable in McNtcp lanes but not in the McArdle RH-7777 lane. The intensity of the 0.9 kb band is consistent with the number of ntcp transgenes incorporated into the genome of the various McNtcp clones. Note the detection of the endogenous Ntcp gene in all DNA samples (depicted by the hand), demonstrating an equivalent amount of DNA in each lane.

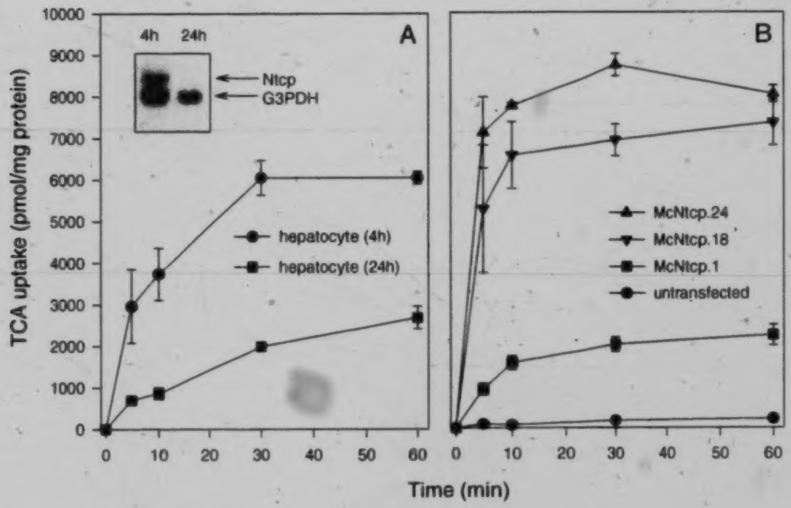

Fig. 3-6. Accumulation of TCA in McNtcp cells and primary hepatocytes. Hepatocytes were cultured in the presence of 0.1 μM dexamethasone and insulin. The amount of taurocholic acid accumulated by primary hepatocyte assayed at 4 h and 24 h after plating reached steady state levels. A similar pattern was observed with McNtcp cells (**B**). Values shown are mean ± S.E. (n=3). The inset in Panel **A** depicts the abundance of the ntcp and G3PDH mRNA in hepatocytes.

the presence of dexamethasone and insulin in the culture medium of primary hepatocytes did not prevent the reduction of transporter activity at 24 h.

The time course of TCA accumulation in McNtcp clones was similar to that in primary hepatocytes (Fig. 3-6B), which reached steady state after 10 min of TCA addition. The maximum level of TCA accumulated in McNtcp cells correlated with Ntcp activity. It is possible that the intracellular concentration of bile acid regulates Ntcp function. Alternatively, the incorporated bile acids may be secreted from the cells. Previous studies show that cultured primary hepatocytes are capable of secreting bile acids (Schwarz *et al.* 1976; Fleischer *et al.* 1989).

To address the possibility that bile acids are secreted by McNtcp cells, the intracellular pool of bile acids in McNtcp cells was equilibrated with radiolabeled TCA, and then the efflux of this pool was followed. As illustrated in Fig. 3-7, the appearance of radiolabeled TCA in the media was rapid. Most of the radioactivity was secreted into the culture medium within the first 10 min after the removal of labeled substrate. This occurred concomitant with the reduction of radioactivity associated with cellular protein. Since at least 95% of cells remained viable throughout the assay, as indicated by trypan blue exclusion, the assay conditions did not have a toxic effect on the cells. The time frame of radiolabeled TCA efflux from cells coincided with the time required for TCA uptake to reach steady state (Fig. 3-6A). A similar pattern of TCA efflux was observed in primary hepatocytes (Fig. 3-7). The bile acid export pump (BSEP) could mediate bile acid efflux from McNtcp cells. However, I could not detect BSEP in McNtcp cells (Fig. 3-8), indicating that this protein does not mediate bile acid efflux from McNtcp cells.

To investigate the specificity of recombinant Ntcp function in McNtcp cells, TCA uptake was measured in the presence of different bile acid species. As expected, conjugated bile acids effectively competed for the uptake of labeled TCA in tested McNtcp clones. Taurodeoxycholic (TDCA) and taurochenodeoxycholic ac-

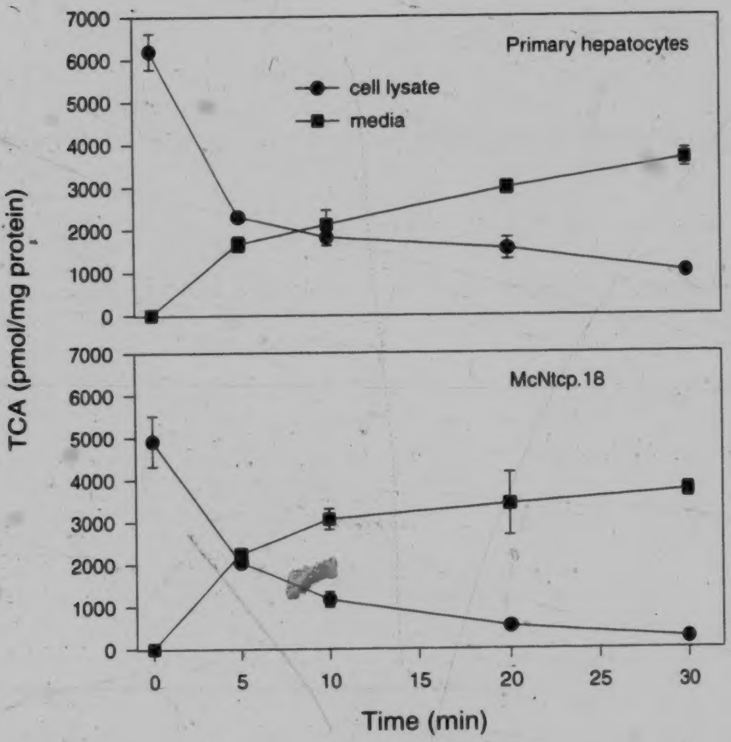

Fig. 3-7. Efflux of TCA from hepatocytes and McNtcp cells. Cells were grown in the absence of dexamethasone and insulin, and were incubated with radiolabelled TCA for 30 min to label the intracellular pool of bile acids. The amount of radioactivity released into the media and remaining in the cells was determined as described in Chapter 2.

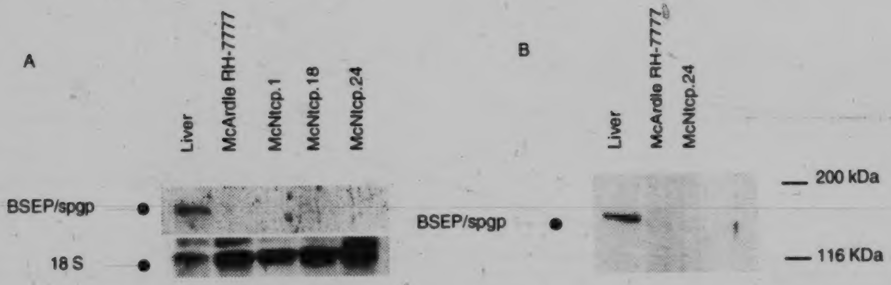

Fig. 3-8. Detection of BSEP/spgp in McNtcp cells. **A**. RNA blotting of total RNA (10 µg) from liver, various McNtcp, and McArdle RH-7777 cells using an BSEP/spgp cDNA probe. A 5 kb spgp transcript was detected in Liver RNA but not in RNA from McNtcp or the parental cell line. **B**. Membrane extracts from liver, McArdle RH-7777, and McNtcp.24 cells were prepared as described in Gerloff *et al.* 1998. Membrane proteins (80 µg) were fractionated on a 5% acrylamide gel and transferred onto a PVDF membrane. A 160-kDa band can be easily detected in liver extracts using an spgp antibody. The same band is not evident in extracts from McNtcp.24 or McArdle RH-7777 cells. Both BSEP/spgp cDNA and antibody were kind gifts of Dr. J. Schuetz (St. Judes Children's Hospital, Memphis, TN).

ids (TCDCA) significantly reduced TCA uptake by 74-78%, 80-90% respectively (Fig. 3-9). Deoxycholic acid (DCA) had a minor but significant effect on the uptake of TCA (65-83% of control). Cholic acid (CA) had no effect on TCA uptake (Fig. 3-9). Later studies have shown that Ntcp does transport unconjugated bile acids, but with much lower affinity than amidated bile acids (Schroeder *et al.* 1998 ; Kouzuki *et al.* 1998). The reduced level of competition that was observed with uncongujated bile acids for TCA uptake in McNtcp cells is consistent with these studies.

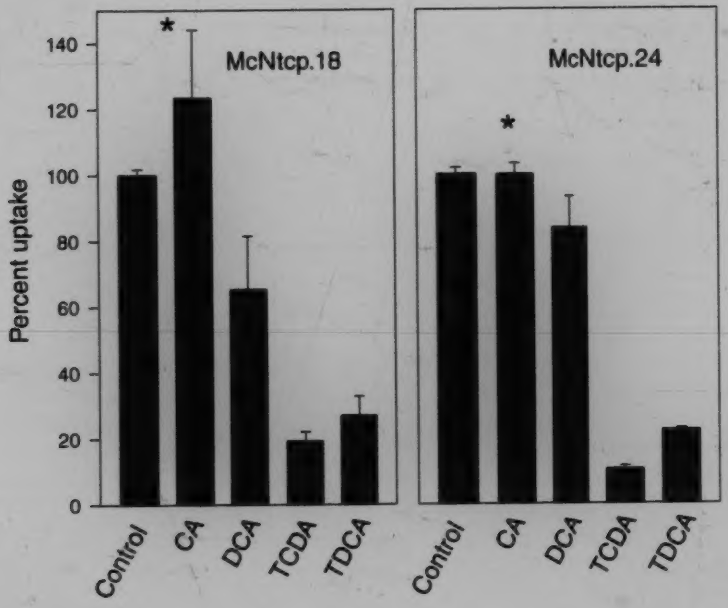

Fig. 3-9. Inhibition of TCA uptake in McNtcp cells by different bile acids. McNtcp cells were assayed for uptake of taurocholic acid (25 µM) in the presence of 100 µM CA, DCA, TCDC, or TDCA acids. Uptake of TCA by cells in the absence of other bile acid species is expressed as 100% (control). Values shown are mean percent of control ± S.E. (n=3). Differences in comparison to control were evaluated using Student's t-test. The asterisk indicates no significant difference.

3.4 DISCUSSION

Primary hepatocytes are not ideal for long term studies due to the decline of liver specific functions. Maintenance of liver specific functions in cultured hepatocytes has been an active area of investigation over the past few decades and a number of significant developments have helped improve the preservation of these functions. For instance, inclusion of dexamethasone and insulin in the culture media of primary hepatocytes appears to help stabilize liver specific functions (Laishes *et al.* 1976a; Laishes *et al.* 1976b). As demonstrated in this chapter, maintenance of primary hepatocytes in the presence of these hormones did not prevent the loss of active bile acid transport activity after 24 h of plating. The loss of activity occurred in parallel with the disappearance of Ntcp mRNA, consistent with an earlier report (Liang *et al.* 1993). The presence of these hormones had no apparent effect on Ntcp function (i.e., no changes in K_m). However, the lower V_{max} value observed in primary hepatocytes cultured in the absence of these hormones suggests that the number of transporter molecules was reduced.

An Ntcp expression vector was stably expressed into McArdle RH-7777 cells. Several clones with different Ntcp activity were isolated and established. The apparent K_m of TCA uptake in these cells ranged from 10.8 ± 1.0 μM to 15.0 ± 5.7 μM, and agreed with that measured in primary hepatocytes. The V_{max} of transport in McNtcp varied from 0.16 to 2.67 nmoles/min/mg protein. This correlated with the abundance of the recombinant Ntcp mRNA and level of the protein (see Fig. 3-2 and 3-4), suggesting that mRNA abundance determined the V_{max} of transport. TCA transport activity in McNtcp cells was much higher than that observed when Ntcp was transiently expressed in COS-7 cells (Boyer *et al.* 1994). Indeed, the highest V_{max} values obtained in McNtcp.24 clones are similar to those reported for freshly isolated hepatocytes (Follman *et al.* 1990). In rat primary hepatocytes and hepatocellular membrane vesicles, a wide ranged of K_m values (15 to 56 μM) have been reported (Schwarz *et al.* 1975; Van Dyke *et al.* 1982; Meier *et al.* 1984; Liang *et al.* 1993). In *Xenopus* oocytes (Hagenbuch *et al.* 1991) and COS cells (Boyer *et al.* 1994) transiently expressing Ntcp, K_m values of 29 and 25 μM have also been observed. Thus, the kinetic parameters of bile acid uptake in McNtcp cells are consistent with previous reports. Although there may be other sodium dependent transporters in the basolateral membrane of hepatocytes (in addition to Ntcp) (Ananthanarayanan *et al.* 1994), the expression of Ntcp alone in McNtcp cells appears to be sufficient to mimic the bile acid transport activity found in freshly isolated hepatocytes.

A major finding in this study is that TCA accumulation in McNtcp cells reached steady state level in a manner similar to that observed in primary hepatocytes. Furthermore, the amount of bile acids accumulated was determined by the absolute levels of bile acid uptake and secretion. The secretion of TCA from McNtcp cells was rapid (Fig. 3-7) and consistent with the notion that the majority of the accumulated intracellular bile acid pool in rat hepatocytes is available for efflux (Stacey 1986; Kuhn *et al.* 1988). Currently, the mechanisms which mediate intracellular bile acid transport in primary hepatocytes (or in McNtcp cells) remain poorly understood. Nevertheless, it would appear that the bile acid secretory pathway remains intact in McNtcp cells. It is interesting that both cultured hepatocytes and this hepatoma cell line retained the ability to secrete bile acids in spite of the loss of active bile acid transport activity. In addition, the bile acid export pump is not detected in McNtcp or its parental cell line (see Fig. 3-8). Secretion of bile acids by McNtcp.24 cells may well use a pathway with broad specificity.

Recombinant Ntcp expressed in McArdle RH-7777 cells appears to function in a manner similar to the native transporter in primary hepatocytes. For example, Ntcp in these cells exhibit the *cis*-inhibition pattern as has been shown for the sodium dependent bile acid transport system in isolated hepatocytes and basolateral hepatocellular membrane vesicles (Frimmer *et al.* 1982; Zimmerli *et al.* 1989). In McNtcp cells, conjugated bile acids such TCDCA and TDCA were highly effective at inhibiting the uptake of TCA, whereas DCA and CA had little or no effect. This result is contrary to what has been found with primary hepatocytes (Frimmer *et al.* 1982; Zimmerli *et al.* 1989). However, the observed discrepancy may depend on the concentrations of TCA and the competing bile acids that were used in these studies.

Ntcp activity is rapidly lost in cultured hepatocytes and is virtually absent in the commonly used hepatoma cell lines (Von Dippe *et al.* 1983; Follman *et al.* 1990; Von Dippe *et al.* 1990; Marchegiano *et al.* 1992). Ntcp mRNA is not detectable in McArdle RH-7777 and HepG2 hepatoma cells (present study and Boyer *et al.* 1993), and likely explains the absence of active bile acid transport activity in these cells. Given the negligible uptake of bile acids by these cells, they are not appropriate model to address the role of bile acids in regulating liver function. For instance, TCA inhibits cholesterol 7α-hydroxylase gene expression in rodents (Pandak *et al.* 1994; Ramirez *et al.* 1994) but has no appreciable effect in HepG2 cells (Chiang *et al.* 1994; Taniguchi *et al.* 1994). The amount of TCA that can accumulate in HepG2 cells may be insufficient to cause any effect. Given the limitations of these models, I endeavored to develop a closer approximation of hepatocyte function by reconstituting bile acid active transport in the McArdle RH-7777 hepatoma cell line.

3.5 REFERENCES

Ananthanarayanan, M., O.C. Ng, J.L. Boyer and F.J. Suchy (1994). Characterization of cloned rat liver Na(+)-bile acid cotransporter using peptide and fusion protein antibodies. *Am. J. Physiol.* 267: G637-643.

Anderson, S., D.N. Davis, H. Dahlback, H. Jornvall and D.W. Russell (1988). Cloning structure and expression of the mitochondrial cytochrome P-450 sterol 26-hydroxylase a bile acid biosynthetic enzyme. *J. Biol. Chem.* 264: 822-829.

Becker, J.E., B. deNechaud and V.R. Potter (1976). Two new rat hepatoma cell lines for studying the unbalanced blocked ontogeny hypothesis. *In* Oncogenic gene expression. W.H. Fishman and S. Sell, eds.: 259-270.

Boyer, J.L., B. Hagenbuch, M. Ananthanarayanan, F. Suchy, B. Stieger, *et al.* (1993). Phylogenic and ontogenic expression of hepatocellular bile acid transport. *Proc. Natl. Acad. Sci. USA.* 90: 435-438.

Boyer, J.L., O.C. Ng, M. Ananthanarayanan, A.F. Hofmann, C.D. Schteingart, *et al.* (1994). Expression and characterization of a functional rat liver Na+ bile acid cotransport system in Cos-7 cells. *Am. J. Physiol.* 266(29): G382-G387.

Cheema, S.K., D. Cikaluk and L.B. Agellon (1997). Dietary fats modulate the regulatory potential of dietary cholesterol on cholesterol 7α-hydroxylase gene expression. *J. Lipid Res.* 38: 315-23.

Chiang, J.Y.L. and D. Stroup (1994). Identification and characterization of a putative bile acid-responsive element in cholesterol 7α-hydroxylase gene. *J. Biol. Chem.* 269: 17502-17507.

Fleischer, B., F.A. Simion and S. Fleischer (1989). Binding and uptake of taurocholate in subcellular organelles in Hepatic Transport of Organic Substances. In: Hepatic transport of organic substances. Petzinger E, R.K.H. Kinne, H. Sies, eds. *Heidelberg: Springer-Verlag, Berlin,* : 240-256.

Follman, W., E. Petzinger and R.K. Kinne (1990). Alterations of bile acid and bumetamide uptake during culturing of rat hepatocytes. *Am. J. Physiol.* 258(27): C700-C712.

Frimmer, M. and K. Ziegler (1982). The transport of bile acids in liver cells. *Biochim. Biophys. Acta.* 947: 75-99.

Gerloff, T., B. Stieger, B. Hagenbuch, J. Madon, L. Landmann, *et al.* (1998). The sister of P-glycoprotein represents the canalicular bile salt export pump of mammalian liver. *J. Biol. Chem.* 273: 10046-10050.

Graham, F.L. and A.J. Van der Eb (1973). A new technique for the assay of infectivity of human adenovirus 5' DNA. *Virology* 52: 456-467.

Hagenbuch, B. (1997). Molecular properties of hepatic uptake systems for bile acids and organic anions. *J. Membrane Biol.* 160: 1-8.

Hagenbuch, B., B. Stieger, H. Foguet, H. Lubbert and P. Meier (1991). Functional expression cloning and characterization of the hepatocyte Na+/bile acid co-transport system. *Proc. Natl. Acad. Sci. USA.* 88: 10629-10633.

Houweling, M., H. Jamil, G.M. Hatch and D.E. Vance (1994). Dephosphorylation of ctp-phosphocholine cytidylyltransferase is not required for binding to membranes. *J. Biol. Chem.* 269: 7544-7551.

Kouzuki, H., H. Suzuki, K. Ito, R. Ohashi and Y. Sugiyama (1998). Contribution of sodium taurocholate co-transporting polypeptide to the uptake of its possible substrates into rat hepatocytes. *J. Pharma. Exp. Therap.* 286: 1043-1050.

Kuhn, W. and D. Gewirtz (1988). A stimulation of taurocholate and glycocholate efflux from the rat hepatocytes by arginine vasopressin. *Am. J. Physiol.* 254(17): G732-G740.

Laishes, B.A. and G.M. Williams (1976a). Conditions affecting primary cell cultures of functional adult rat hepatocytes. I. The effects of insulin. *In vitro Cell. Dev. Biol.* 12: 521-532.

Laishes, B.A. and G.M. Williams (1976b). Conditions affecting primary cell cultures of functional adult rat hepatocytes. II. The effects of dexamethasone. *In vitro Cell. Dev. Biol.* 12: 821-832.

Liang, D., B. Hagenbuch, B. Stieger and P.J. Meier (1993). Parallel decrease of Na+-taurocholate cotransport and its encoding mRNA in primary cultures of rat hepatocytes. *Hepatology* 18: 1162-1166.

Marchegiano, P., F. Carubbi, C. Tiribeli, S. Amarri, M. Stebel, *et al.* (1992). Transport of sulfobromophthalein and taurocholate in the HepG2 cell line in relation to the expression of membrane carrier proteins. *Biochem. Biophys. Res. Comm.* 183: 1203-1208.

Meier, P.S.T., A. Meier, C. Barrett and J.L. Boyer (1984). Mechanisms of taurocholate transport in canalicular and basolateral rat liver plasma membrane vesicles. *J. Biol. Chem.* 259: 10614-10622.

Pandak, W., R.Z. Vlahcevic, D.M. Heuman, K.S. Redford, J.Y.L. Chiang, *et al.* (1994). Effects of different bile salts on steady-state mRNA levels and transcriptional activity of cholesterol 7α-hydroxylase. *Hepatology* 19: 941-947.

Ramirez, M.I., D. Karaoglu, D. Haro, C. Barillas, R. Bashirzadeh, *et al.* (1994). Cholesterol and bile acids regulate cholesterol 7α-hydroxylase expression at the transcriptional level in culture and in transgenic mice. *Mol. Cell. Biol.* 14: 2809-2821.

Schroeder, A., U. Eckhardt, B. Stieger, R. Tynes, C.D. Schteingart, *et al.* (1998). Substrate specificity of the rat liver Na+ - bile salt cotransporter in Xenopus laevis oocytes and in CHO cells. *Am. J. Physl.* 274(37): G370-G375.

Schwarz, L.R., R. Burr, M. Schwenk, E. Pfaff and H. Greim (1975). Uptake of taurocholic acid into isolated rat-liver cells. *Eur. J. Biochem.* 55: 617-623.

Schwarz, L.R., M. Schwenk, E. Pfaff and G. H (1976). Excretion of taurocholate from isolated hepatocytes. *Eur. J. Biochem.* 71: 369-373.

Stacey, N. (1986). Effects of ethinyl estradiol on substrate uptake and efflux by isolated rat hepatocytes. *Biochem. Pharm.* 35: 2495-2500.

Tanabe, S., H. Sherman, L. Smith, L.A. Yang, R. Fleming, *et al.* (1989). Biogenesis of plasma lipoproteins in rat hepatoma McA-RH7777: Importance of diffusion-mediated events during cell growth. *In vitro Cell Dev. Biol* 25: 1129-1140.

Taniguchi, T., J. Chen and A.D. Cooper (1994). Regulation of cholesterol 7α-hydroxylase gene expression in Hep-G2 cells. *J. Biol. Chem.* 269: 10071-10078.

Van Dyke, R., J.E. Stephens and B.F. Scharschmidt (1982). Bile acid transport in cultured rat hepatocytes. *Am. J. Physiol.* 243(6): G484-G492.

Von Dippe, P. and D. Levy (1983). Characterization of bile acid transport in normal and transformed hepatocytes. *J. Biol. Chem.* 268: 8896-8901.

Von Dippe, P. and D. Levy (1990). Expression of bile acid transport protein during liver development and in hepatoma cells. *J. Biol. Chem.* 265: 5942-5945.

Zimmerli, B., J. Valantinas and P.J. Meier (1989). Multispecificity of Na+-dependent taurocholate uptake in basolateral (sinusoidal) rat liver plasm membrane vesicles. *J. Pharm. Exp. Ther.* 250: 301-308.

Chapter 4: Bile acid-induced morphological changes in McNtcp.24 cells

A version of this chapter was been published in European Journal of Cell Biology (1997) 74, 190-196.

4.1 INTRODUCTION

The establishment of primary hepatocyte cultures represents one of the most significant advances in the study of hepatocyte function. However, as detailed in Chapter 1, hepatocytes in primary culture lose a myriad of hepatocyte-specific functions. For example, primary hepatocytes rapidly lose cyp7a, cyp27a, and ntcp gene expression (Hylemon *et al.* 1992; Stravitz *et al.* 1996, Chapter 3), concomitant with a decrease in bile acid uptake activity (Chapter 3). The expression of these liver specific genes is either severely reduced or absent in most immortalized liver cell lines (Labonte *et al.* 2000, Chapter 3).

In the previous Chapter, I described the reconstitution of active bile acid transport in the hepatoma cell line, McArdle RH-7777. Several lines were created displaying various levels of bile acid uptake activity in comparison to primary hepatocytes. As detailed in Chapter 1, bile acids may mediate hepatocyte cytotoxicity in cholestatic liver disease. Therefore, it was important to test the cellular response of McNtcp cells to bile acids. In the present chapter, I describe the alteration of cellular morphology in McNtcp.24, one of the McNtcp cell lines which displayed the highest level of bile acid uptake activity, following extended incubation with taurine-conjugated bile acids.

4.2 METHODS

4.2.1 Culture conditions

McNtcp.24 and McArdle RH-7777 cells were maintained as described in Section 2.2. Bile acids were added to the culture medium to a final concentration of 100 µM unless otherwise indicated. The cells were typically incubated in bile acid-containing medium for 12 to 14 h before analysis. Cell viability was routinely monitored by trypan blue exclusion. Lactate dehydrogenase activity in the cell culture medium was determined as described previously in Section 2.8.

4.2.2 Light microscopy

Routine light microscopy was done using a Zeiss Televal inverted microscope with phase contrast optics. Cytochemical staining of McNtcp.24 cells was done following established procedures. Briefly, McNtcp.24 cells were grown on sterile coverslips in the presence of 100 µM TCA. After treatment, the cells were rinsed, fixed with 6% paraformaldehyde for 30 min at room temperature, rinsed with 50 mM ammonium chloride and then with PBS. Cells were then treated with a solution containing 2.5% potassium chromate and 1% osmium tetroxide for 1 h at RT and then rinsed with distilled water. To visualize neutral lipids, the cells were stained with 0.5% Oil-red-O stain (Sigma Chemical Co., St. Louis, MO) at RT for 4 h. The cells were washed and then counterstained with Gill's hematoxylin. Stained cells were viewed under brightfield illumination. To visualize cholesterol, the cells were treated with filipin (Sigma Chemical Co., St. Louis, MO) as previously described (Kruth *et al.* 1986), except that the glass coverslips were mounted on the microscope slides with 100% glycerol. In some experiments, cells were incubated with 10 nM fluorescein diacetate (FDA) (Molecular Probes, Eugene, OR) at 37 °C for 30 min. For intracellular localization of fluorescent bile acids, cells were grown as before and incubated at 37 °C for 20 min in DMEM containing 0.2 % BSA and 20 µM Cholylglycylamidofluorescein (CgamF), a kind gift of Dr. A. F. Hofmann (University of California, San Diego). After several washes with ice cold PBS containing 1 mM TCA and 0.2 % BSA, cells were left in PBS for fluorescent examination. Stained cells were viewed with a Leica inverted (DM IRB/E) microscope (Leica Microsystems Inc., Richmond Hill, ON) or an Olympus BX-50 microscope (Olympus Corp., Melville, NY) equipped with fluorescence filters and an image capture device.

4.2.3 Electron microscopy

Confluent cultures of McNtcp.24 cells grown in the presence or absence of TCA were fixed *in situ* with 2% glutaraldehyde for 60 min at RT. After fixation, the cells were scraped from plates, washed with 0.2 M sodium phosphate buffer (pH 7.2) containing 1.7% sucrose and the post-fixed with 2% OsO_4 (in 0.2 M phosphate containing 1.7 %sucrose) for 30 min at RT. The cells were then washed with 0.2M sodium phosphate buffer (pH7.2), dehydrated by serial incubation in an increasing concentration of ethanol, and then embedded in Epon 812. Thin sections (80-120 nm thick) were mounted on copper grids. Before examination in the electron microscope, the sections were stained with lead citrate and uranyl acetate. Photographs were obtained with a Phillips EM-420 electron microscope operated at 100 kV.

4.2.4 Labeling of the intracellular bile acid pool

McNtcp.24 cells were plated to 60% confluency at the start of the experiment. The cellular bile acid pool was homogeneously labeled by replacing the culture medium with fresh medium containing 25 µM radiolabeled TCA (20 mCi/mmol). After 12 h incubation, the cells were washed and incubated in bile acid-free culture medium. The efflux of radiolabeled TCA from the loaded cells was followed by replacing the culture medium at regular intervals over 4 h and measuring the radioactivity in the collected culture medium. The amount of radiolabeled TCA remaining in the cells after the incubation period was also determined.

4.2.5 Measurement of fatty acid oxidation rate

The release of ^3H_2O by McNtcp.24 cells was used to quantitate the oxidation rate of exogenous [^{3}H]-palmitate using a previously described procedure (Saddik *et al.* 1991). Briefly, cells were incubated in DMEM without serum but containing [^{3}H]-palmitate, unlabeled palmitate, and fatty acid-free BSA as a carrier. The medium was collected at 15 min intervals over the course of 60 min. [^{3}H]-palmitate was extracted and the level of ^3H_2O in the culture medium was determined by liquid scintillation spectrometry.

4.2.6 Measurement of glycolytic rate

The release of ^3H_2O by McNtcp.24 cells was used to quantitate the rate of glycolysis by the metabolism of exogenous [^{3}H]-glucose as previously described (Saddik *et al.* 1991). Briefly, Cells were incubated in DMEM containing D-[2-^{3}H]-glucose and unlabeled glucose. The medium was collected at 15 min intervals over the course of 60 min, and $^{3}H_2O$ generated by glycolysis was separated from D-[2-^{3}H]-glucose by passing media (200 µl) through a column containing Dowex 1–X4 anion exchange resin resuspended in 0.2 M potassium tetraborate. The column was further washed with 800 µl of water, and the level of $^{3}H_2O$ in the effluent determined by liquid scintillation spectrometry.

4.2.7 Lipid analysis

To determine lipid content, bile acid-treated and untreated McNtcp.24 cells were washed with PBS, scraped from the plates, and then sonicated. The concentration of protein in the sonicated cell suspension was determined as described in Chapter 2. The resulting suspension was extracted with chloroform:methanol (2:1, v:v) and the lipids were separated by TLC as previously described in (Wang *et al.* 1998). Bands corresponding to cholesterol, triacylglycerol and phospholipids were scraped and the lipids extracted. The total mass of the extracted lipids was determined using commercial diagnostic kits (Sigma Chemical Co., St. Louis, MO; Roche Molecular Biochemicals, Laval, PQ). Total phospholipid content was determined as described by Fiske and Subbarrow (Fiske *et al.* 1925).

4.3 RESULTS

4.3.1 Effect of bile acid treatment on McNtcp.24 cell ultrastructure

As described in Chapter 3, McNtcp.24 cells displayed enhanced TCA uptake activity compared to primary hepatocytes. Under normal culture conditions, McNtcp.24 cells are morphologically indistinguishable from the parental McArdle RH-7777 rat hepatoma cells. Addition of 100 μM TCA to the culture medium of McArdle RH-7777 cells did not cause any discernible alteration in cell morphology, consistent with the observed inability of these cells to take up TCA from the culture medium. Incubation of these cells in medium containing >200 μM TCA caused some cell death. This effect is most likely due to the detergent properties of the bile acids. Incubation of McNtcp.24 cells (Fig. 4-1A) in medium containing 5-100 μM TCA promoted the formation of vesicular structures (Fig. 4-1B). Several small vesicles were evident 6 h after the addition of TCA (100 μM) to the culture medium. By 24 h, most cells contained what appeared to be one large vesicle. Since the vesicles were not evident in the parental McArdle RH-7777 cells, their formation is related to the ability of McNtcp.24 cells to take up bile acids from the culture medium.

Light microscopic examination of TCA-treated McNtcp.24 cells in suspension showed retention of the vesicles. In addition, the vesicles remained associated with the cells after passage (i.e. trypsinization of adherent cells and re-plating of single cells). These observations suggest that the vesicles are intracellular. The passaged cells adhered to the culture dish and continued to grow in bile acid-free culture medium. The size and number of vesicles in the cells decreased as the time after passage and growth in bile acid-free culture medium increased. By 24 h, greater than 95% of the bile acid-treated cells returned to normal morphology. The

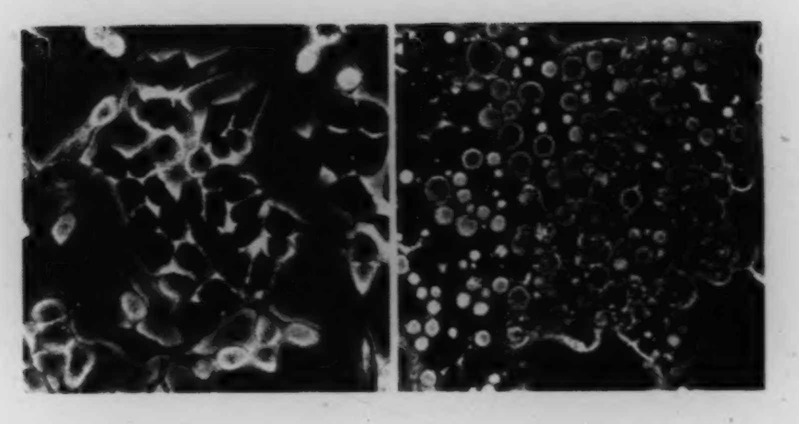

Fig. 4-1. Phase contrast photomicrographs of untreated (**A**) and TCA-treated (**B**) McNtcp.24 cells. Original magnification= 200X.

size of the vesicles in the remainder of the cells was dramatically reduced. Thus, the morphological change associated with incubation of McNtcp.24 cells in bile acid-containing medium is reversible.

In general, the formation of the intracellular vesicles was induced by taurine-conjugated bile acids. TCA induced the most profound changes in cellular morphology. TCDCA was slightly less effective whereas TUDCA (the 7ß epimer of TCDCA) was the least effective. Both of these bile acids are transported by the ntcp, since both compete with TCA for uptake into McNtcp.24 cells (Fig. 4-2). However, the amount of these bile acids accumulated by the cells might differ. The unconjugated forms of these bile acids species did not significantly alter cellular morphology after 24 h of treatment, but this may simply reflect the reduced affinity of unconjugated bile acids for ntcp (See Chapter 3 and Schroeder *et al.* 1998).

Although the growth of McNtcp.24 cells in medium containing TCA was slightly slower compared to the parental cell line, the majority of the cells (>95%) on the culture dish excluded trypan blue. Exclusion of trypan blue indicates that the plasma membrane of McNtcp.24 was not compromised in the presence of TCA. Moreover, there was no significant increase in lactate dehydrogenase activity in the medium after 24 h of bile acid treatment (see the FDA experiments in section 4.5.8). These observations indicate that the TCA treatment did not affect cell viability.

4.3.2 Electron microscopic analysis

Transmission electron microscopic analysis of TCA-treated McNtcp.24 cells confirmed that the vesicles are located intracellularly (Fig. 4-3A). Smaller and irregularly shaped vesicles were also evident in some cells. The large electron light vesicles do not appear to be enclosed by a membrane but structures that resemble membrane fragments are apparent along the inner perimeter (Fig. 4-3A). In some

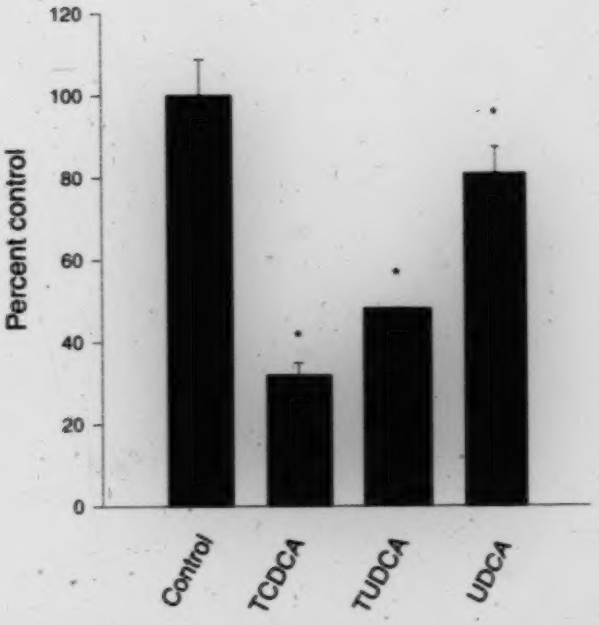

Fig. 4-2. Inhibition of TCA uptake by various bile acids. McNtcp.24 cells were assayed for uptake of TCA (25 μM) in the presence of 100 μM TCDCA, TUDCA, and UDCA. Uptake of TCA alone is expressed as 100%. Values are the mean percent of control ± SD (n=3). Differences in comparison to control were determined using Student's t-test. Asterisk represents $p<0.0001$.

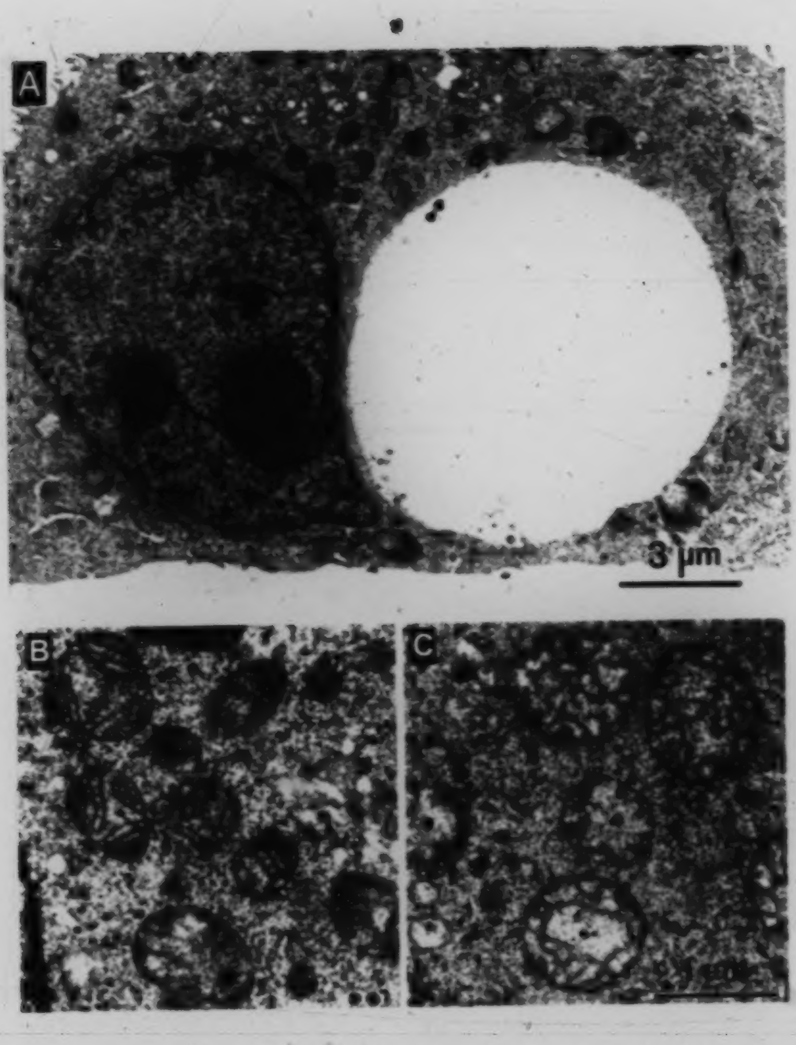

Fig. 4-3. Electron micrograph of McNtcp.24 cells. **A**. Thin-section of McNtcp.24 cells incubated with 100 μM TCA for 12 h. Electron micrograph of mitochondria of untreated (**B**) and TCA-treated (**C**) McNtcp.24 cells. Note the disrupted internal mitochondrial structure and the bloated appearance of mitochondria in TCA-treated cell.

cells, the nucleus assumed irregular shapes (e.g. see Fig. 4-3A), but this feature did not correlate with the size or number of vesicles present within the cell. The fingerlike projections (microvilli) from the plasma membrane were visible on McNtcp.24 cells, regardless of whether the changes in cellular morphology were accompanied by a profound alteration of mitochondrial ultrastructure. The mitochondria of McNtcp.24 cells grown in the absence of bile acids appeared normal (Fig. 4-3B), whereas those in the TCA-treated McNtcp.24 cells were enlarged and assumed a rounded shape (Fig. 4-3C). The most striking feature was the alteration of the inner mitochondrial structure. In particular, the cristae of mitochondria in the TCA-treated McNtcp.24 cells appeared as tubular structures within the lumen of the mitochondria. In some cases, these structures were found arranged around the entire circumference of the inner wall (e.g. see Fig. 4-3C). Inspection of the several photomicrographs suggested that the overall number of mitochondria in TCA-treated McNtcp.24 cells was increased.

4.3.3 Analysis of fatty acid oxidation and glycolytic rates

The changes in mitochondrial structure suggested a probable aberration of mitochondrial function. To examine this possibility, the efficiency of fatty acid and glucose utilization was measured in untreated and bile acid-treated McNtcp.24 cells. Surprisingly, analysis of intact McNtcp.24 cells after TCA treatment did not reveal any impairment in the ability to use exogenous palmitate (Fig. 4-4A). Likewise, the rate of utilization of exogenous glucose by McNtcp.24 cells via glycolysis was not overtly different in TCA- and TCA-untreated cells (Fig. 4-4B), implying that mitochondrial function was unchanged under TCA treatment. Thus despite the extreme changes in mitochondrial structure, the overall ability of the TCA-treated McNtcp.24 cells to metabolize fatty acids and glucose remained unaffected.

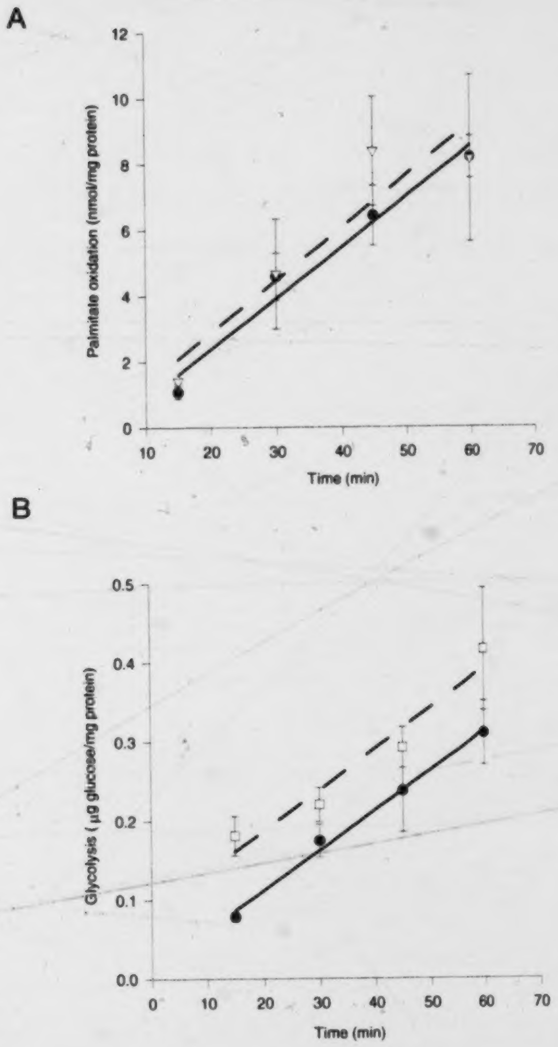

FIG. 4-4 ^3H_2O production from exogenous [^{3}H]-palmitate or [^{3}H]-glucose by McNtcp.24 cells. **A**. The rate of fatty acid oxidation of McNtcp.24 cells grown in the presence (*open triangles)* or absence (*closed circles*) of 100 µM TCA was estimated by measuring the release of ^3H_2O from [^{3}H]-palmitate. **B**. The rate of glycolysis of McNtcp.24 cells grown in the presence (*open squares*) or absence (*closed circles*) of 100 µM TCA was estimated by measuring the release of ^3H_2O from D-[2-^{3}H]-glucose. Mean ± SD (n=3) are shown for each point. Linear regression lines were generated using the computer program SigmaPlot v 5.0 (SPSS inc.).

4.3.4 Cytological staining of lipid in McNtcp.24 cells

The general appearance of the vesicles suggested that they might be lipid droplets. However, there were no large changes in total lipid composition after treatment of McNtcp.24 cells with bile acids. Despite the extensive morphological changes, the total cellular cholesterol and triacylglycerol content were comparable between untreated and TCA-treated McNtcp.24 cells (Table 4-1). The cells were analyzed using cytochemical procedures to determine if there was redistribution of cellular lipids. Oil-red-O stain was used to visualize the localization of neutral lipids. Punctate red staining was clearly evident in the cytoplasm of untreated and TCA-treated McNtcp.24 cells (Fig. 4-5A, B). Although occasional dark red staining could be seen within the large vesicles, the vesicles themselves did not become stained with Oil- red-O (Fig. 4-5B). This finding indicates that neutral lipids are not a major component of the intracellular vesicles.

Unesterified cholesterol was visualized by filipin staining and fluorescence microscopy. In untreated McNtcp.24 cells, filipin staining was evident in the cell membrane and appeared as a shell surrounding the invisible cytoplasm with another intensely staining shell (the nuclear membrane) suspended within (Fig. 4-5C). In some cells, small spherical structures with intense staining were also visible. In TCA-treated McNtcp.24 cells, the intracellular vesicles appeared as voids within the cells (Fig. 4-5D). The intensely staining perimeter of the vesicles gave the impression of a large spherical structure within the cell. Thus, the intracellular vesicles likely do not contain an appreciable amount of free cholesterol.

	Cholesterol	Triacylglycerol	Phospholipids [a]
McNtcp.24	27.1 ± 4.0	27.4 ± 4.0	42.3 ± 4.0
McNtcp.24 +100 µM TCA	33.5 ± 1.3	28.9 ± 4.0	56.1 ± 4.0

Table 4-1. Lipid composition of McNtcp.24 cells. Lipids were extracted from cells, separated by thin-layer chromatography and quantitated as described in Section 4.2.5. -[a] The phospholipid values were determined using a phosphorous assay. The values shown (nmol/mg cell protein) represent the mean ± SD of three plates of cells per treatment.

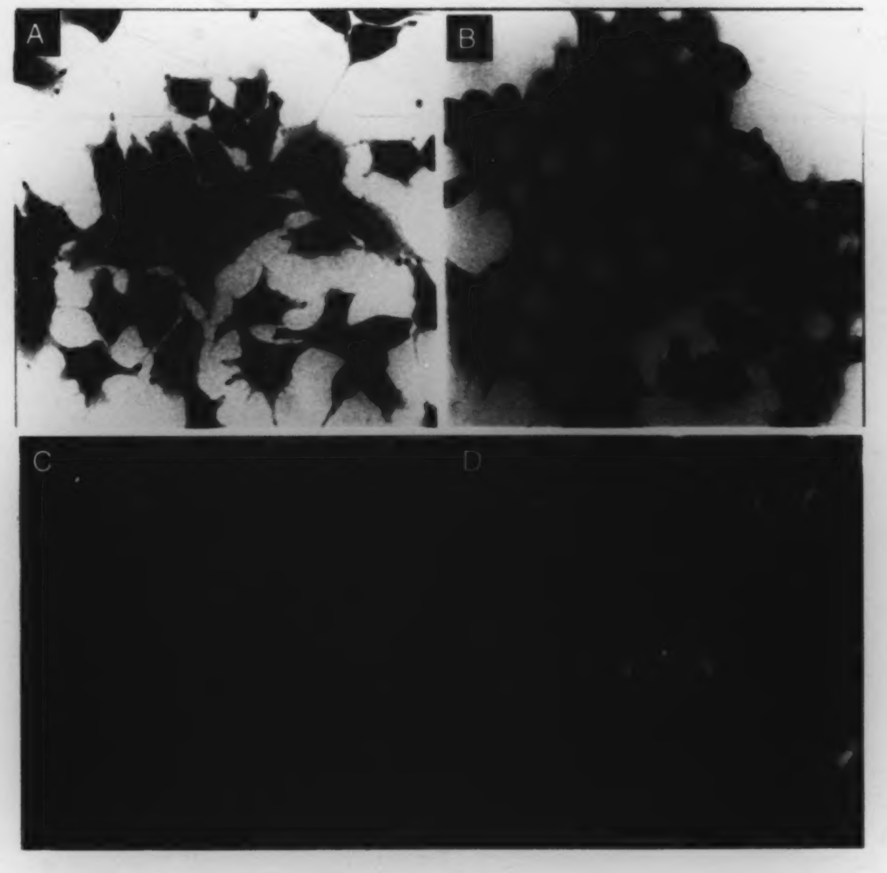

Fig. 4-5 Photomicrographs of TCA-treated McNtcp.24 cells stained with Oil-red-O and filipin. (Top set) Phase contrast photomicrographs of Oil-red-O stained, untreated (**A**) and TCA-treated (**B**) McNtcp.24 cells. (Bottom set) Fluorescent photomicrographs of untreated (**C**) and TCA-treated (**D**) McNtcp.24 cells stained with filipin. Cells were viewed under U.V. illumination with FITC-emission filters. Note the absence of staining inside of the vesicles (**B**,**D**). Original magnification 200X.

4.3.5 Metabolic labeling of the intracellular bile acid pool

As detailed in Section 3.3.2, bile acids from the culture medium are taken up by McNtcp.24 cells and secreted. It is possible that bile acids accumulate in McNtcp.24 cells, since these cells constitutively express ntcp. Because McNtcp cells do not express BSEP (Chapter 3), the efflux of bile acids from McNtcp.24 cells might not be as efficient as the uptake process. To test this possibility, McNtcp.24 were grown in medium containing radiolabeled TCA for 12 h to homogeneously label the intracellular bile acid pool. The cells were then washed and the medium was replaced with bile acid–free medium. The amount of the TCA accumulated by the parental McArdle RH-7777 cells was insignificant compared to McNtcp.24 cells (Fig. 4-6), consistent with the inability of these cells to take up bile acids. By contrast, McNtcp.24 cells accumulated and secreted radiolabeled TCA. After 4 h, the amount of radioactivity remaining in TCA-treated McNtcp.24 cells was substantially reduced (Fig. 4-6), indicating that the majority of the TCA taken up by the cells had been secreted. However, the size of the vesicles within the cells appeared unchanged. These observations suggest that the vesicles are not intracellular stores of bile acids and that the formation of vesicles is indirectly related to the cellular trafficking of bile acids.

4.3.6 Localization of microvilli-lined vesicles

Previous studies have suggested that the biogenesis of bile canalicular membrane involves the intracellular formation of microvilli-lined vesicles (Chiu *et al.* 1989; Remy *et al.* 1989; Sormunen *et al.* 1993; Zaal *et al.* 1994). These vesicles have been found inside of rat and human liver hepatocytes (Remy *et al.* 1989; Zaal *et al.* 1994) and in a variety of human hepatoma cell lines, including HepG2 (Remy

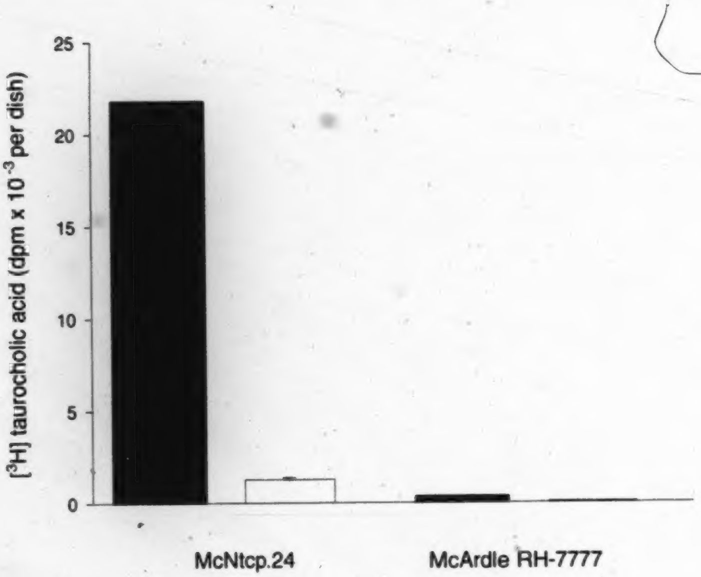

Fig. 4-6. Cell associated [^{3}H]-TCA in McNtcp.24 and McArdle cells. Cells were incubated in medium containing [^{3}H]-TCA for 12 h. The amount of radioactivity associated with washed cells at the end of the labeling period (*solid bars*) and after 4 h incubation in bile acid-free medium (*open bars*) was determined. Values shown are mean ± SD (n=6 per determination). The amount of cellular protein per dish of McNtcp.24 and McArdle RH-7777 cells were not significantly different.

et al. 1989; Sormunen *et al.* 1993). Similar structures were also found in McNtcp.24 cells (Fig. 4-7A). FDA is commonly used to assess the viability of cultured cells (Rotman *et al.* 1966). In liver cells, FDA is rapidly metabolized and fluorescein is secreted into the bile canalicular spaces, making it a useful tool for labeling canalicular structures (Barth *et al.* 1982; Yumoto *et al.* 1996). Addition of FDA to TCA-treated McNtcp.24 cells resulted in bright green fluorescence inside the cells (Fig. 4-7B). This feature is further support of the viability of TCA-treated cells. In some cells, intense focal intracellular fluorescence was also evident (Fig. 4-7B, arrow heads), and the location of the fluorescence corresponded with the location of vesicular structures that were visible under brightfield illumination (Fig. 4-7C). These structures likely represent intracellular canalicular spaces. However, the great majority of the large vesicles clearly did not exhibit fluorescence (Fig. 4-7B).

Fluorescent bile acid derivatives have been used to study bile acid transport in both isolated hepatocytes and perfused livers. CgamF is a fluorescein labeled bile acid derivative that has been shown to be specific for the hepatic bile acid transport system and undergo hepatobiliary secretion as shown in liver perfusion studies (Schteingart *et al.* 1992; Holizinger *et al.* 1997). CgamF accumulates in canalicular spaces of hepatocyte couplets and polarized Wif B cells (Maglova *et al.* 1995; Bravo *et al.* 1998). In untreated McNtcp.24 cells, CgamF localized to small vesicular structures observable under brightfield illumination (Fig. 4-8). This finding is consistent with the results of the FDA experiments, suggesting that McNtcp.24 spontaneously form canalicular-like structures. In comparison, CgamF localized to some, but not all, of the large vesicles formed In TCA-treated cells (Fig. 4-9). This observation is consistent with the FDA experiment showing that most of the vesicles induced by TCA-treatment did not accumulate fluorescein.

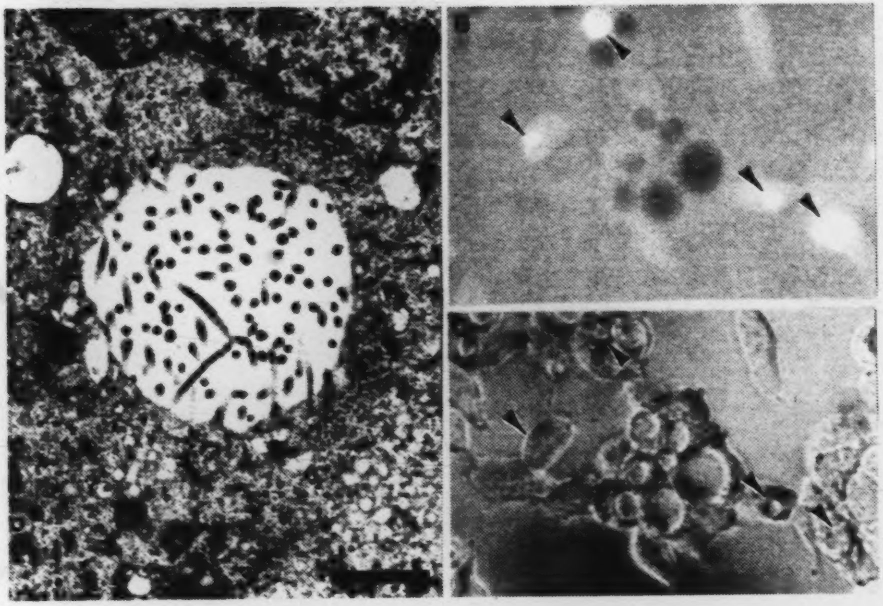

Fig. 4-7 Localization of microvilli-lined vesicles in McNtcp.24 cells. **A**. A microvilli vesicle resembling a bile canaliculus can be seen within the cytoplasm of McNtcp.24 cells. **B**. McNtcp.24 cells were treated with FDA following a 16 h incubation with TCA and viewed by fluorescent microscopy (abs= 473 nm, em=514 nm for fluorescein). **C**. The same field was viewed under brightfield illumination. The *arrowheads* (**B**, **C**) show intense focal intracellular fluorescence and their corresponding location in the same field viewed under brightfield illumination. Original magnification= 200 X (**B**, **C**). Bar 1 mm (**A**).

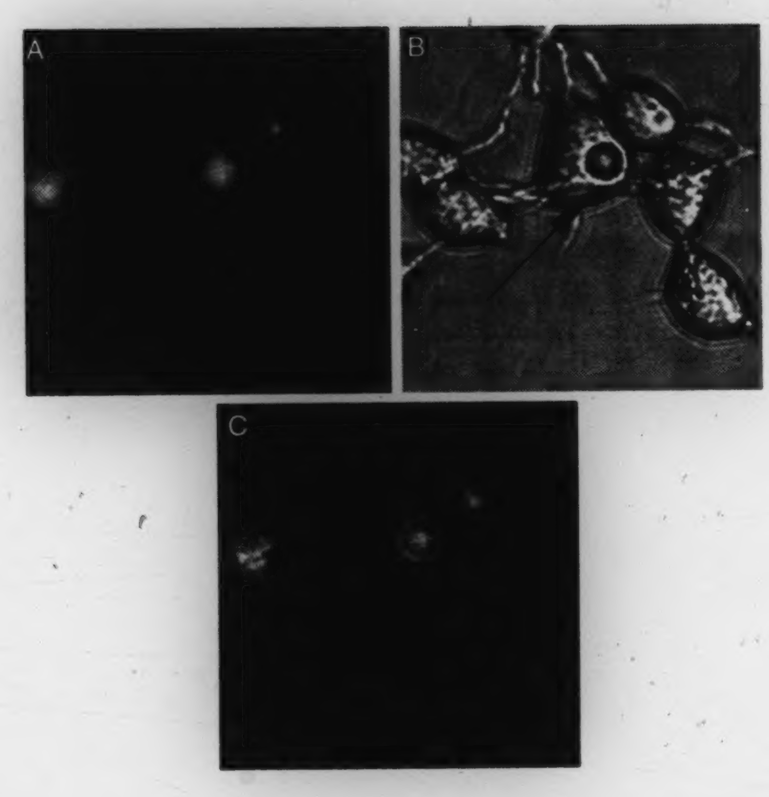

Fig. 4-8 Cellular localization of CgamF in untreated McNtcp.24 cells. CgamF stained cells were viewed under fluorescent microscopy as detailed for FDA. **A**. Diffuse fluorescence was evident in untreated McNtcp.24 cells incubated with CgamF. Bright domains of fluorescence were visible in some fields. These domains co-localized with small vesicular structures (*arrow*) when the same field was viewed under brightfield illumination (**B**). **C**. Images were superimposed to verify co-localization. Original magnification= 200X.

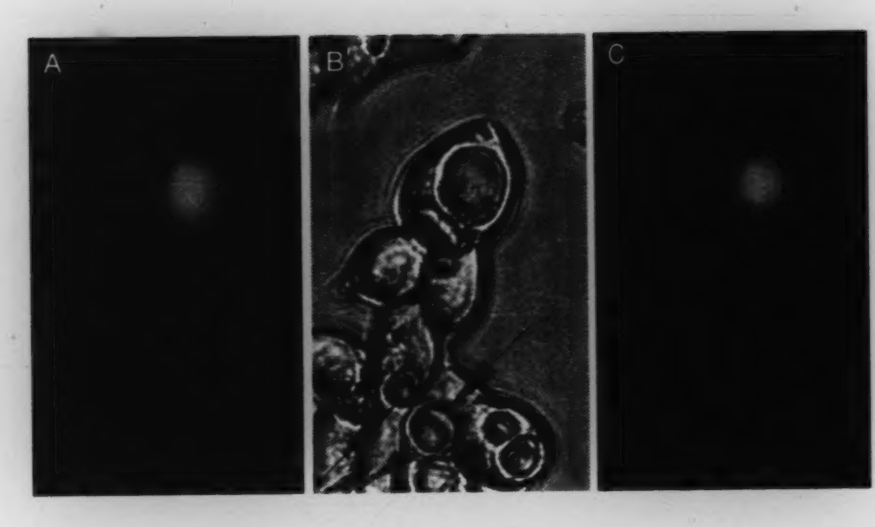

Fig. 4-9. Cellular localization of CgamF in TCA-treated McNtcp.24 cells. Cells were incubated with TCA for 16 h and then incubated with CgamF as described in Fig. 4.7. **A**. As with untreated McNtcp.24 cells, TCA-treated cells displayed a diffuse pattern of fluorescence. However there were bright domains of fluorescence in most fields. These domains co-localized with some of the large vesicular structure when the same field was viewed under brightfield illumination (**B**). However, not all the vesicular structures observed under brightfield illumination (*arrows*) displayed bright fluorescence. (**C**) Superimposition of images (**A**, **B**) Original magnification= 200X.

4.4 DISCUSSION

Taurine-conjugated bile acids caused overt morphological and ultrastructural changes in McNtcp.24 cells. In particular, the treated cells showed the accumulation of large vesicular structures. We subjected McNtcp.24 cells to electron microscopic, histochemical and biochemical analysis to characterize the changes that occur in McNtcp.24 cells after bile acid treatment. Electron microscopy confirmed that the vesicles are intracellular in nature. Morphological and ultrastructural changes have been shown to occur in hepatocytes of cholestatic liver (Schaffner *et al.* 1971; Phillips *et al.* 1983; Degott *et al.* 1992; Center *et al.* 1993). Large clear vesicles have been documented in hepatocytes of cholestatic animals (Shefer *et al.* 1983; Center *et al.* 1993). In bile duct-occluded cats, these vesicles are found to be rich in lipids (Center *et al.* 1993). Histochemical analysis using Oil-red-O and filipin stains revealed that the vesicles in McNtcp.24 cells did not contain significant amounts of lipids, consistent with the results of biochemical analysis. Moreover, the structures do not appear to represent intracellular stores for bile acids, because these structures remained after the efflux of the intracellular bile acids. The balance of the available data indicated that the interior of these structures are devoid of lipophilic material.

Expansion of mitochondrial volume (Schaffner *et al.* 1971; Krahenbuhl *et al.* 1992) and aberration of mitochondrial ultrastructure (Schaffner *et al.* 1971; Shefer *et al.* 1983; Center *et al.* 1993) are additional notable changes in cholestatic hepatocytes that are also apparent in bile acid-treated McNtcp.24 cells. Surprisingly, the altered mitochondrial structure induced by the TCA treatment did not appear to have any significant effect on the ability of McNtcp.24 cells to metabolize fatty acids or glucose. TCA-treated McNtcp.24 cells grew slightly slower but were clearly viable. In fact, the TCA-treated cells continued to grow and returned to normal morphology within 24 h after the withdrawal of bile acids from the culture medium. Krähenbühl and coworkers suggested that the increase in mitochondrial volume fraction documented in hepatocytes of bile duct-ligated rats might represent a compensatory mechanism to maintain energy metabolism in the cholestatic liver (Krahenbuhl *et al.* 1992). The same mechanism may also be responsible for the unaffected overall ability of TCA-treated McNtcp.24 cells to metabolize exogenous palmitate.

It is clear that the alteration of cellular morphology after bile acid treatment is a specific consequence of the ability of the McNtcp.24 cells to take up bile acids, since the same changes are not evident in the parental McArdle RH-7777 cells. Treatment of McNtcp.24 cells with taurine-conjugated bile acids at concentrations <200 µM did not cause cell death. This is intriguing because hepatocyte death, which is typically observed in cholestatic liver, is generally attributed to the toxic effect of bile acids. Indeed, glycochenodeoxycholic acid (GCDCA) has been shown particularly effective in inducing apoptosis when present in the medium of cultured rat hepatocytes (Patel *et al.* 1994). This suggests the possibility that different species of bile acid may have different biological activities (see Chapter 5). Cytoplasmic vacuolation has been observed in other model systems following incubation with weak bases such as procaine hydrochloride (Yang *et al.* 1965; Henics *et al.* 1997). Drug-induced vacuolation in these systems is reversible and appears to an adaptive and survival response to cellular stress (Henics *et al.* 1999). A similar mechanism may operate in TCA-treated McNtcp.24 cells.

Experiments with FDA and CgamF indicate that untreated McNtcp.24 cells are capable of forming canalicular-like structures. In polarized Wif B cells and hepatocyte couplets, CgamF localizes to bile canalicular spaces (Maglova *et al.* 1995; Bravo *et al.* 1998). However, not all canalicular structures in these cells were able to accumulate CgamF, implying that not all canalicular structures were functional (Maglova *et al.* 1995; Bravo *et al.* 1998). In TCA-treated cells, FDA and CgamF failed to localize to most of the large vesicular structures, implying that these structures are not functional canalicular spaces. TCA has been shown to increase the volume of the canalicular space and promote canalicular secretion in hepatocyte couplets (Gautam *et al.* 1989). This bile acid has also been shown to regulate the insertion of apical transporters into the canaliculus by activation of cellular signalling pathways (Gatmaitan *et al.* 1997; Misra *et al.* 1999). It is possible that TCA may promote the formation of vesicular observed in McNtcp.24 cells by activation of signal transduction pathways or direct interaction with intracellular organelles. Further studies should reveal the relationship between the TCA-induced vesicular structures in McNtcp.24 cells and the hepatocyte canaliculus.

4.6 REFERENCES

Barth, C. and L. Schwarz (1982). Transcellular transport of fluorescein in hepatocytes monolayers: Evidence for functional polarity of cells in culture. *Proc. Natl. Acad. Sci. USA.* 79: 4985-4987.

Bravo, P., V. Bender and D. Cassio (1998). Efficient in vitro vectorial transport of a fluorescent conjugated bile acid analogue by polarized hepatic hybrid WIF-B and WIF-B9 cells. *Hepatology* 27: 576-583.

Center, S., L. Guida, M. Zanlli, E. Dougherty, J. Cumming, *et al.* (1993). Ultrastructural hepatocellular features associated with severe hepatic lipidosis in cats. *Am. J. Vet. Res.* 54: 724-731.

Chiu, J.-H., C.-P. Hu, W.-Y. Lui, S. Lo and C. Change (1989). The formation of bile canaliculi in human hepatoma cell lines. *Hepatology* 11: 834-842.

Degott, C., G. Feldman, D. Larrey, A. Duran-Schneier, D. Grange, *et al.* (1992). Drug-induced prolonged cholestasis in adults: A histological semiquantitative study demonstrating progressive ductopenia. *Hepatology* 15: 244-251.

Fiske, C. and Y. Subbarrow (1925). The colorimetric determination of phosphorous. *J. Biol. Chem.* 66: 375-400.

Gatmaitan, Z.C., A.T. Nies and I.M. Arias (1997). Regulation and translocation of ATP-dependent apical membrane proteins in rat liver. *Am. J. Physiol.* 272: G1041-G1049.

Gautam, A., O.C. Ng, M. Strazzabosco and J.L. Boyer (1989). Quantitative assessment of canalicular bile formation in isolated hepatocyte couplets using microscopic optical planimetry. *J. Clin. Invest.* 833: 565-573.

Henics, T. and D.N. Wheatley (1997). Vacuolar cytoplasmic phase separation in cultured mammalian cells involves the microfilament network and reduces motional properties of intracellular water. *Int. J. Exp. Path.* 78: 343-354.

Henics, T. and D.N. Wheatley (1999). Cytoplasmic vacuolation, adaptation and cell death: a view on new perspectives and features. *Biol. Cell* 91: 485-498.

Holizinger, F., C.D. Schteingart, H.-T. Ton-Nu, S.A. Eming, M.J. Monte, *et al.* (1997). Fluorescent bile acid derivatives: relationship between chemical structure and hepatic and intestinal transport in the Rat. *Hepatology* 26: 1263-1271.

Hylemon, P.B., E.C. Gurley, R.T. Stravitz, J.S. Litz, W.M. Pandak, *et al.* (1992). Hormonal regulation of cholesterol 7 α-hydroxylase mRNA levels and transcriptional activity in primary rat hepatocyte cultures. *J. Biol. Chem.* 267(24): 16866-71.

Krahenbuhl, S., S. Krahenbuhl-Glauser, J. Stucki and R. Gehr (1992). Sterological and functional analysis of liver mitochondria from rats with secondary biliary cirrhosis: impaired mitochondrial metabolism and increased mitochondrial content per hepatocyte. *Hepatology* 15: 1167-1172.

Kruth, H., M. Comly, J. Butler, M. Vanier, J. Fink, *et al.* (1986). Type C Niemann-Pick Disease. Abnormal metabolism of low density lipoprotein in homozygous and heterozygous fibroblasts. *J. Biol. Chem.* 261: 16769-16774.

Maglova, L.M., A.M. Jackson, X.-T. Meng, M.W. Carruth, C.D. Schteingart, *et al.* (1995). Transport Characteristics of three fluorescent conjugated bile acid analogs in isolated rat hepatocytes and couplets. *Hepatology* 22: 637-647.

Labonte, E.D., Q. Li and L.B. Agellon (2000). Expression bile cholesterol 7α-hydroxylase restores bile acid synthesis in McArdle RH7777 cells. *Arch. Biochem. Biophys. in press*

Misra, S., P. Ujhazy, L. Varticovski and I. Arias (1999). Phosphoinositide 3-kinase lipid products regulate ATP-dependent transport by sister of P-glycoprotein and multidrug resistance associated protein 2 in bile canalicular membrane vesicles. *Proc. Natl. Acad. Sci. USA* 96: 5814-5819.

Patel, T., S. Bronk and G. Gores (1994). Increases of intracellular Magnesium promote glycodeoxycholate-induced apoptosis in rat hepatocytes. *J. Clin. Invest.* 94: 2183-2192.

Phillips, M., R. Fisher, D. Anderson, S.-P. Lan, J. Lachin, *et al.* (1983). Ultrastructural evidence of intrahepatic cholestasis before and after chenodeoxycholic acid therapy in patients with cholelithiasis: The national cooperative gallstone study. *Hepatology* 3: 209-220.

Remy, L., C. Chalver, J. Ripert and A. Gerolami (1989). Intracellular lumina and bile canaliculi in rat hepatocytes in vitro - a cytochemical study. *Acta Histochem.* 85: 87-92.

Rotman, B. and B. Papermaster (1966). Membrane properties of living mammalian cells as studied by enzymatic hydrolysis of fluorogenic esters. *Proc. Natl. Acad. Sci. USA* 55: 134-141.

Saddik, M. and G. Lopaschuk (1991). Myocardial triglyceride turnover and contribution to energy substrate utilization in isolated working rat hearts. *J. Biol. Chem.* 266: 8162-8170.

Schaffner, F., P. Bacchin, F. Hutterer, H. Scharnbeck, L. Sarkozi, *et al.* (1971). Mechanism of Cholestasis. 4. Structural and biochemical changes in the liver and serum in rats after bile duct ligation. *Gastroenterology* 60: 888-897.

Schroeder, A., U. Eckhardt, B. Stieger, R. Tynes, C.D. Schteingart, *et al.* (1998). Substrate specificity of the rat liver Na+ - bile salt cotransporter in Xenopus laevis oocytes and in CHO cells. *Am. J. Physl.* 274(37): G370-G375.

Schteingart, C.D., S. Eming, H.-T. Ton-Nu, D.L. Crombie and A.F. Hofmann (1992). Synthesis, structure, and transport properties of fluorescent derivatives of conjugated bile acids. In Bile acids and the Hepatobiliary system : Falk symposium 68. G. Paumgartner, A. Stiehl, and W. Gerok. Kluwer Academic publishers: Dordrecht: 177-183.

Shefer, S., F. Zaki and G. Salen (1983). Early morphologic and enzymatic changes in livers of rats treated with chenodeoxycholic and ursodeoxycholic acids. *Hepatology* 3: 201-208.

Sormunen, R., S. Eskelinen and V. Lehto (1993). Bile canaliculus formation in cultured HepG2 cells. *Lab. Invest.* 68: 652-662.

Stravitz, R.T., Z. Vlahcevic, T.L. Russell, M.L. Heizer, N.G. Avadhani, *et al.* (1996). Regulation of sterol 27-hydroxylase and an alternative pathway of bile acid biosynthesis in primary cultures of rat hepatocytes. *J. Steroid Bioch. Mol. Biol.* 57(5-6): 337-47.

Wang, W., D. Merriam, A. Moses and G. Francis (1998). Enhanced Cholesterol Efflux by Tyrosyl Radical-oxidized High Density Lipoprotein Is Mediated by Apolipoprotein AI-AII Heterodimers. *J. Biol. Chem.* 273: 17391–17398.

Yang, W., F.F. Strasser and C.M. Pomerat (1965). Mechanism of drug-induced vacuolization in tissue culture. *Exp. Cell Res.* 38: 495-506.

Yumoto, A.U., S. Watanabe, M. Hirose, T. Kitamura, Y. Yamaguchi, *et al.* (1996). Structure and functional features of bile canaliculi in rat hepatocyte spheroids. *Liver* 16: 61-66.

Zaal, K., J. Kok, R. Sormunen, S. Eskelinen and D. Hoekstra (1994). Intracellular sites involved in the biogenesis of bile canaliculi in hepatic cells. *Eur. J. Cell. Biol.* 63: 10-19.

Chapter 5: Cytotoxicity of bile acids in cells of hepatic and non-hepatic origin

A version of this chapter will be submitted for publication in
Molecular Biology of the Cell.

5.1 INTRODUCTION

As detailed in Chapter 1, considerable progress has been made in understanding how bile acids are internalized by polarized cells such as hepatocytes and ileocytes. Asbt mediates the active reclamation of conjugated bile acids in the ileum (Wong *et al.* 1994; Love *et al.* 1998), and ntcp is quantitatively the most important transporter of conjugated bile acids in hepatocytes (Hagenbuch *et al.* 1991; Hagenbuch 1997). Although 3HSD and HBAB have been implicated in the translocation of bile acids from the basolateral to the apical poles of hepatocytes, this area of bile acid transport remains poorly understood (Stolz *et al.* 1989). In addition, the intracellular targets that mediate the various effects of bile acids on cellular function remain poorly characterized.

With the discovery that bile acids are the natural ligands for the nuclear receptor termed farnesoid x receptor (FXR;NR1H4) (Makishima *et al.* 1999; Parks *et al.* 1999; Wang *et al.* 1999), it has become evident that bile acids may be important regulators of gene expression in the liver and small intestine. The genes regulated by FXR encode proteins involved in the biosynthesis and transport of bile acids (Gustafsson 1999; Russell 1999). As discussed in Chapter 1, bile acids modulate various cellular functions such as the secretion of apolipoprotein B from hepatocytes (Lin *et al.* 1996a; Lin *et al.* 1996b) and the signaling pathways that lead to the translocation of bile acid transporters to the canalicular membrane (Misra *et al.* 1998). In McNtcp cells, which are liver-derived cells engineered to actively transport bile acids (Chapter 3), taurine-conjugated bile acids induce the formation of intracellular vesicles that resembles structures observed in cholestatic liver cells without apparent cellular cytotoxicity (Chapter 4). In contrast, glycine-conjugated bile acids are potent inducers of apoptosis in these cells, concordant with that observed in primary cultures of hepatocytes (Patel *et al.* 1994; Roberts *et al.* 1997).

Glycine-conjugated bile acids have been also shown to induce apoptosis in McNtcp.24 cells by activation of the Fas receptor through a FasL-independent mechanism (Faubion *et al.* 1999). Thus, it would appear that McNtcp cells have distinctive responses to different species of bile acids. Whereas taurine-conjugated bile acids were well tolerated, glycine-conjugated bile acids displayed extreme cytotoxicity to McNtcp cells. In the present chapter, I determine if this differential response is limited to cells of hepatic origin, and whether expression of HBAB can attenuate the cytotoxic response of McNtcp.24 cells to glycine-conjugated bile acids.

5.2 METHODS

5.2.1 Cell lines

McNtcp.24 and CHO cells were cultured as detailed in Section 2.2. To establish cell lines stably expressing asbt, a cDNA encoding the hamster asbt (Torchia *et al.* 1996) protein was cloned into a pBK-CMV expression vector (Stratagene, La Jolla, CA). The prokaryotic promoter embedded in the 5'-UTR region of the encoded recombinant mRNA was removed from the resulting plasmid. Megan Forbes-Blacker, a former technician with Dr. L. B. Agellon, cloned the human bile acid binder (HBAB) cDNA (Stolz *et al.* 1993) into a derivative of pCep4 (Invitrogen Corp., Carlsbad, CA) lacking the EBNA 1 gene. The lipofectamine reagent was used to transfect the expression plasmids into CHO, McArdle RH-7777, and McNtcp.24 cells following the procedure detailed by the manufacturer (Life Tech., Burlington, ON). The cell medium was replaced 24 h post-transfection with medium containing G418 (400 µg/ml) or hygromycin (500 µg/ml) to select for stable transfectants. Surviving colonies were expanded and assayed for the ability to take up [^{3}H]-TCA from the culture medium as described in Section 2.6 or screened for the expression of HBAB by RNA blot analysis.

5.2.2 Immunoblot analysis

For immunodetection of asbt protein, cells were lysed in a solution of 50 mM Tris-HCl (pH 7.4), 1% NP-40%, 0.25% sodium deoxycholate; 150 mM NaCl, 1 mM EGTA, 1 mM Na_3VO_4, 1 mM NaF, containing a protease inhibitor cocktail (Sigma-Aldrich Canada Ltd.). Cell extracts were fractionated using polyacrylamide gel electrophoresis and transferred to Immobilon-P membrane (Millipore Ltd., Nepean, ON). Asbt was detected using a rabbit antiserum directed against the last 14 amino acids of the carboxyl terminal of the hamster asbt protein. HBAB protein was detected as previously described (Stolz *et al.* 1993).

5.2.3 Visualization of Genomic DNA fragmentation

Cells (10^6 per 60 mm dish) were grown for 16 h. After washing with PBS, the cells were incubated with 50 µM bile acids for 3 h at 37 °C. Adherent and non-adherent cells were dissolved in Tris-buffered saline [pH 7.6] containing 10 mM EDTA and 0.5% sarkosyl, and genomic DNA was isolated as described in Section 2.5. The resulting DNA was treated with RNAse A and then analyzed by conventional agarose gel electrophoresis (Wyllie 1980). The genomic DNA fragments were visualized with U.V. light following ethidium bromide staining.

5.2.4 Caspase activity assays

Cells (10^6 per 60 mm dish) were grown for 16 h. After washing with PBS, the cells were incubated with 50 to 100 µM bile acids for 1 to 2 h as detailed in the figure legends. After the incubation period, the medium was discarded and adherent cells were scraped in PBS. Cells were collected by centrifugation (500x g) and resuspended in buffer containing 50 mM Tris-HCl (pH 7.5), 1% Nonidet P-40, and 150 mM NaCl. Following a 10 min incubation on ice, lysed cells were centrifuged for 10 min, 10, 000 x g at 4 °C. The supernatant was assayed for caspase activity in 20 mM PIPES (pH 6.8), 100 mM NaCl, 1 mM EDTA, 1% CHAPS, and 10% sucrose (Stennicke *et al.* 1997; Stennicke *et al.* 1999) with Z-IETD-AFC for caspase 8 and Z-DEVD-AFC for caspase 3 (Talanian *et al.* 1997; Earnshaw *et al.* 1999). The release of the fluorogenic-leaving group was detected by excitation at 400 nm and emission at 505 nm. Free AFC was used to generate a standard curve for quantitation.

5.2.5 Phosphatidylinositol 3-kinase assays

Crude membrane fractions were isolated from CHO.asbt and McNtcp.24 cells as described previously (Courtneidge *et al.* 1980). To prepare a lipid suspension, phosphatidylserine and phosphatidylinositol (1:1, wt:wt) were sonicated in a solution containing 25 mM MOPS (pH 7.0), 1 mM EGTA, 1 mM Na_3VO_4. Cell extracts were assayed in a solution containing 25 mM MOPS (pH 7.5), 5mM $MgCl_2$, 1mM EGTA, 1 mM Na_3VO_4, 130 μM ATP, 20 μCi [γ-^{32}P]-ATP (3000 Ci/mmol) and 0.2 mg/ml sonicated lipids. The reaction was allowed to proceed for 10 min at 37 °C and stopped by addition of 300 μl of 1N HCl:methanol (1:1, v:v). Lipids were extracted twice with 350 μl chloroform and the organic phases from both extractions were combined then washed once with 700 μl 1N HCl:methanol (1:1, v:v). Lipids were dried, resuspended in chloroform:methanol (1:1, v:v). The samples were spotted along with pure phosphoinositide phosphate standards (Avanti Polar Lipids, Alabastar, Alabama) onto 1.2% potassium oxalate empregnated TLC plates (Traynor-Kaplan *et al.* 1989). The chromatogram was developed in chloroform: methanol: water: aqeous ammonia (90:70:17:3) (Arcaro *et al.* 1993). [^{32}P] incorporation was quantitated by phosphorimaging using a Fuji BAS1000 phosphorimager. Visualization of standards was done by dipping TLC plates in 10% $CuSO_4$, 10 % H_3PO_4 and heating at 200 °C for 10 min.

5.3 RESULTS

5.3.1 Bile acid uptake in CHO.asbt cells

To determine if non-liver derived cells also possess differential cytotoxicity to bile acids, Chinese hamster ovary (CHO) cells were engineered to actively take up bile acids by expression of asbt. I constructed an asbt expression vector as detailed in Section 5.2.1 and introduced it into CHO cells, which lack endogenous bile acid transport activity (Chapter 3). Colonies surviving the selection with G418, were assayed for the ability to take up $[^3H]$-TCA from the culture medium. I chose several clones showing a range of transport activity for further analysis.

As shown in Fig. 5-1A, uptake of TCA into various clones was saturable with an apparent K_m ranging between 22 to 25 μM. V_{max} values ranged from 0.32 to 2.76 nmol/mg protein/min and correlated with the asbt transgene expression in total RNA from CHO.asbt cells (Fig. 5-1A, inset). Correspondingly, in lysates made from CHO.asbt cells, an immunoreactive band of comparable size to rat asbt protein (~45-kDa) was detected using asbt antiserum (Fig. 5-1B, inset). The uptake of 25 μM TCA in CHO.asbt.8 and 35 cells reached a steady state within 10 min (Fig. 5-1B), implying the presence of an efflux pathway for bile acids in CHO.asbt cells. Indeed, it was possible to chase the radiolabel from CHO.asbt cells after preincubating cells with radiolabeled bile acids (Fig. 5-1C). These experiments demonstrate that CHO.asbt cells express a fully functional asbt protein.

5.3.2 Cytotoxic potential of bile acid in CHO.asbt.35 cells

To determine the cytotoxic potential of bile acids in CHO.asbt cells, lactate dehydrogenase (LDH) activity was assayed in the culture medium of both CHO.asbt

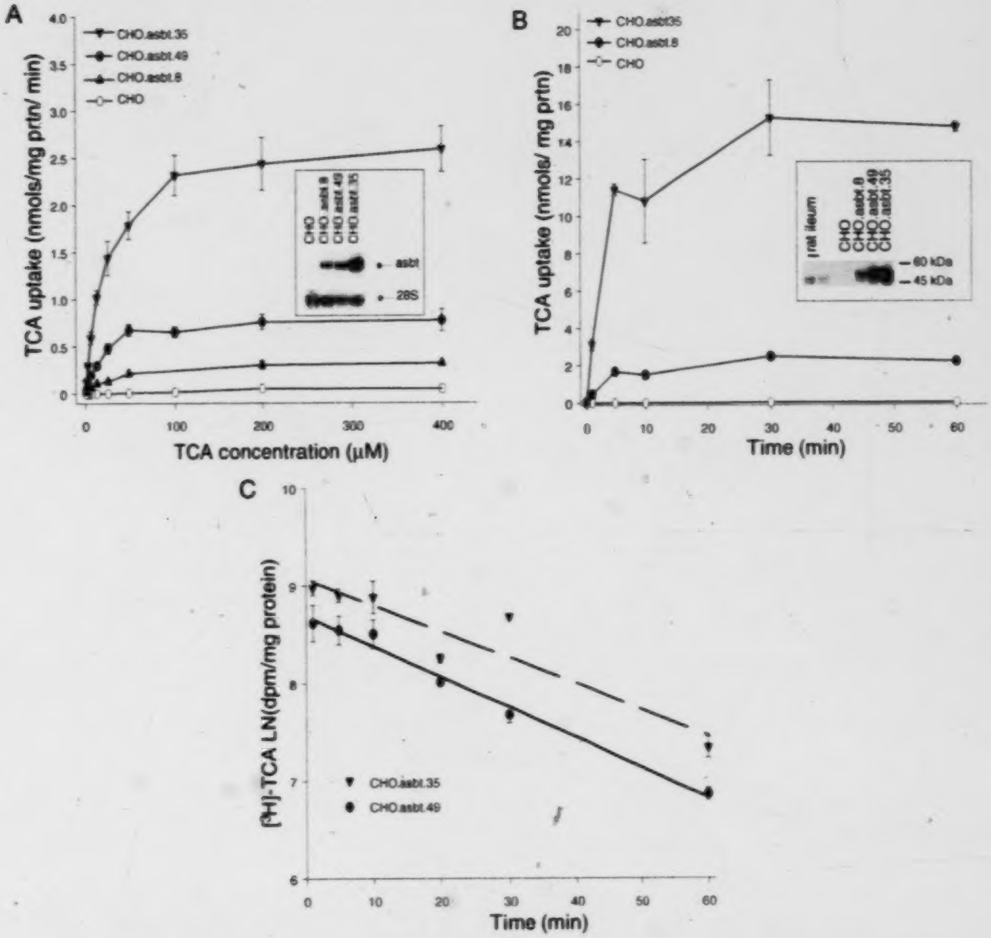

Fig 5-1 Functional expression of asbt in CHO.asbt cells. **A**. CHO.asbt cells showed concentration dependent uptake of TCA that was saturable with greater than 100 µM concentrations. The apparent K_m for TCA uptake ranged between 22.4-25.9 µM. Inset shows RNA blot analysis using an asbt cDNA probe to detect asbt expression in total RNA (10 µg) of CHO.asbt cells. A 1.7 kb message is readily detectable in CHO.asbt cells, but is absent in CHO cells. **B**. Time dependent uptake of TCA in CHO.asbt and CHO cells. TCA uptake in CHO.asbt cells reached steady state levels by 10 min. Inset shows the detection of asbt by immunoblotting of total cell extracts (20 µg) from CHO.asbt, but not from CHO cells. The recombinant protein is similar in size to the rat asbt. **C**. Efflux of TCA from CHO.asbt.35 and CHO.asbt.49 cells. Cells were incubated with 25 µM [^{3}H]-TCA for 20 min to label the intracellular pool of bile acids. The amount of radioactivity retained by the cells was determined as described in Chapter 2. The means ± SD (n=3) are shown for each point.

and McNtcp.24 cells after incubating these cells with glycine- and taurine-conjugated bile acids. CHO.asbt.35 cells were chosen to characterize the cytotoxic response to bile acids because this cell line has bile acid uptake activity that is similar to McNtcp.24 cells (Chapter 3). The amount of LDH activity in the culture medium was normalized to the amount of LDH activity that remained on the culture dish following bile acid treatment. Within 2 h of incubating McNtcp.24 cells with 100 µM of glycine conjugates of cholic acid, chenodeoxycholic acid, and deoxycholic acid (GCA, GCDCA, GDCA, respectively), LDH activity in the culture medium of these cells increased by 20 to 34% and remained constant for 9 h. Of the bile acids tested, GCDCA proved the most potent cytotoxin (Fig. 5-2A). In contrast, incubation with 100 µM of either taurine- and glycine-conjugated bile acids resulted in a time-dependent increase of LDH activity in the culture medium of CHO.asbt.35 cells (Fig. 5-2A). GCA and GDCA were the most potent cytotoxins as LDH activity in the medium of cells treated with these bile acids reach 40% within 6 h. TCA was the most potent cytotoxin of the taurine-conjugated bile acid tested (See Fig. 5-2A). Because LDH activity did not significantly increase in the culture medium of the respective parental cell lines following incubations with amidated bile acids (Fig. 5-2B), bile acid uptake is a prerequisite for bile acid cytotoxicity at low concentrations. Moreover, cytotoxicity was specific to amidated bile acids as cholic acid had a negligible effect on LDH activity in the culture medium of CHO.asbt.35 cells in comparison to untreated controls (Fig 5-3).

In Chapter 4, I showed that taurocholic acid was well tolerated in McNtcp.24 cells. In contrast, GCDCA was shown to induce apoptosis in McNtcp.24 cells concordant with what has been documented for hepatocytes in primary cultures (Roberts *et al.* 1997). Consistent with these observations, GCDCA was able to induce genomic DNA fragmentation in McNtcp.24 cells (Fig 5-4). Indeed, the glycine-conjugated bile acids that were tested induced DNA ladders in these cells, but

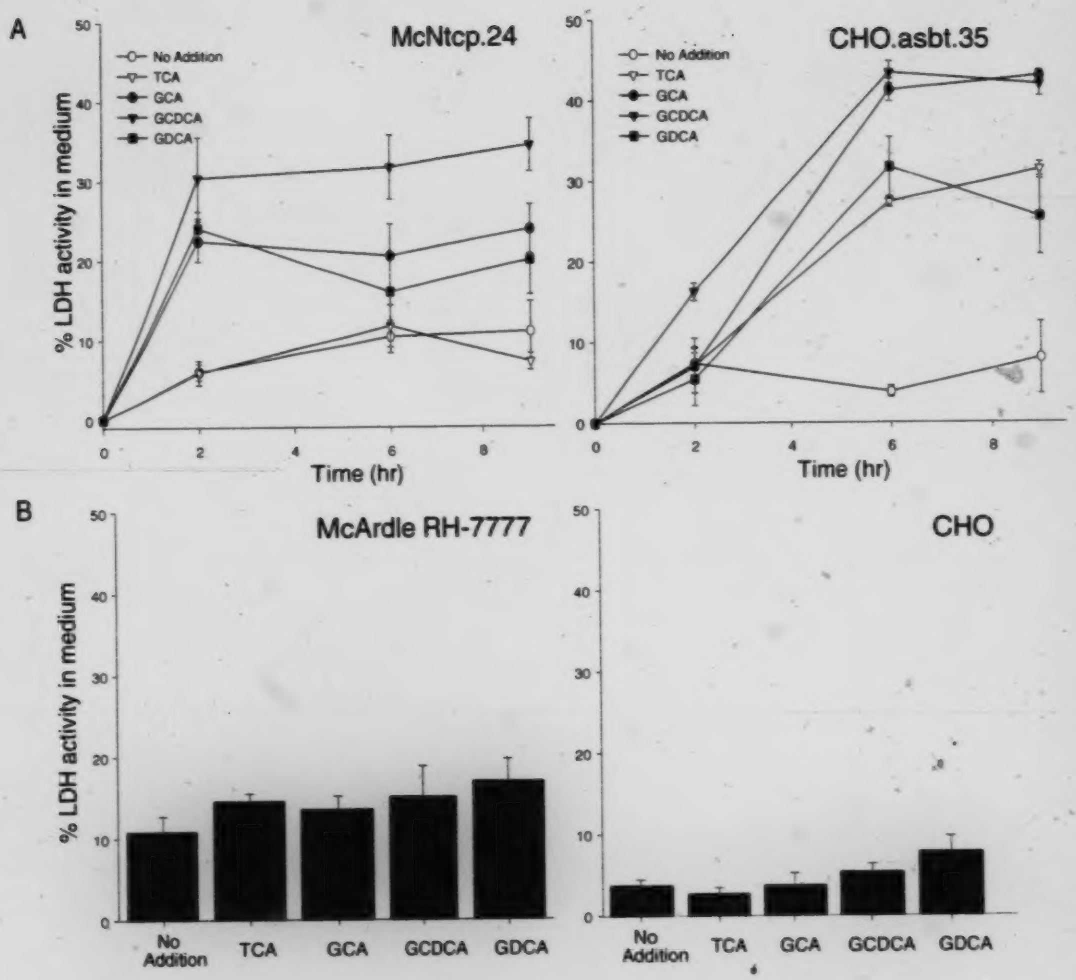

Fig 5-2 Detection of LDH activity in the medium of bile acid-treated cells. **A**. McNtcp.24 and CHO.asbt.35 cells were incubated with 100 µM bile acids. Glycine-conjugated bile acids increased LDH activity in the culture medium of McNtcp.24 in a time dependent manner. Incubation of McNtcp.24 cells with TCA did not result in a significant increase in LDH activity in comparison to control cells (no addition column). In contrast, both glycine and taurine-conjugated bile acids induced the time-dependent increase of LDH activity in medium of treated CHO.asbt.35 cells. **B**. Glycine- and taurine-conjugated acids had a negligible effect on LDH activity in treated McArdle RH7777 or CHO cells after a 5 h incubation period. The means ± SD (n=3) are shown per time point.

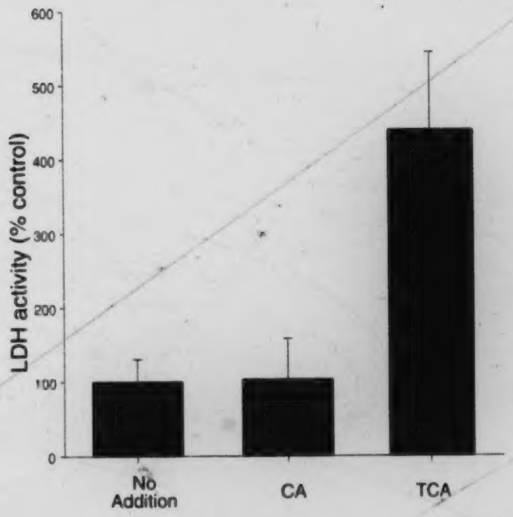

Fig 5-3 LDH activity in medium of bile acid-treated CHO.asbt.35 cells. Cells were treated with 100 μM bile acids for 5 h and the LDH activity in the medium was measured as detailed in Section 2.8. LDH activity is shown as % of control (No Addition group). The means ± SD (n=5) are shown for each group.

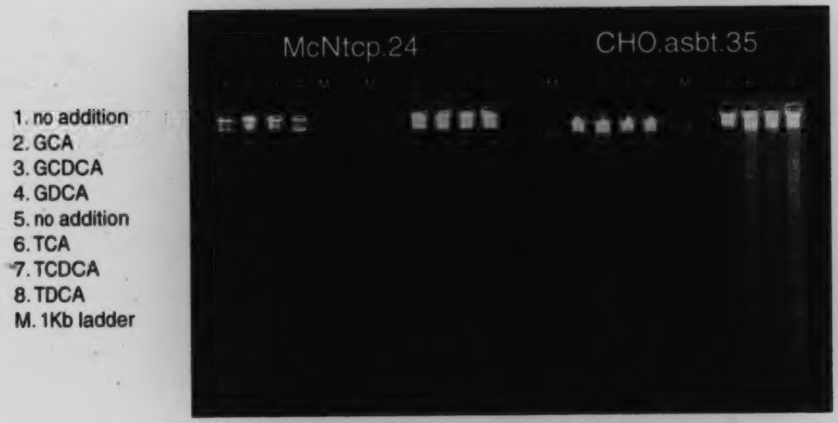

Fig 5-4 Genomic DNA fragmentation in bile acid-treated CHO.asbt.35 and McNtcp.24 cells. Cells were incubated with 50 μM taurine- or glycine-conjugated bile acids for 3 h and genomic DNA was isolated as described in Section 5.2.3. Only glycine-conjugated bile acids induced the typical DNA laddering pattern in McNtcp.24 cells, whereas both types of bile acids induced DNA laddering in CHO.asbt.35 cells. Concentrations as low as 5 μM induced genomic DNA fragmentation in both cell lines. Original magnification = 400X

taurine-conjugated bile acid did not (Fig. 5-4). Therefore, I determined if amidated bile acids could induce apoptosis in CHO.asbt.35 cells. As shown in Fig. 5-4, glycine-conjugated bile acids induce DNA fragmentation as observed in McNtcp.24 cells. However, taurine-conjugated bile acids also induced DNA laddering in CHO.asbt.35 cells, indicating that both amidated bile acids are apoptogenic in this non-hepatic derived cell line with bile acid transport activity. These experiments indicate that CHO.asbt.35 cells undergo apoptosis when challenged with amidated bile acids.

5.3.3 Mechanism of bile acid-mediated cell death

Members of the caspase family of cysteine proteases have been implicated in the initiation and execution phase of apoptosis induced by a variety of different stimuli (Budihardjo *et al.* 1999). In addition, studies using McNtcp.24 cells and hepatocytes have implicated the caspase cascade in apoptosis triggered by toxic bile acids (Faubion *et al.* 1999; Miyoshi *et al.* 1999). Caspase activity was therefore measured after bile acid treatment in CHO.asbt.35 cells to determine if toxic bile acids could activate the caspase cascade in this cell line. As shown in Fig. 5-5A, activation of caspase 8 was evident in CHO.asbt.35 cells after either taurine- or glycine-conjugated bile acid treatment. In contrast, treatment of McNtcp.24 cells with GCDCA resulted in the induction of caspase 8 activity, whereas TCA treatment had negligible effect as compared to untreated controls (Fig. 5-5B). The exclusiveness of caspase 8 activation by glycine-conjugated bile acids is consistent with the notion that taurine-conjugated bile acids may be nontoxic to liver-derived cell lines. Because incubation of the respective parental cell lines with amidated bile acids did not result in activation of caspase 8 (Fig. 5-5, open bars), toxic bile acids must be first internalized before they can trigger apoptosis. More-

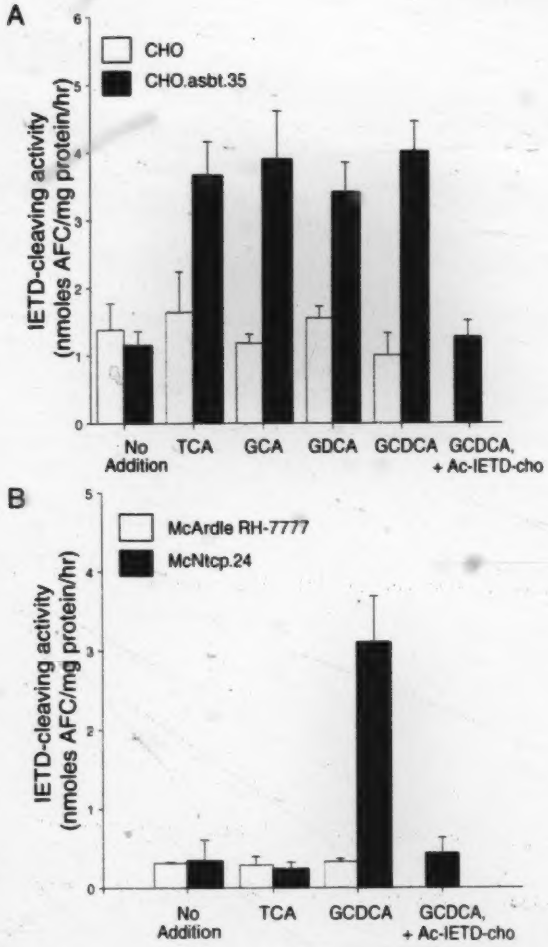

Fig 5-5 Activation of caspase 8 in bile acid-treated cells. Cells were grown overnight, treated with various bile acids (100 µM) for 2 h, and caspase 8 activity was assayed in cellular extracts using the fluorogenic substrate, Z-IETD-AFC. The time and concentration for bile acid incubation was selected to be consistent with the LDH experiments depicted in Fig. 5-2. **A**. Both glycine- and taurine-conjugated bile acids induced the activation of caspase 8 in CHO.asbt.35 cells (dark bars). Extracts from TCA- and GCDCA- treated CHO cells did not show any significant change in caspase 8 activity as compared to controls (white bars). **B**. In contrast, only glycine-conjugated, but not taurine-conjugated, bile acids induced the activation of caspase 8 in McNtcp.24 cells (dark bars). No activation of caspase 8 was observed in McArdle RH-7777 cells with amidated bile acids (open bars). Caspase 8 activity in GCDCA treated cells could be inhibited by addition of the caspase 8 inhibitor Ac-IETD-cho to the cell extracts. The data (mean ± SD, n=3) is representative of several experiments.

over, unconjugated bile acids failed to elicit apoptosis and activate caspase 8 in CHO.asbt.35 cells (Fig. 5-6).

To further characterize the initiation of the caspase cascade in CHO.asbt.35 cells, I determined the time dependent activation of caspase 8 activity by bile acids. As shown in Fig. 5-7, caspase 8 activation in both CHO.asbt.35 and McNtcp.24 cells by GCDCA was be first detected at 30 min and began to plateau within 60 min of the start of the time course. In contrast, TCA-mediated activation of caspase 8 was first detected at 60 min and reached the levels induced by GCDCA by 120 min. The profile of caspase 8 activation by GCDCA and TCA suggest a subtle difference in the mode that these bile acids triggered apoptosis in CHO.asbt.35 cells. Given the different profile of caspase 8 activation by GCDCA and TCA in CHO.asbt.35 cells, it is possible that the type of bile acids transporter expressed in the different cell lines may play a role in conferring sensitivity of glycine or taurine conjugated bile acids. To address this possibility, McArdle RH-7777 cells expressing asbt (Fig. 5-8A) were challenged with bile acids. As shown in Fig. 5-8B, expression of asbt in McArdle RH-7777 did not confer sensitivity to taurine-conjugated bile acids, whereas GCDCA remained cytotoxic.

Caspase 3 may mediate the execution phase of apoptosis and has been shown to be a downstream target of the caspase 8 (Budihardjo *et al.* 1999). I assayed the activity of the caspase 3 in CHO.asbt.35 and McNtcp.24 cells following a bile acid challenge to determine if this caspase was also involved in apoptotic response induced by bile acids. As shown in Fig. 5-9, 1 h incubation with GCDC (50 μM) resulted in activation of caspase 3 in McNtcp.24 cells, whereas TCA treatment showed no activation. In contrast, both amidated bile acids activated caspase 3 in CHO.asbt.35 cells, but in a manner consistent with the time dependent activation of caspase 8 (see Fig. 5-7). These findings suggest that the apoptotic potential of bile acids in McNtcp.24 cells depends on the type of amino acid conjugated

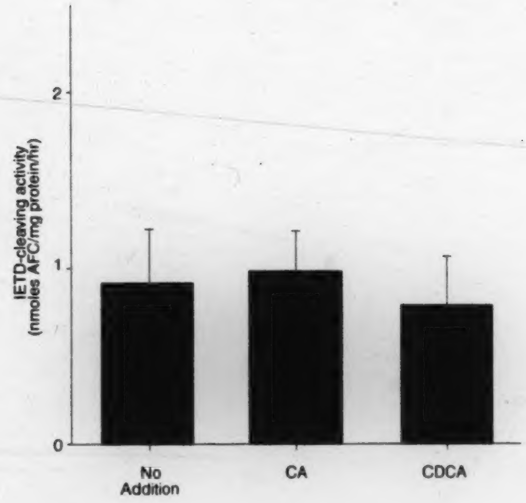

Fig 5-6 Caspase 8 activity in CHO.asbt.35 cells treated with unconjugated bile acids. CHO.asbt.35 cells were treated with 100 μM bile acids for 2 h and caspase 8 activity was determined in cellular extracts as detailed in Section 5.2.4. The mean ± SD, n=3 is shown for each bar.

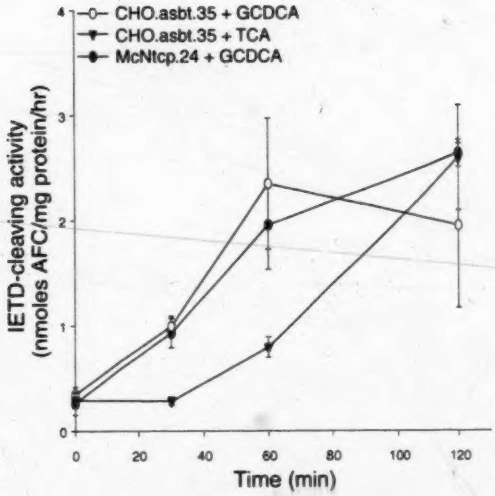

Fig 5-7 Time dependent activation of caspase 8 in bile acid-treated CHO.asbt.35 and McNtcp.24 cells. Cells were treated with 50 μM bile acids. After a time interval, cellular extracts were isolated and assayed for caspase 8 activity as described in Section 5.2.4. The means ± SD (n=3) are shown for each time point.

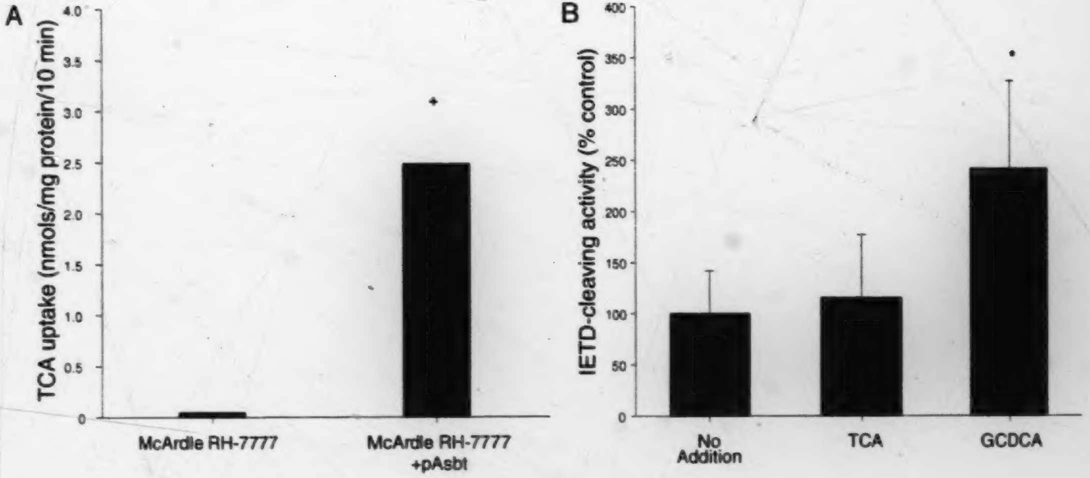

Fig 5-8 Caspase 8 activity in McArdle RH-7777 cells expressing asbt and treated with bile acids. McArdle cells were transfected with the pASBT vector using the lipofectamine reagent. Transfected cells were divided into several groups and incubated with G418. One group that showed significant accumulation of bile acids compared to parental cells (**A**) was assayed for caspase 8 activity following a 2 h incubation with 100 μM bile acid (**B**). The time and concentration of bile acid treatment was selected to be consistent with the LDH experiments of Fig. 5-2. Only treatment with GCDCA resulted in significant activation of caspase 8. The mean ± SD, n=6 is shown for each bar. Differences in comparison to control cells were evaluated using a Student's t-test. * = $p<0.005$, + = $p<0.0001$

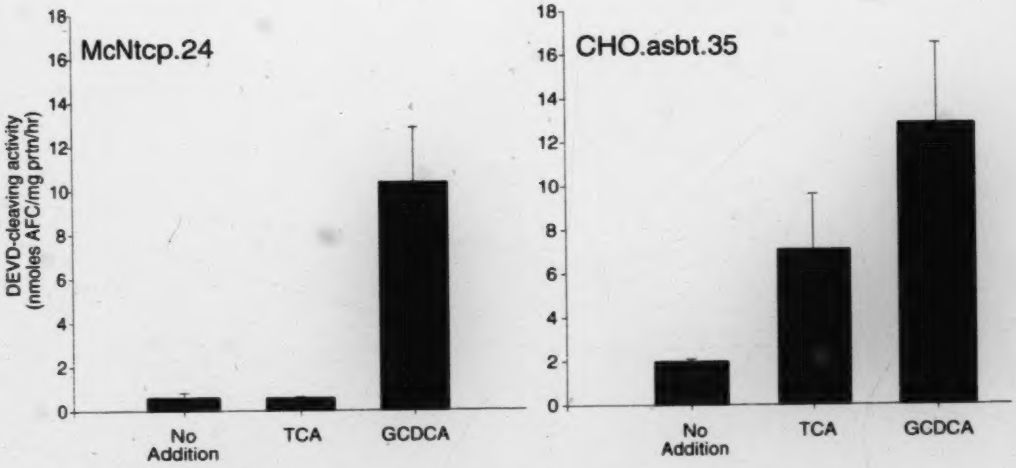

Fig 5-9 Caspase 3 activity in bile acid-treated cells. Cells were treated with bile acids for 1 h and cellular extracts were prepared as detailed in Section 5.2.4. Caspase 3 activity was assayed using the fluorogenic substrate, Z-DEVD-AFC. **A**. In McNtcp.24 cells, GCDCA-treatment resulted in a dramatic activation of caspase 3, whereas TCA had no effect in comparison to control cells. **B**. In CHO.asbt.35 cells, both TCA and GCDCA treatment activated caspase 3. The mean ± SD, n=3 is shown for each bar.

to the steroid nucleus, but does not depend on the type of transporter used to internalized the bile acids.

5.3.4 Differential sensitivity

Several studies in the last few years have shown that bile acids activate a variety of cellular signaling pathways (reviewed in Bouscarel *et al.* 1999). In addition, a recent paper has suggested that TCDCA activates a PI3K dependent pathways in McNtcp.24 cells that leads cellular survival from bile acid cytotoxicity (Rust *et al.* 2000). Consistent with the findings of this study, a 30 min pretreatment of McNtcp.24 cells with 20 μM of the PI3K inhibitor, LY-294002, resulted in sensitivity to TCA or TCDCA (Fig. 5-10A). In addition, pretreatment of McNtcp.24 cells with either TCDCA or TCA ameliorated the cytotoxic effects of GCDCA (Fig. 5-10B), suggesting that induction of a "protective pathway" by taurine-conjugated bile acids is dominant over the apoptotic pathway activated by glycine-conjugated bile acids. The inability of taurine-conjugated bile acids to activate survival pathways in CHO.asbt.35 cells may help to explain the sensitivity of this cell line to both taurine and glycine conjugated bile acids. I therefore assayed PI3K activity in crude cellular membrane preparations from bile acid-treated cells. As shown in Fig. 5-11, treatment of CHO.asbt.35 cells with amidated bile acids did not result in a significant increase in PI3K activity, suggesting that bile acids do not activate a survival pathway in these cells. In contrast, treatment of McNtcp.24 cells with TCA and TCDCA significantly increased PI3K activity (Fig. 5-11), consistent with the experiments using the LY-294002 compound (see Fig. 5-10A).

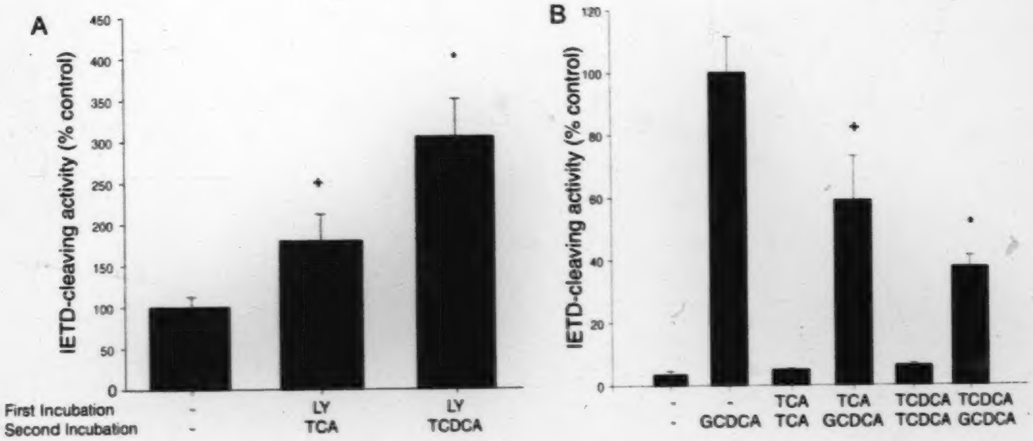

Fig 5-10 Caspase 8 activity in bile acid-treated McNtcp.24 cells after pretreatment with LY-294002. **A**. McNtcp.24 cells were incubated for 30 min with 20 μM of the specific PI3K inhibitor LY-294002 prior to a 2 h challenge with 100 μM TCA or TCDCA. Caspase 8 activity was then assayed in cellular extracts as described Section 5.2.4. Differences in comparison to control cells were evaluated using a Student's t-test **B**. McNtcp.24 cells were incubated with TCA or TCDCA for 30 min before 1 h incubation with 50 μM GCDCA. The data (means ± SD, n=3) is representative of several experiments. Differences in comparison to GCDCA-treated cells were evaluated using a Student's t-test. + = $p<0.05$, * = $p<0.001$

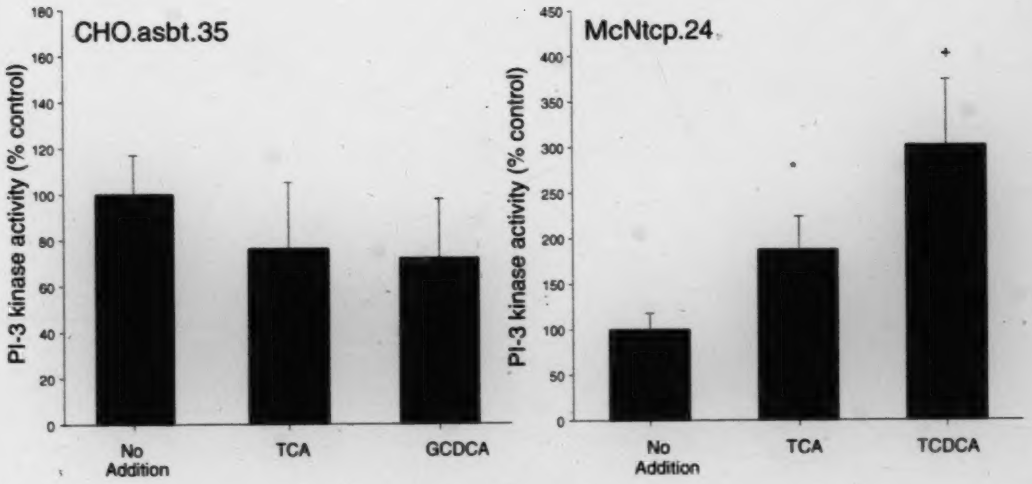

Fig 5-11 PI3K activity in bile acid-treated cells. Cells treated with 100 μM bile acid for 1 h and crude membrane fractions were isolated as described Section 5.25. **A**. TCA treatment did not activate PI3K in membrane fractions of CHO.asbt.35 cells. **B**. In contrast, both TCA and TCDCA induced the activation of PI3K in McNtcp.24 cells. The data (mean ± SD, n=3) is representative of several experiments. Differences in comparison to control cells were evaluated using a Student's t-test. * = $p<0.02$, + = $p<0.01$

5.3.5 Cytotoxic Potential of bile acids in HBAB-expressing McNtcp.24 cells

Activation of survival pathways provides a mechanism by which hepatocytes may escape the potential toxic effects of bile acids. As detailed in Chapter 1, 3HSD has been proposed to play a role in hepatocyte bile acid transport (Stolz *et al.* 1989) and may protect hepatocytes from potentially cytotoxic bile acids. The human bile acid binder (HBAB) is a high-affinity bile acid binding version of the rat 3HSD (Stolz *et al.* 1993[illegible]o determine if sequestration of bile acids could rescue McNtcp.24 cells from apoptosis induced by glycine-conjugated bile acids, I introduced a HBAB expression plasmid into McNtcp.24 cells. Several clones were chosen following the selection procedure for further analysis. These cell lines were designated as BNs, and had 200 to 1000 times greater expression of the HBAB transgene compared to the parental cell line (Fig. 5-12A). A commensurate level of HBAB protein was present in cellular extracts from these BN cells (Fig 5-12B).

To determine if the expression of HBAB affected cellular transport in BN cells, I examined both cellular uptake and efflux of [^{3}H]-TCA in these cells. As shown in Fig. 5-13A, BN.16 and BN.25 cells had similar ability to accumulate bile acids from the culture medium compared to McNtcp.24 cells. Although BN. 30, 49 and 46 displayed a modest increase in bile acid uptake (~30% increase), the high level of HBAB mRNA abundance (200-1000 times) in these cells did not correlate with the overall increase in transport activity (see Fig. 5-12 and 5-13). As depicted in Fig. 5-13B, expression of HBAB did not appear to affect the ability of these cells to secrete radiolabeled bile acids. These experiments suggest that HBAB expression does not overtly affect cellular uptake and secretion of bile acids under the experimental conditions used.

Since GCDCA was the most potent cytotoxin to McNtcp.24 cells (Fig. 5-2), I used this bile acid to test the ability of HBAB to protect BN cells against bile acid

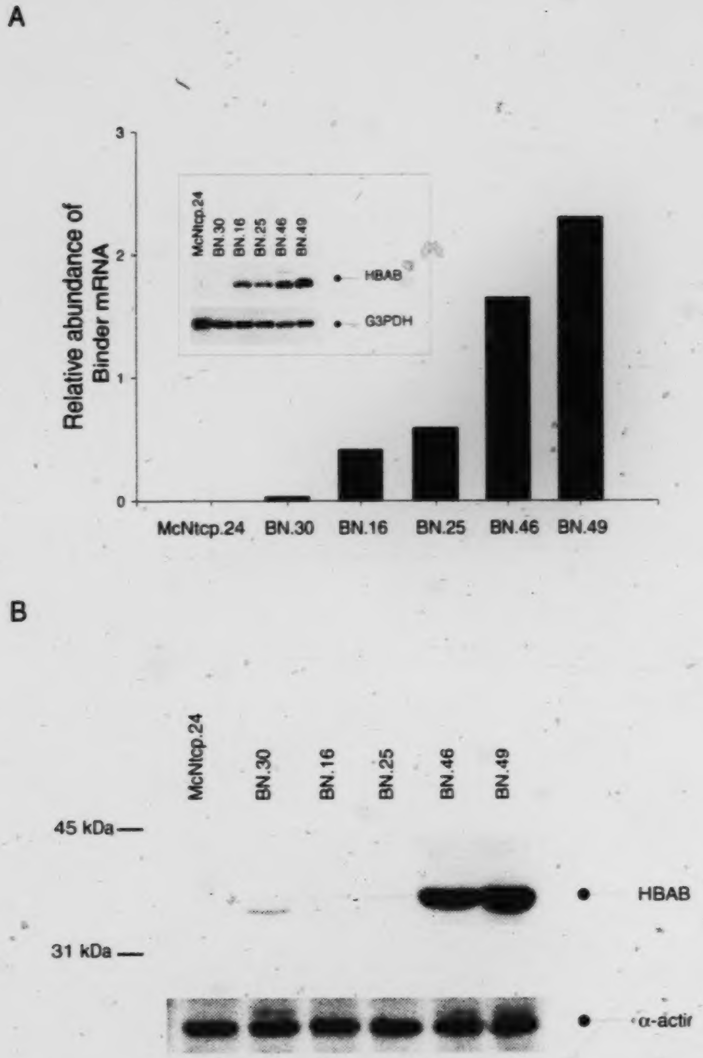

Fig 5-12 Stable expression of HBAB in McNtcp.24 cells. **A**. Total RNA was isolated from BN, McNtcp.24 and McArdle RH-7777 cells and the relative abundance of the 2.O kb HBAB message detected by RNA blotting using a HBAB cDNA probe. The blots were stripped and reprobed with G3PDH cDNA. **B**. Detection of HBAB and α-actin protein in cellular extracts from BN and McNtcp.24 cells by immunoblotting.

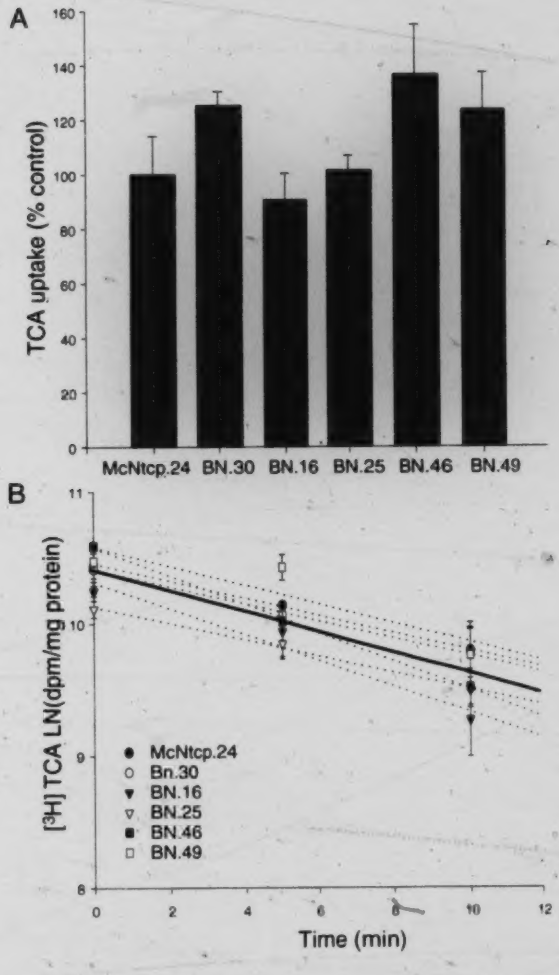

Fig 5-13 TCA uptake and efflux in BN and McNtcp.24 cells. **A**. Uptake of TCA from the culture media by BN and McNtcp.24 cells. The values represent the % uptake of TCA compared to McNtcp.24 cells. **B**. Efflux of TCA from BN and McNtcp.24 cells. Cells were incubated with 25 μM radiolabeled TCA for 20 min to label the intracellular pool of bile acids and the amount of radioactivity retained by the cells was determined as described in Chapter 2. The natural log of the means ± SD (n=3) are shown for each time point. The slopes of regression lines obtained from BN were compared to the slope of the regression line obtained from McNtcp.24 cells by analysis of variance. There was no statistical difference between the slopes of these curves.

induced cytotoxicity. As shown in Fig. 5-14A, LDH activity in culture media of BN cells treated with 100 µM GCDCA was not different than that in the medium of GCDCA-treated McNtcp.24 cells. As shown in Fig. 5-14B, expression of HBAB did not prevent the activation of caspase 8 after incubation of BN cells with 50 µM GCDCA. It would thus appear that expression of HBAB does not protect cells from the bile acid induced cytotoxicity.

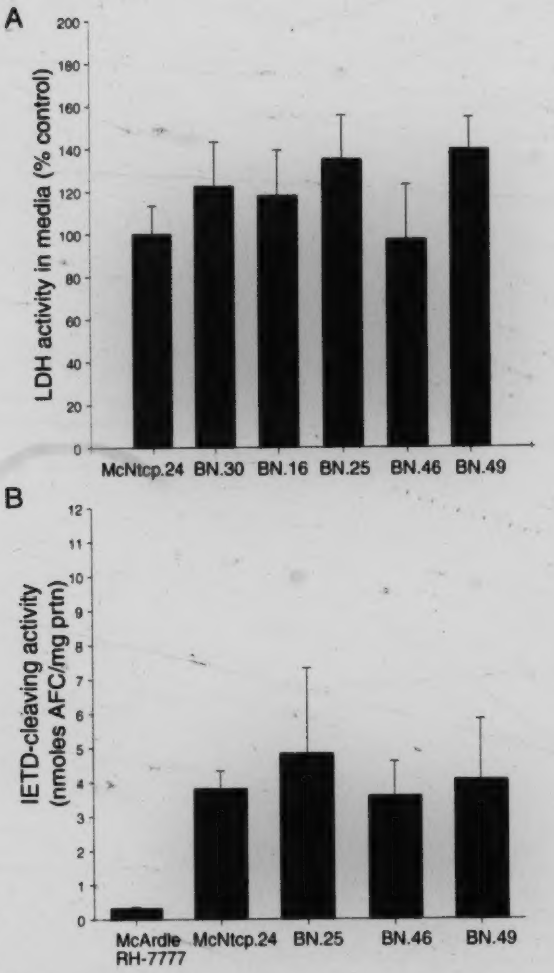

Fig 5-14 Cytotoxic potential of GCDCA in BN and McNtcp.24 cells. **A**. Cells were treated with 100 μM GCDCA for 4 h and LDH activity in the media and cells was assayed. The values (means ± SD, n=6) represent % of LDH activity in the media of BN cells compared to McNtcp.24 cells. **B**. Cells were treated with 50 μM GCDCA for 1 h and caspase 8 activity was assayed in cellular extracts as detailed in Section 5.2.4. Expression of HBAB in McNtcp.24 did not prevent the activation of caspase 8 by GCDCA. Caspase 8 activity in GCDCA-treated McArdle RH-7777 is shown as an additional control. The means ± SD (n=3) are shown.

5.4 DISCUSSION

The last few years have brought great progress in understanding how hepatocytes and ileocytes take up and secrete bile acids. However, the molecular fate of bile acids within these cells remains poorly understood. With the current interest in how bile acids regulate gene transcription via FXR, understanding how bile acids can modulate cellular function is important in interpreting any *in vitro* experiment using cells that transport bile acids. To gain further insight into how bile acids can be toxic to cells, I stably expressed a bile acid transporter in the non-bile acid transporting cell line, Chinese hamster ovary cells (CHO). CHO.asbt cells expressed recombinant asbt of approximately 48-kDa, and displayed bile acid uptake activity which was saturable with an apparent K_m ranging from 22 to 25 μM. The molecular weight and K_m are consistent with reported values for recombinant asbt (Wong *et al.* 1994; Sippel *et al.* 1997). These observations suggest that asbt is fully functional in CHO.asbt cells. It is not known if CHO cells have pathways capable of facilitating the efflux of bile acids. A related system that recognizes bile acids may exist in CHO cells and other mammalian cells. The apparent efflux observed in CHO.asbt.35 cells could be attributed to the fact that asbt is a bidirectional transporter of bile acids (Weinman *et al.* 1998). Moreover, yeast cells and plants express ABC related proteins capable of active bile acid transport (Ortiz *et al.* 1997). Because these organisms do not make bile acids, bile acid transport in these cells may represent a generalize pathway for cellular excretion of organic anions.

I challenged CHO.asbt.35 cells with both taurine- and glycine-conjugated bile acids to determine their cytotoxic potential in this non-hepatic derived, bile acid transporting cell line. Upon TCA treatment, CHO.asbt.35 or other clones did not evolve the vesicle structures observed in McNtcp.24 cells under identical experimental conditions (Chapter 4). This observation would imply that the vesicle structures are unique to the McNtcp.24 cells and are indicative of subtle differences between these model systems. More importantly, unlike McNtcp.24 cells, taurine-conjugated bile acid induced cell death, as indicated by the increase of LDH activity in the culture media of CHO.asbt.35 cells. TCA appeared to be the most potent toxin of the taurine-conjugated bile acids tested. Because CA was unable to elicit significant release of LDH into the culture medium of treated CHO.asbt.35 cells, it is unlikely that the observed cytotoxicity of TCA could be attributed simply to the intracellular accumulation of bile acids. In contrast, glycine-conjugated bile acids were both effective at increasing LDH activity in culture medium of both McNtcp.24 and CHO.asbt.35 cells. GCDCA was the most potent of the glycine-conjugated bile acids to induce cell death. Differential sensitivity of liver derived cells to glycine and taurine-conjugated bile acids has been shown in primary hepatocytes culture (Webster *et al.* 1998) as well as in the bile acid-transporting Wif-B cells (Boyer *et al.* 1994). In particular, Wif-B cells tolerated 1mM TCA concentrations in their culture media for 10 days without apparent cytotoxicity (Koniecko *et al.* 1999). However, taurine-conjugated bile acids can be cytotoxic in CHO.asbt.35 cells. The differential sensitivity displayed by McNtcp.24 and CHO.asbt.35 cells to amidated bile acids suggests that liver cells have a mechanism to distinguish and differentially elaborate the biological activities of taurine- and glycine-conjugated bile acids.

Using McNtcp.24 cells and primary mouse hepatocytes, Gores and co-workers have shown that glycine conjugated bile acids (GDCA, DCA) induced apoptosis through activation of the Fas receptor in a FasL-independent manner (Faubion *et al.* 1999). Moreover, they demonstrated that GCDCA activates both initiator and effector caspases (Wolf *et al.* 1999), and that the apoptotic response can be blocked with the caspase 8 inhibitor, Crm A (Faubion *et al.* 1999). The mechanism by which bile acids stimulate the activation of Fas receptor remains unclear. In Fas deficient hepatocytes, toxic bile acids were still able to induce cell death, implying that bile acids may signal through multiple pathways to initiate cell death (Miyoshi *et al.* 1999).

Both glycine- and taurine-conjugated bile acids induce apoptotic cell death in CHO.asbt.35 cells, as demonstrated by the presence of genomic DNA fragmentation in treated cells. Involvement of the caspase cascade in CHO.asbt.35 cells was shown by the fact that amidated bile acids activate both caspase 8 and caspase 3. Interestingly, caspase 3 has been implicated in CHO apoptosis induced by staurosporine (Wang *et al.* 1996), and indicates that different apoptotic stimuli may signal through the same effector molecules, at least in this cell line. At this time, It is not clear how amidated bile acids activate caspases in CHO.asbt.35 cells. Activation of caspases does not appear to be related to expression of asbt in CHO.asbt.35 cells because TCA did not induce cell death or activate caspase 8 in McArdle RH-7777 cells expressing asbt. The differential response observed in McNtcp.24 cells to amidated bile acids would appear to depend on activation of a PI3K dependent survival pathway. Consistent with the findings of a previous report (Rust *et al.* 2000), pretreatment of McNtcp.24 cells with low concentrations of LY-294002 rendered these cells susceptible to the TCA and TCDCA cytotoxicity. TCA did not increase PI3K activity in CHO.asbt.35 cells, implying a mechanism to explain the different response observed with taurine-conjugated bile acids in these cell lines. Although inhibition of PI3K activity in McNtcp.24 cells rendered these cells susceptible to apoptosis, I have shown that extended incubations of McNtcp.24 cells with TCA does not result in permanent cellular damage and these cells continue to grow after removal of TCA from the culture medium (Chapter 4). This observation implies either that taurine-conjugated bile acids are not inherently toxic to liver derived cell lines, or that inhibition of signaling pathways may make these cells indirectly susceptible to bile acids. Activation of PI3K by TCA in membrane fractions from McNtcp.24 is consistent with the findings that show increased PI3K activity in canalicular membrane vesicles after TCA treatment (Misra *et al.* 1998). However, activation of type I PI3K in this report was associated with recruitment of p-sister of glycoprotein and other multidrug resistance gene proteins to the canalicular membrane (Misra *et al.* 1998). Activation of phosphatidylinositol kinases may help to explain the vesicle formation observed when McNtcp.24 cells were incubated with TCA for extended periods (Chapter 4).

I have shown that different species of amidated bile acids can be differentially cytotoxic in McNtcp.24 cells. However, the role of cytosolic bile acid binding proteins in conferring cytoprotection against the toxic effects of bile acids remains unknown. Several proteins that bind bile acids have been identified in hepatocytes (review in Agellon *et al.* 1999). The balance of the available data suggest that 3HSD is the major bile acid binding protein in the cytosol of rat hepatocytes (Stolz *et al.* 1989). However, the role of this class of protein in bile acid transport remains unproven. The human bile acid binder (HBAB), which binds bile acids with high affinity, is thought to play a similar role in human hepatocytes (Stolz *et al.* 1989). With the intent of increasing the intracellular bile acid binding capacity in McNtcp.24 cells, I expressed HBAB in these cells. HBAB expression had a negligible effect on the ability of the BN cells to take up or secrete bile acids. Expression of HBAB did not prevent GCDCA from inducing cell death in BN cells (Fig. 5-14). Interestingly, BN cells also formed intracellular vesicles with TCA observed with McNtcp.24 cells.

Given the high rate of bile acid uptake in the parental cell line, McNtcp.24, the level of bile acids associated with a single cell may be higher than the number of HBAB molecules expressed in that cell. From Fig 3-6 and assuming that a single cell has 300 pg of total protein (Darnel *et al.* 1986), there would be 2.55×10^{-15} moles or 1.56×10^{9} molecules of taurocholic acid associated with a single cell at steady-state levels of bile acid uptake. Assuming that HBAB (36-kDa) constitutes

5% of total cellular protein in BN.49 cells, then 4.17 x 10^{-16} moles or 0.25 x 10^{9} molecules of HBAB would be expressed per cell. However, because bile acids interact with organelles and other cellular proteins (see Section 1.3), the actual concentration of free bile acids within a cell may be much lower than the value calculated above. Future studies are needed to determine the relationship between the free bile acid concentration and the total cytosolic bile acid binding capacity of BN cells.

5.5 REFERENCES

Agellon, L.B. and E.C. Torchia (1999). Intracellular transport of bile acids. *Bioch. Biophys. Acta* 1486: 198-209

Arcaro, A. and M.P. Wymann (1993). Wortmanin is a potent phosphatidylinositol 3-kinase inhibitor: the role of phosphatidyl 3,4,5 -trisphosphate in neutrophil responses. *Biochem. J.* 296: 297-301.

Bouscarel, B., S.D. Kroll and H. Fromm (1999). Signal transduction and hepatocellular bile acid transport: cross talk between acids and second messengers. *Gastroenterology* 117: 433-452.

Boyer, J.L., O. Ng, M. Ananthanarayanan, A.F. Hofmann, C.D. Schteingart, *et al.* (1994). Expression and characterization of a functional rat liver Na+ bile acid cotransport system in COS-7 cell. *Am. J. Physiol.* 266(29): G382-G387.

Budihardjo, I., H. Oliver, M. Lutter, X. Luo and X. Wang (1999). Biochemical pathways of caspase activation during apoptosis. *Annu. Cell. Dev. Biol.* 15: 269-90.

Courtneidge, S.A., A.D. Levinson and J.M. Bishop (1980). The protein encoded by the transforming gene of avian sarcoma virus (pp60 src) and a homologous protein in normal cells (pp60 proto-src) are associated with the plasma membrane. *Proc. Natl. Acad. Sci. USA* 77: 3783-3787.

Darnell, J. E., H. F. Lodish, and D. Baltimore (1986). Molecular cell biology. New York, Scientific American books, distributed by W.H. Freeman: 137.

Earnshaw, W.C., L.M. Martins and S.H. Kaufmann (1999). Mammalian caspases: structure, activation, substrates, and functions during apoptosis. *Annu. Rev. Biochem.* 68: 383-424.

Faubion, W.A., G.M. E, H. Miyoshi, S.F. Bronk, P.J. Roberts, *et al.* (1999). Toxic bile salts induce rodent hepatocyte apoptosis via direct activation of Fas. *J. Clin. Invest.* 103: 137-145.

Gustafsson, J.A. (1999). Seeking ligands for lonely orphan receptors. *Science* 284: 1285.

Hagenbuch, B. (1997). Molecular properties of hepatic uptake systems for bile acids and organic anions. *J. Membrane. Biol.* 160: 1-8.

Hagenbuch, B., B. Stieger, M. Foguet, H. Lubbert and P.J. Meier (1991). Functional expression cloning and characterization of hepatocyte Na+/bile acid cotransport system. *Proc. Natl. Acad. Sci. U.S.A.* 88: 10629-10633.

Koniecko, E.M. and J.M. Crawford (1999). Trophic effects of taurocholate on bile secretory phenotype of Wif-B hepatoma cells. in Falk symposium: Bile Acids and Cholestasis (Titisee, Germany). G. Paumgartner, A. Stiehl, W. Gerok, D. Keppler and U. Leuschner, Kluwer Academic Publishers, Lancaster. 108: 166-171.

Lin, Y., R. Havinga, I.J. Schippers, H.J. Verkade, R.J. Vonk, *et al.* (1996a). Characterization of the inhibitory effects of bile acids on very-low-density lipoprotein secretion by rat hepatocytes in primary culture. *Biochem. J.* 316: 531-538.

Lin, Y., R. Havinga, H.J. Verkade, H. Moshage, M.J. Slooff, *et al.* (1996b). Bile acids suppress the secretion of very-low density lipoprotein by human hepatocytes in primary cultures. *Hepatology* 23: 218-28.

Love, M.W. and P.A. Dawson (1998). New insights into bile acid transport. *Current Opinion in Lipidology* 9: 225-229.

Makishima, M., A.Y. Okamoto, J.J. Repa, H. Tu, R.M. Learned, *et al.* (1999). Identification of a nuclear receptor for bile acids. *Science* 248: 1362-1365.

Misra, S., P. Ujhazy, Z. Gatmaitan, L. Varticovski and I.M. Arias (1998). The role of phosphoinositide 3-kinase in taurocholate-induced trafficking of ATP-dependent canalicular transporters in rat liver. *J. Biol. Chem.* 273: 26633-26644.

Miyoshi, H., C. Rust, P.J. Roberts, L.J. Burgart and G.J. Gores (1999). Hepatocyte apoptosis after bile duct ligation in the mouse involves Fas. *Gastroenterology* 117: 669-677.

Ortiz, D.F., M.V. St. Pierre, A. Abdulmessih and I.M. Arias (1997). A Yeast ATP-binding Cassette-type protein mediating ATP-dependent bile acid transport. *J. Biol. Chem.* 272: 15358-15365.

Parks, D.J., S.G. Blanchard, R.K. Bledsoe, G. Chandra, T.G. Consler, *et al.* (1999). Bile acids: natural ligands for an orphan nuclear receptor. *Science* 284: 1365-1368.

Patel, T., S.F. Bronk and G.J. Gores (1994). Increases of intracellular magnesium promote glycodeoxycholate-induced apoptosis in rat hepatocytes. *J. Clin. Invest.* 94: 2183-2192.

Roberts, L.R., H. Kurosawa, S.F. Bronk, P.J. Fesmier, L.B. Agellon, *et al.* (1997). Cathepsin B contributes to bile salt-induced apoptosis of rat hepatocytes. *Gastroenterology* 113: 1714-1726.

Russell, D.W. (1999). Nuclear orphan receptors control cholesterol catabolism. *Cell* 97: 539-542.

Rust, C., L.M. Karnitz, C.V. Paya, M. J, R.D. Simari, et al. (2000). The bile acid taurochenodeoxycholate activates a phosphatidylinositol 3-kinase-dependent survivalsignaling cascade. *J. Biol. Chem.* 275: 20210–20216.

Sippel, C.J., P.A. Dawson, T. Shen and D.H. Perlmutter (1997). Reconstitution of bile acid transport in a heterologous cell by cotransfection of transporter for bile acid uptake and efflux. *J. Biol. Chem.* 272: 18290-18297.

Stennicke, H.R. and G.S. Salvesen (1997). Biochemical characteristics of caspase-3, -6, -7, and -8. *J. Biol.Chem.* 272: 25719-25723.

Stennicke, H.R. and G.S. Salvesen (1999). Caspases: preparation and characterization. *Methods* 17: 313-319.

Stolz, A., L. Hammond, H. Lou, H. Takikawa, M. Ronk, *et al.* (1993). cDNA cloning and expression of the human hepatic bile acid-binding protein. *J. Biol. Chem.* 268: 10448-10457.

Stolz, A., H. Takikawa, M. Ookhtens and N. Kaplowitz (1989). The role of cytoplasmic proteins in hepatic bile acid transport. *Ann. Rev. Physiol.* 51: 161-76.

Talanian, R.V., C. Quinlan, S. Trautz, M.C. Hackett, J.A. Mankovich, *et al.* (1997). Substrate specificities of caspase family proteases. *J. Biol. Chem.* 272: 9677-9682.

Torchia, E.C., S.K. Cheema and L.B. Agellon (1996). Co-ordinate regulation of bile acid biosynthetic and recovery pathways. *Bioch. Biophys. Res. Com.* 225: 128-133.

Traynor-Kaplan, A.E., B.L. Thompson, A.L. Harris, P. Taylor, G.M. Omann, *et al.* (1989). Transient increase in phosphatidylinositol 3,4-bisphosphate and phosphatidylinositol trisphosphate during activation of human neutrophils. *J. Biol. Chem.* 264: 15668-15673.

Wang, H., J. Chen, K. Hollister, L.C. Sowers and B.M. Forman (1999). Endogenous bile acids are ligands for the nuclear receptor FXR/BAR. *Mol. Cell* 3: 543-553.

Wang, X., N.G. Zelenski, J. Yang, J. Sakai, M.S. Brown, *et al.* (1996). Cleavage of sterol regulatory element binding proteins(SREBPs) by CPP32 during apoptosis. *EMBO J.* 15(5): 1012-20.

Webster, C.R.L. and M.S. Anwer (1998). Cyclic adenosine monophosphate-mediated protection against bile acid-induced apoptosis in cultured rat hepatocytes. *Hepatology* 27: 1324-1331.

Weinman, S.A., M.W. Carruth and P.A. Dawson (1998). Bile acid uptake via the human apical sodium-bile acid cotransporter is electrogenic. *J. Biol. Chem.* 273: 34691-5.

Wolf, B.B. and G.D. R (1999). Suicidal tendencies: apoptotic cell death by caspase family proteinases. *J. Biol. Chem.* 274: 20049-30052.

Wong, M.H., P. Oelkers, A.L. Craddock and P.A. Dawson (1994). Expression cloning and characterization of the Hamster ileal sodium-dependent bile acid transporter. *J. Biol. Chem.* 269: 1340-1347.

Wyllie, A.H. (1980). *Nature* 284: 555-556.

Chapter 6: Disruption of the murine ilbp gene

6.1 INTRODUCTION

As detailed in Chapter 1, the enterohepatic circulation (EHC) of bile acids is very efficient, and small losses of bile acids from the EHC are replenished daily by bile acid production in the liver. The activities of bile acid transporters in the liver and small intestine are crucial for efficient circulation of bile acids enterohepatically. Defects in the bile acid biosynthetic or recovery pathways, as illustrated by the gene disruption of cyp7a (Ishibashi et al. 1996) or by mutations in the human asbt gene (Oelkers et al. 1997), can seriously compromise the size of bile acid pool in EHC and lead to malabsorption of lipophilic nutrients in the proximal gut. In contrast to the defined role of bile acid transporters, the role of intracellular bile acid binding proteins in the trafficking of bile acids in the EHC remains unclear. I have shown in Chapter 5 that expression of a putative intracellular bile acid binding protein, HBAB, was unable to protect McNtcp.24 cells from cytotoxic bile acids or overtly affect the ability of these cells to take up or secrete bile acids.

Another putative intracellular bile acid protein is the ileal bile acid binding protein (ilbp). As discussed in Section 1.3.2, several studies have implicated *ilbp* in the reclamation of bile acids in the ileum (Kramer *et al.* 1993; Kramer *et al.* 1995; Kramer *et al.* 1997; Kramer *et al.* 1998). Ilbp may modulate asbt function and/or translocate bile acids from the apical to basolateral membranes of ileocytes for secretion. To determine if ilbp expression is crucial for the conservation of bile acids in the EHC, I undertook the targeted disruption of the murine *ilbp* gene. In the present Chapter, I describe the construction and initial characterization of *ilbp* null mice.

6.2 METHODS

6.2.1 Construction of targeting vector for the *ilbp* gene

Bac clones containing the murine *ilbp* gene were isolated from a 129/SV Mouse embryonic stem (ES) genomic library (Genome Systems Inc., St. Louis, MO). The library was screened by Dr. Liqing Yu, a former post-doctoral fellow in Dr. L. B. Agellon's Lab, by DNA amplification using primers (set 1(*ilbp*A1,B1), set 2(*ilbp*A2,B2)

Sense *ilbpA1*: 5’-AGT AGT GGC TAG CCT TCC TTC A-3’
Antisense *ilbpB2*: 5’-GCC TGC CAG CGA TCC TTA A-3’

Sense *ilbpA2*: 5’-CCA GTG TGG TCA ATT CTG C-3’
Antisense *ilbpB2*: 5’-TGG ATG GAT GAG TTC TGT CC-3’

based on the published murine *ilbp* gene sequence (Crossman *et al.* 1994). Set 1 was designed to generate a 313-bp amplification product from the 3‘ end of the *ilbp* gene, spanning exon IV; set 2 was designed to generate a 1017- bp amplification product from the 5’ end of the *ilbp* gene. Clones isolated from the library were characterized by restriction enzyme mapping. Restricted DNA was then blotted and hybridized with *ilbp* cDNA (Crossman *et al.* 1994) and exon IV DNA radiolabeled probes. BamHI fragments containing all four exons of the *ilbp* gene (see Fig. 6-1A) were subcloned into the pZero plasmid (Invitrogen, Carlsbad, CA) and further characterized by restriction enzyme mapping. The pKO scrambler vector V915 (Lexicon genetics Inc., Woodland, TX) was used as a scaffold to construct the *ilbp* targeting plasmid. Fragments containing exons I and IV of the *ilbp* gene were subcloned into pV915 as depicted in Fig. 6-1B. DNA cassettes expressing the Neomycin phosphotransferase and Herpes thymidine kinase (TK) genes (Lexicon genetics Inc., Woodland, TX) were then sub-cloned into the AscI and RsrII restriction sites, respectively, on the V915 vector. The Neomycin phosphotransferase gene confers resistance to the antibiotic G418, while the TK gene confers sensitivity to nucleoside analog such as [1-(2'-deoxy-2'-flouro-b-D-arabinofuranosyl)-5-iodouracil] or FIAU.

6.2.2 Disruption of ilbp gene in R1 ES cells

I performed the following experiments at the Embryonic Stem Cell Targeted Mutagenesis Facility (ESTM) at the University of Calgary. R1 ES cells (Nagy *et al.* 1993) were cultured as outlined in Section 2.2. To generate R1 cells containing a mutated *ilbp* allele, 100 µg of the *ilbp* targeting vector (Section 6.2.1, and Fig. 6-1B) was linearized by a Sal I digest, electroporated into 1.4 x 10^7 RI ES cells using a Bio-Rad Gene pulser (Bio-Rad Laboratories, Mississauga, ON) at 230 V, 500 µF. ES cells that underwent homologous recombination at the *ilbp* locus were enriched by positive-negative selection using G418 (300 µg/ml) and FIAU (1.25 µM) as described in (Tsuzuki *et al.* 1998). G418/FIAU resistant cell lines were isolated, expanded, and screened for targeting events by DNA amplification using primers (PA1, PB1) based on the predicted sequence of a targeted *ilbp* allele (See Fig. 6-1C). The cycle profile was: 95 °C for 5 min, 30 cycles of [95 °C for 1 min, 55 °C for 2 min, 72 °C for 2 min], 72 °C for 10 min, 4 °C hold. This primer set amplified a unique 1.7-kb fragment from the new junction created by homologous recombination at the 5' end of the *ilbp* gene (Fig. 6-1C). DNA from positive cell lines was then digested with Xba I, fractionated by agarose electrophoresis, blotted, and hybridized with an exon IV radiolabeled probe.

Sense	PA1: 5'-GCA GAG GAT CAG GAG ATT CAG-3'
Antisense	PB1: 5'-GCG CAT GCT CCA GAC TGC CTT G-3'

6.2.3 Production of germ line competent chimeras and genotyping of germline progeny.

Cell lines from Section 6.2.2 containing the mutated *ilbp* allele were karyotyped as previously described (Nagy *et al.* 1993). Briefly, growing cells were treated with 0.05 µg/ml colcemid (Life Tech., Burlington, ON) for 90 min at 37 °C. Colcemid prevents the formation of the spindle apparatus responsible for cell division, thereby arresting cells at the metaphase stage of mitosis. The cells were collected and incubated in a 0.075 M KCl (hypotonic) solution, fixed in methanol:acetic acid (3:1, v:v), spotted onto clean slides and left on a slide warmer at 60 °C for 18 h. Slides were then dipped into PBS containing 1% Giemsa for 3 min, subsequently rinsed in distilled $H_2$0, and dried at 60 °C for 16 h. Slides were examined by light microscopy and the chromosomal spreads counted. Cell lines having a strong modal number of 40 in their karyotypes and absence of gross abnormalities in chromosomal ultrastructure were injected into C57BL/6 blastocysts for chimera production. Technicians at ESTM facility injected 6-10 ES cells from selected cell lines into the blastocoel cavity of C57BL/6 embryos and transferred surviving blastocysts to the uteri of pseudopregnant C57BL/6 females. Pseudopregnant mice were generated by mating females with vasectomized males. Chimeric animals were backcrossed to C57BL/6 mice to determine germ line competency. F1 animals and their progeny were screened from DNA isolated from tail biopsy by DNA amplification using three primers (PA2, PB1, PB2) based on the

Sense	PA2: 5'-ACG ATG AGT TCA TGA AGC GC-3'
Antisense	PB2: 5'-TCC TTG ACA ATT GCA TGG C-3'
	PB1: (see section 6.2.2 for sequence)

sequence of the wild type and mutated ilbp alleles (see Fig. 6-1). Primers PA2 and PB2 amplified a 1145-bp fragment from a wild type *ilbp* allele, while primers PA2 and PB1 amplified a 450-bp fragment from a *ilbp* mutated allele. The genotype of animals was confirmed by DNA blot analysis as described for ES cells (Section 6.2.2). F1 heterozygous animals were subsequently crossed to generate mice homozygous for the *ilbp* gene mutation. Chimeric and F1 animals were initially housed at the ESTM facility. Because this facility was infected with the murine hepatitis virus (mhv), F1 mice were not transferred to the University of Alberta Health Sciences Laboratory Animal Service (HSLAS) until their progeny could be cleansed of mhv. To remove this pathogen, embryos from heterozygous mating (F2 mice) were implanted into the uteri of pseudopregnant females at HSLAS. Mice born at HSLAS with the *ilbp* mutation were used to establish a breeding colony. In addition, the mice born at the HSLAS are currently being backcrossed with C57BL/6 animals to dilute the contribution of the 129 genetic strain. For the purpose of this thesis, the initial characterization of *ilbp* null mice was done on mice of mixed genetic background (129:C57BL/6).

6.2.4 Bile acid analysis

The liver, gall bladder and intestine of 55-day old mice were collected and snap frozen in liquid nitrogen. Extraction of bile acids was done as previously detailed (Hedenborg *et al.* 1986). Briefly, frozen tissue was homogenized in 95% ethanol containing 0.1% ammonia. Homogenates were incubated at 80 °C after addition of [24-^{14}C]-GCA (<2 nmols per sample) as an internal standard. Resulting extracts were filtered and a fraction from each extract was dried down and resuspended in 1 ml of methanol. A 100-µl aliquot was dried down for scintillation counting. Concentration of total bile acids was determined using a diagnostic bile acid kit from the Sigma corp. (St. Louis, MO). Individual bile acid species were resolved on silica G HPTLC plates (Merck Ltd., Darmstadt, Germany) using a mobile phase containing n-butanol, glacial acetic acid, water (7:1:2, v:v:v) to resolve conjugated bile acids (Robb *et al.* 1984) and a mobile phase containing iso-octane, ethylacetate, acetic acid, n-butanol (10:5:1.5:1.5, v:v:v:v) to resolve free bile acids (Sundaram *et al.* 1971).

6.3 RESULTS

6.3.1 targeted gene disruption of the *ilbp* locus in ES cells

As detailed in Section 1.3.2, *ilbp* is a single copy gene (Crossman *et al.* 1994) belonging to the family of small cytosolic lipid binding proteins (lbp) (Bernlohr *et al.* 1997). The primary sequence of the murine *ilbp* gene has been previously published (Crossman *et al.* 1994), and like other members of the lbp family, the *ilbp* gene is composed of 4 exons dispersed within a small region of genomic DNA (~ 6-kb) (Fig. 6-1A). Deletion of the middle exons of the *ilbp* gene should render this gene nonfunctional. In addition, pluripotent murine ES cells are routinely used to generate mice with specific mutations. Thus, a possible strategy to disrupt *ilbp* gene was to replace exons II and III of the *ilbp* gene with a selective marker (e.g. a gene conferring Neomycin resistance, Neo^r) in murine ES cells and use these cells to produce mice harboring a nonfunctional *ilbp* gene.

To introduce a mutation into the *ilbp* locus, I constructed a replacement vector containing homologous DNA from *ilbp* gene. Primers were designed from the published sequence to amplify fragments from the 5' and 3' end of the gene. A 129 ES genomic BAC library was subsequently screened using these primers, and clones containing the *ilbp* gene were isolated, characterized, and sub-cloned as detailed in Section 6.2.1. As shown in Fig. 6-1B, a short region (1.5-kb) of homology containing exon I was cloned between the TK and Neo^r cassettes of backbone vector (pKO V915), and the large region of homology (4.0-kb) containing exon IV was cloned 3' to the Neo^r cassette. The choice for selecting regions of homology to construct the replacement vector was dependent on the availability of endonuclease restriction sites on both the *ilbp* gene and the V915 plasmid.

The linearized targeting vector was introduced into R1 ES cells by

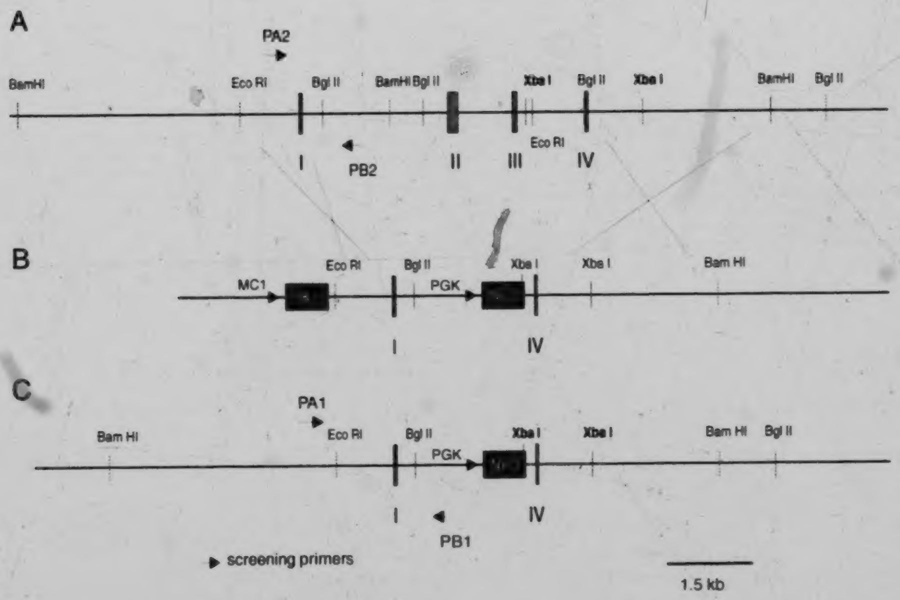

Fig 6-1 Strategy for disrupting the murine *ilbp* locus. **A**. Architecture of the murine *ilbp* gene. It is a single copy gene located on mouse chromosome 11 containing 3 introns and 4 exons. **B.** Structure of ilbp replacement vector. Fragments containing exon I and IV were subcloned into the V915 vector. A Neo^r expression cassette was subcloned between the two *ilbp* regions of homologies. The TK cassette was subcloned 5' of *ilbp* fragments. **C.** After successfully targeting the *ilbp* gene, exon II and III would be replaced with the Neo^r cassette. The arrows depict DNA amplification primers used to identify disrupted and wild type alleles in genomic DNA. Note the position of Xba I restriction sites. These sites were used to devise a strategy for to identify *ilbp* mutated alleles by DNA blotting.

electroporation (Thomas *et al.* 1987). About 50% of ES cells survived electroporation and were cultured as detailed in Section 2.2. After 24 h, the cells were incubated for 10 days in medium containing both G418 and FIAU. G418 selects for ES that have incorporated the Neo^r gene into their genome, while FIAU selects against random insertion (non-homologous recombination) of the targeting vector. This positive and negative selection scheme enriches for cells that have undergone a homologous double recombination event at the *ilbp* locus (Fig. 6-1C).

Surviving ES colonies were isolated, expanded, and screened for the incorporation of the mutated *ilbp* allele. Primers for DNA amplification were designed based on the predicted structure of a mutated *ilbp* allele (Fig. 6-1C). Fig. 6-2A shows the initial screen of 4 ES cell lines using these primers. A unique 1.7-kb fragment was amplified from genomic DNA containing an mutated *ilbp* allele (see below). From the 160 ES cell lines screened, 24 cell lines were positive for the 1.7-kb fragment. A 1.5-kb fragment was also amplified in most reactions (Fig. 6-1C), including reactions with wild type genomic DNA. This band is unrelated to the *ilbp* gene as determined by DNA blotting with an *ilbp* cDNA probe. Cell lines identified by DNA amplification underwent DNA blot analysis to confirm the mutation of the *ilbp* allele. A DNA blotting strategy was devised to take advantage of the presence of Xba I restriction sites in both the endogenous and mutated alleles (see Fig. 6-1A, C). Fig. 6-2B shows the expected hybridization pattern with exon IV radiolabeled probe after Xba I digest of DNA containing the wild type and mutated alleles. The 24 positive clones identified by DNA amplification gave the expected 1.2-kb after DNA blotting analysis (Fig. 6-1C), indicating that these cells contained the correct targeted mutation at the *ilbp* locus. These ES cell lines were expanded and verified for the presence of the mutated *ilbp* allele. Of the 24 cell lines tested, 18 contained the *ilbp* disruption. DNA blotting analysis after Bgl II digestion of ES genomic DNA further verified the genotype of the 18 positive ES cells. As shown in

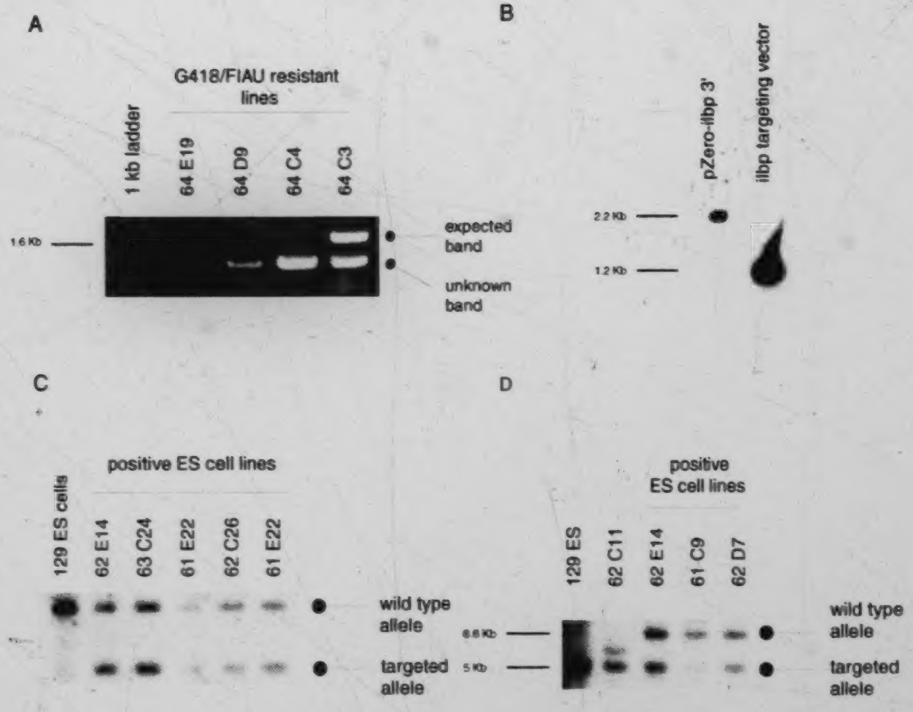

Fig 6-2 Screening of ES cell DNA for presence of a disrupted *ilbp* allele. **A.** Using the primers described in Section 6.2.2, a unique 1.7-kb fragment was identified in ES DNA containing a disrupted *ilbp* allele. An unknown and unrelated band of 1.5-kb was amplified in most reactions. Only cell line 64 C3 in this set showed the expected 1.7-kb band. **B.** Expected hybridization pattern for detecting an ilbp disrupted allele. Digestion of wild type (129) genomic DNA with Xba I yields a 2.2-kb fragment as detected by DNA blotting using an exon IV probe. Digestion of a mutated allele with Xba I yields a fragment of 1.2-kb, confirming the structure of the 3' end of the disrupted gene. **C.** DNA blot analysis after Xba I digestion of positive ES cell line DNA using an exon IV probe. Note the absence of the 1.2-kb band in wild type ES DNA. **D.** DNA blot analysis after Bgl II digestion of DNA from expanded ES cell lines. After hybridization with exon IV probe, detection of a 6.6-kb band confirmed the presence of a mutated allele at the *ilbp* locus. A,C,D are representative of numerous DNA amplification reactions and DNA blot hybridizations.

Fig. 6-2D, digestion of a mutated allele released a unique 6.6-kb band that hybridized with an exon IV radiolabeled probe. Fig. 6-3 summarizes the protocol and time-line to obtain ES cells with a disrupted *ilbp* allele.

6.3.2 Creation of *ilbp*-deficient mice

The ability of ES cells to generate chimeric animals after blastocyst injection and implantation depends on the genetic integrity of the cells. ES cells that have undergone spontaneous mutations (e.g., loss or gain of a chromosome) will have a decreased propensity to form chimeric animals or transmit their genetic information to the germline (Abbondanzo *et al.* 1993; Nagy *et al.* 1993; Stewart 1993). To verify the genetic integrity of the positive ES cell lines identified in the previous section, I karyotyped these cells by making chromosomal spreads of cells arrested during mitosis and counting the numbers of chromosomes (See Section 6.2.3). As shown in Fig. 6-4A, euploid ES cells have 40 acrocentric chromosomes, and deviations from 40 chromosomes (aneuploidy) or presence of metacentric chromosomes (a Robertsonian translocation) (Fig. 6-4A, arrow) indicates a reduced potency of the cells to form chimeras (Abbondanzo *et al.* 1993). Fig. 6-4B shows the distribution of chromosome spreads in two positive ES cell lines. The modal number was 40 in chromosomal spreads from these cells, and no other obvious mutations were observed (e.g. presence of metacentric chromosomes). Chromosomal abnormalities were present in karyotypes of other cell lines, but these were observed infrequently. ES cell lines having a low number of aneuploid karyotypes were injected into C57BL/6 blastocyst for chimera production as detailed in Section 6.2.3.

Chimeric animals were identified by the presence of agouti stripes (coat color of 129 mice) intermingled with areas of black fur (coat color of C57BL/6 mice) (Fig. 6-5A). Resulting chimeras were bred with normal C57BL/6 mice to determine germline

Day	
1	Electroporation of R1 cells 1.4×10^7 cells
2	Begin selection with G418/FIAU
10-13	Pick colonies and transfer to 12 well dishes with MEFs (220 colonies picked)
19-23	Triplate Cells into 12 well dishes (160 colonies grew)
23-26	Freeze 2/3 and 1/3 grown for DNA analysis.
104	Genomic DNA blotting 24 ES (+/-) identified
149	Expand positives for confirmation and karyotype analysis 18 of 24 ES(+/-) cell lines reconfirmed

Fig 6-3 Protocol and approximate time line for generating ES cells with a single disrupted *ilbp*

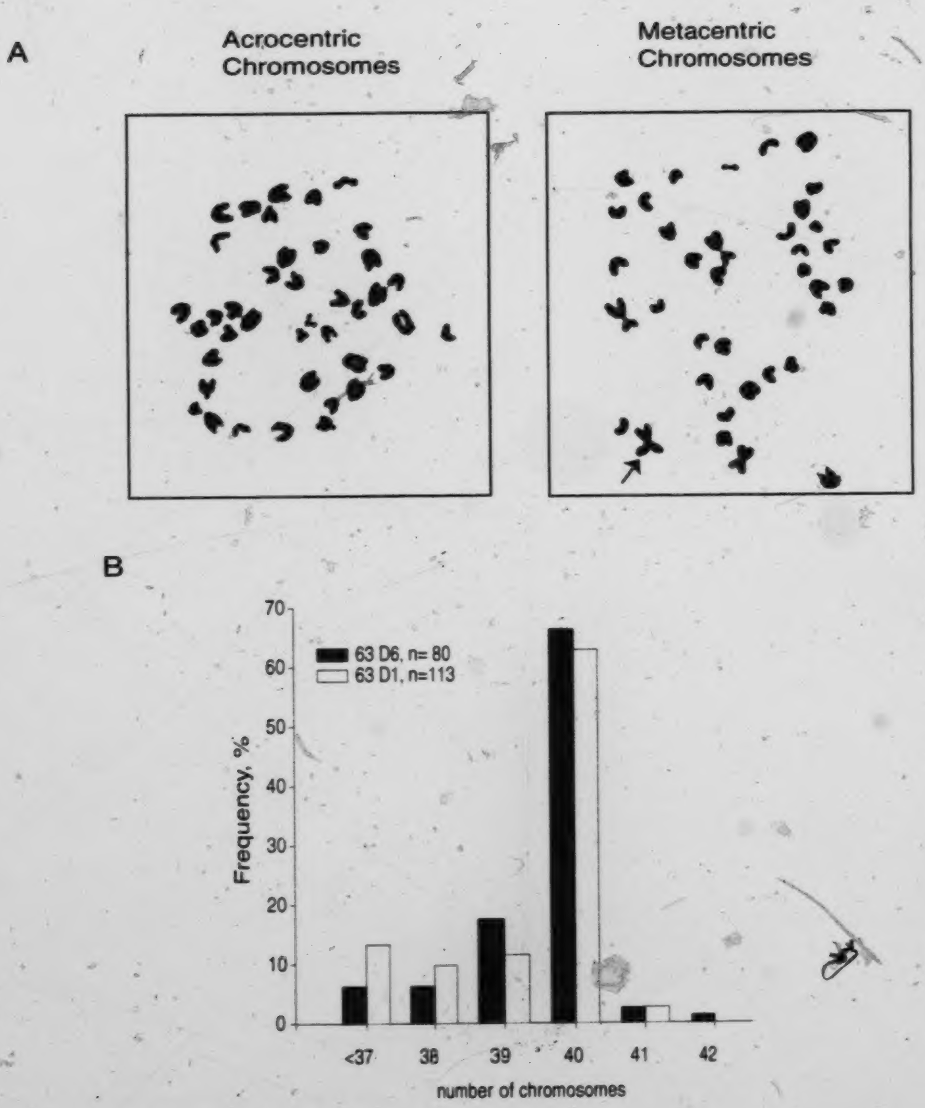

Fig 6-4 Karyotype of positive ES cell lines. Metaphase spreads were prepared as detailed in Section 6.2.3. **A.** The left panel shows the karyotype of euploid ES cell with 40 acrocentric chromosomes. This spread was representative of most karyotypes analyzed. The right panel shows the presence of metacentric chromosomes (arrow) in a chromosomal spread. **B.** Distribution of chromosome spreads from two positive ES cells. Original magnification 800 X.

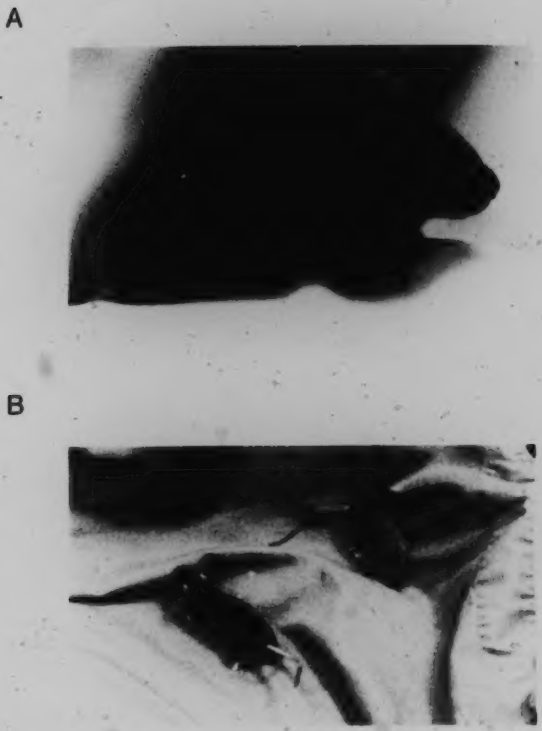

Fig 6-5 A germline chimera and one of its progeny. **A**. Chimeric animals were identified by the presence of agouti strips (light areas) among black fur. This mouse displays 65% or greater chimerism. ES with the *ilbp* mutation contributed to the germ cells of the chimera in (**A**) and gave rise to a 100% agouti pup in (**B**). Note the black C57BL/6 mother.

competency. As shown in Fig 6-5B, the presence of agouti offspring indicated that the phenotype of the 129 derived ES cells had been transmitted to the germline. Of 20 chimeric animals identified and crossed to C57BL/6 animals, only 3 germline mice were obtained (Table 6-1). All 3 germline mice were derived from a single positive ES cell line, designated 63 D6. Chimera production was stopped when I was able to confirm that *ilbp* mutation had been transmitted to the F2 generation (See below).

F1 mice were screened by DNA amplification for the presence of the *ilbp* mutation using the strategy outlined for ES cells (Section 6.2.2). F1 heterozygotes were interbred and the resulting offspring were screened by DNA amplification using primers designed to distinguish between wild type, heterozygous, and homozygous animals (Section 6.2.3). As shown in Fig. 6-6A, I was able to identify mice homozygous for the *ilbp* mutation. The genotype of F2 mice was subsequently confirmed by DNA blot analysis (Fig. 6-6B). These experiments show that I had successfully created mice that carried a gene disruption in the *ilbp* locus.

6.3.3 Characterization of disrupted *ilbp* mice.

To determine if disruption of the *ilbp* locus resulted in a nonfunctional transcript from the *ilbp* promoter, I analyzed the pattern of *ilbp* gene expression in wild type (*ilbp*$^{+/+}$), heterozygous (*ilbp*$^{+/-}$), and homozygous (*ilbp*$^{-/-}$) animals from Section 6.3.2. As detailed in Chapter 1, *ilbp* mRNA expression in the ileum is not detectable until 2 weeks after birth and reaches adult levels near post natal day 50 (Sacchettini *et al.* 1990). Therefore, I collected Ileal sections from 52-day old *ilbp*$^{+/+}$, *ilbp*$^{+/-}$, *ilbp*$^{-/-}$ mice, isolated total RNA, and examined *ilbp* gene expression by RNA blotting. As shown in Fig. 6-7, the 600-bp *ilbp* message was readily detectable in total mRNA in *ilbp*$^{+/+}$, *ilbp*$^{+/-}$ mice. However, *ilbp* mRNA was absent in total RNA from ileal

Targeted Cell lines	Transfers	Live pups	Chimeras	% Chimerism	Germline Transmission
63 D1	7	8	1	30	0
62 E5	9	7	2	20-50	0
63 D16	9	22	4	5-50	0
64 C3	8	14	6	5-40	0
63 D6	8	22	6	40-65	3
63 C24	2	3	1	40	0
totals	43	76	20		3

Table 6-1 Summary of blastocyst injection and chimera production.

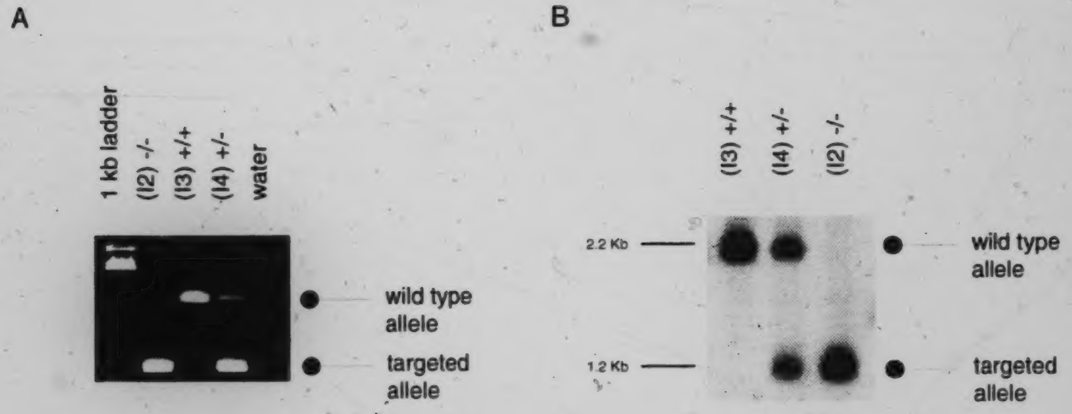

Fig 6-6 Representative genotyping of *ilbp* null mice. **A.** Wild type, heterozygous, and homozygous mice for the *ilbp* mutation were identified using the primers described in Section 6.2.3. A 1145-bp fragment was amplified in Wild type mice, while a 450-bp fragment was amplified in homozygous mice. Amplification of both fragments indicated that the mice were heterozygous for the *ilbp* mutation. **B**. Corresponding DNA blot analysis after Xba I digest of genomic DNA from (**A**). Note the absence of the 2.2-kb band in -/- lane, indicating an *ilbp* null

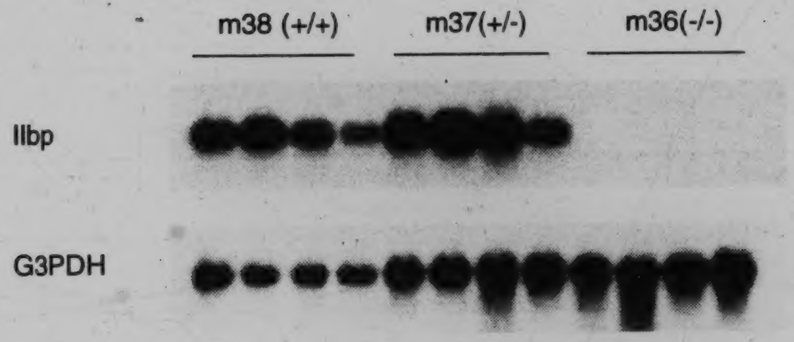

Fig 6-7 Detection of ilbp gene expression in ileal sections of *ilbp*$^{+/+}$, *ilbp*$^{+/-}$, and *ilbp*$^{-/-}$ mice. Total RNA preparations (10 µg) were hybridized with a mouse ilbp cDNA probe. The ilbp message was detected in total RNA from *ilbp*$^{+/+}$, *ilbp*$^{+/-}$ mice. Note the absence of hybridization in the m36(-/-) lane, indicating that the ilbp message not expressed in *ilbp*$^{-/-}$ mice (top panel). The same RNA was hybridized with a G3PDH cDNA probe, showing the presence of intact RNA in all lanes (bottom panel).

sections of *ilbp* null mice. To confirm the disruption of *ilbp* gene expression in *ilbp* null mice, intestinal extracts were probed with an *ilbp* antibody for expression of *ilbp* protein. As shown in Appendix II, Fig. 1, *ilbp*$^{-/-}$ animals did not express *ilbp*, while *ilbp* expression in *ilbp*$^{+/+}$ animals was restricted to the terminal small intestine. These experiments show that I have functionally disrupted the expression of the *ilbp* gene in mice.

Ilbp null mice were indistinguishable from heterozygotes and wild type mice, and were clearly viable. There was no gross change in body weight at post natal day 77 between the three groups (Table 6-2). However, others and I have noticed that homozygous mice appeared docile compared to *ilbp*$^{+/+}$ and *ilbp*$^{+/-}$ mice. To determine if disruption of *ilbp* expression altered the size and composition of the bile acid pool in the EHC, bile acids were extracted from the liver, gall bladder and small intestine of *ilbp*$^{+/+}$, *ilbp*$^{+/-}$, and *ilbp*$^{-/-}$ mice. As shown in Table 6-3, *ilbp*$^{-/-}$ mice contained similar levels of bile acids in their EHC as did *ilbp*$^{+/+}$ and *ilbp*$^{+/-}$ mice. In addition, there was no statistical difference between the sexes from the different groups (Table 6-3). The speciation of bile acids in the EHC of *ilbp*$^{-/-}$ mice was determined by HPTLC as detailed in Section 6.2.4. Taurine conjugates of cholic acid and β-muricholic acid (3α,6β,7β-trihydroxy-5β-cholanic acid) are the predominant bile acid species in mice (Schwarz *et al.* 1996; Turley *et al.* 1998). As shown in Fig. 6-8A, bile acids extracted from *ilbp*$^{-/-}$ and *ilbp*$^{+/+}$ mice were predominantly taurine-conjugated. In addition, *ilbp*$^{-/-}$ had a normal distribution of conjugated to free bile acids in comparison to wild type mice (Fig. 6-8B). These experiments indicated that ilbp expression was not critical for conservation of bile acids in the EHC of mice.

	Males	n	Females	n
+/+	28.9±2.2	3	22.1±1.8	7
+/-	27.8±2.3	5	23.0±2.2	5
-/-	31.7±1.3	5	23.2±1.8	5

Table 6-2 Body weights of 77 day old *ilbp*$^{+/+}$, *ilbp*$^{+/-}$, and *ilbp*$^{-/-}$ mice.

	Males	Females	Combined	n
+/+	5.37±1.38	4.53±1.36	5.05±1.35	8
+/-	5.18±1.92	5.68±1.70	5.43±1.70	8
-/-	6.90±4.30	7.27±3.46	7.07±2.72	9

Table 6-3 Determination of the size of the bile acid pool in *ilbp*$^{+/+}$, *ilbp*$^{+/-}$, and *ilbp*$^{-/-}$ mice. Bile acids were isolated from liver, gall bladder and small intestine *Ibp*$^{+/+}$, *ilbp*$^{+/-}$, and *ilbp*$^{-/-}$ mice as detailed in Section 6.2.4. Means (μmol bile acids/g wet weight of tissue)± SD are shown for each group and gender.

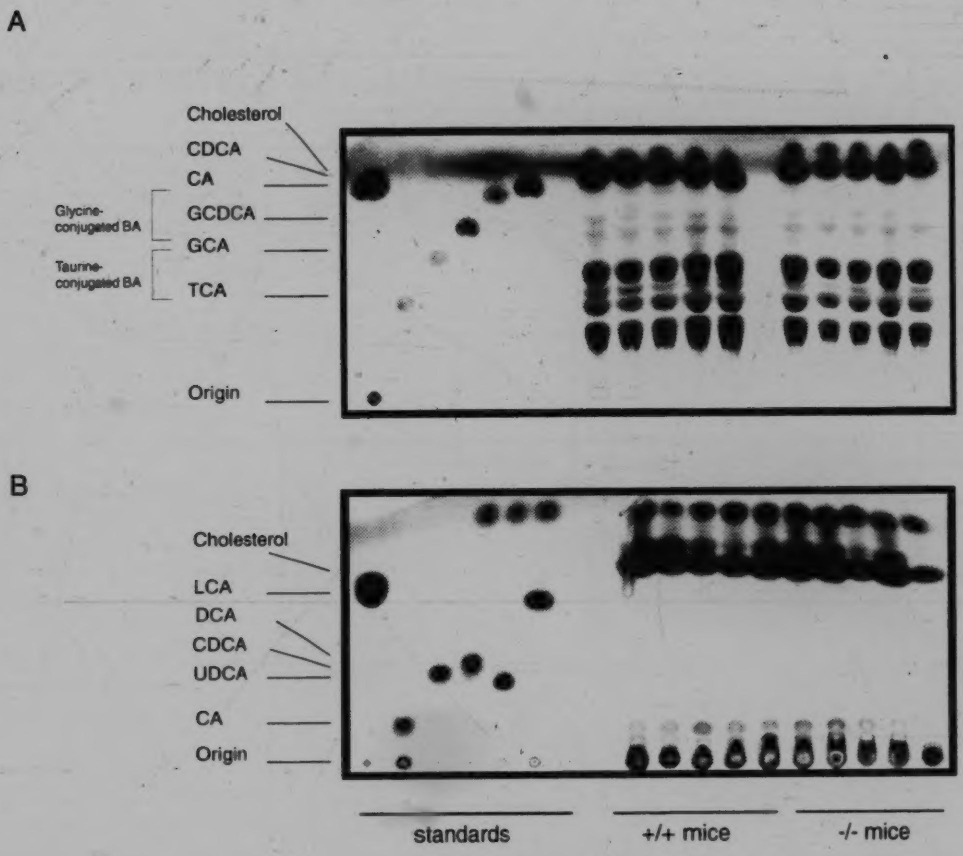

Fig. 6-8 Speciation of bile acids isolated from *ilbp*$^{+/+}$ and *ilbp*$^{-/-}$ mice. Bile acids were extracted from the liver, gall bladder and small intestine of *ilbp*$^{+/+}$ and *ilbp*$^{-/-}$ mice. Equivalent volumes of the extracts were spotted from 5 different mice in each group and resolved by HPTLC as detailed in Section 6.2.4. **A**. *Ilbp*$^{-/-}$ mice produced a normal complement of conjugated bile acids (taurine to glycine) as compared to wild type mice. **B**. Free bile acids constituted a small portion of the bile acid pool of both *ilbp*$^{+/+}$ and *ilbp*$^{-/-}$ mice, indicating that bile acids were metabolize in a similar manner in both strains. Spots running above or below the bile acid standards represent other lipid species (e.g. neutral lipids and phospholipids).

6.4 DISCUSSION

To elucidate the *in vivo* function of ilbp, I created mice deficient in *ilbp* gene expression. I introduced an ilbp targeting vector into 129-derived ES cells and enriched for cells that had undergone homologous recombination at the *ilbp* locus using a positive/negative selection scheme. The frequency of recombination in these types of experiments appears to depend on the extent of homology between the targeting vector and the gene target (Deng *et al.* 1992). Since the extent of homology between the *ilbp* targeting vector and *ilbp* gene was 5.5-kb, the expected frequency of targeting at the *ilbp* locus would fall between 10^{-6} and 10^{-5} (Deng *et al.* 1992). The identification of 18 cell lines carrying the *ilbp* mutation is consistent with this prediction.

The majority of the *ilbp*$^{-/+}$ ES cell lines had normal euploid karyotypes with a strong modal chromosomal number of 40. Contribution of the *ilbp*$^{-/+}$ ES cells to the formation of chimeric animals ranged from 5% to 65% (Table 6-1). High probability of germline transmission is generally associated with a high percentage of chimerism (Stewart 1993). Indeed, only three chimeras (F0) with the highest degree of *ilbp*$^{-/+}$ ES contribution were able to produce germline offspring. F1 mice carrying the *ilbp* mutation were bred to produce *ilbp* null mice. *Ilbp* null mice did not express *ilbp* mRNA message or protein, demonstrating that the *ilbp* gene has been functionally disrupted in these mice.

At least three proteins may be responsible for ileal bile acid recovery. Asbt mediates the active bile acid uptake on the brush border membranes of ileocytes (Love *et al.* 1998; Dawson 1999). T-asbt or a yet unidentified organic anion exchanger secretes bile acids from ileocytes at the basolateral pole (Weinberg *et al.* 1986; Lazaridis *et al.* 2000). The intracellular ilbp may play role in ileal bile acid transport. Asbt appears to be a crucial component of the ileal bile acid recovery system. Early studies have demonstrated that re-sectioning of the ileum in both dogs and humans results in loss of bile acids from the EHC, diarrhea and steatorrhea (Payoust *et al.* 1965; Shearman *et al.* 1989). Mutations in the human *Asbt* gene that abolish bile acid uptake activity can cause primary bile acid malabsorption (Oelkers *et al.* 1997). These studies imply that asbt function is critical for intestinal recovery of bile acids. The formal proof of this concept will await the gene disruption of the murine *Asbt* gene.

Ilbp null mice were clearly viable and phenotypically indistinguishable from wild type or heterozygotes littermates. *Ilbp*$^{-/-}$ mice had similar body weight and levels of bile acids in EHC as *ilbp*$^{-/+}$ and *ilbp*$^{+/+}$ mice. In addition, the speciation pattern of bile acids in the EHC of *ilbp*$^{-/-}$ mice appeared normal. These experiments indicated that *ilbp* expression was not crucial for conservation of bile acids in the EHC. In addition, because *ilbp*$^{-/-}$ mice were phenotypically normal and had normal bile acid pool size, *ilbp* did not appear to be a critical component of the ileal bile acid transport system. *Ilbp* may nevertheless play a subtler role in the ileal conservation of bile acids than the current experiments reveal. Compensatory mechanisms may exist to maintain bile acids levels in the EHC of *ilbp* null mice at normal levels. For example, in mice fed a bile acid sequestrant, cyp7a gene expression increases in response to bile acid depletion (Torchia *et al.* 1996). Transport in extra-ileal sites (e.g. jejunum) may upregulate to compensate for an ileal bile acid transport dysfunction.

Members of the lbp gene family expressed in the gut have been postulated to play a role in the cellular transport of lipophilic molecules (reviewed in Storch *et al.* 2000). However, the targeted disruption of the murine *Fabp-i* gene resulted in a paradoxical increase in the transfer of fatty acids from the gut to the plasma compartment of *Fabp-i*$^{-/-}$ mice, suggesting that Fabp-i may act to hinder or retard fatty acid transport in gut (Vassileva *et al.* 2000). Ilbp may play an analogous role with respect to bile acid conservation in the EHC. Future studies will have to address this possibility. Unlike the situation in rats, murine ilbp gene expression is first detected at very low levels in the intestine of 18 day old embryos (Shneider *et al.* 1997; Gong *et al.* 1996; Crossman *et al.* 1994). This period coincides with time of the proximal to distal wave of cytodifferentiation in the gut epithelium of the mouse (Crossman *et al.* 1994). After birth, ilbp gene expression is restricted to the ileum and remains low until day 13, when its mRNA abundance rises to reach adult levels (Crossman et al. 1994). It is possible that ilbp may play a role in the differentiantion or morphogenesis of the small intestine or specifically the ileum.

6.5 REFERENCES

Abbondanzo, S.J., I. Gadi and C.L. Stewart (1993). Derivation of embryonic stem cell lines. *Methods Enzymol.* 225: 803-822.

Bernlohr, D.A., M.A. Simpson, A. Vogel Hertzel and L.J. Bamaszak (1997). intracellular lipid binding proteins and their genes. *Annu. Rev. Nutr.* 17: 277-303.

Crossman, M.W., S.M. Hauft and J.I. Gordon (1994). The mouse Ileal lipid-binding Protein gene: a model for studying axial patterning during gut morphogenesis. *J. Cell Biol.* 126: 1547-1564.

Dawson, P.A. (1999). Intestinal bile acid transport. *Falk symposium: Bile Acids and Cholestasis (Titisee, Germany).* Eds., G. Paumgartner, A. Stiehl, W. Gerok, D. Keppler and U. Leuschner. Kluwer Academic Publishers, Lancaster. **108:** 1-28.

Deng, C. and M.R. Capecchi (1992). Re-examination of gene targeting frequency as a function of the extent of homology between the targeting vector and the target locus. *Mol. Cel. Biol.* 12(8): 3365-3371.

Gong, Y.Z., T. Kato, D.A. Schwartz, J.S. Norris and F.A. Wilson (1996). Ontogenic and glucocorticoid-accelerated expression of rat 14 kDa bile acid-binding protein. *Anat. Record* 245: 532-538.

Hedenborg, G., A. Norlander and A. Norman (1986). Bile acid conjugates present in tissues during extrahepatic cholestasis. *Scand. J. Clin. Lab. Invest.* 46: 539-544.

Hofmann, A.F. (1999). The continuing importance of bile acids in liver and intestinal disease. *Arch. Intern. Med.* 159: 2647-2658.

Ishibashi, S., M. Schwarz, P.K. Frykman, J. Herz and D.W. Russell (1996). Disruption of cholesterol 7α-hydroxylase gene in mice: i. postnatal lethality reversed by bile acid and vitamin supplementation. *J. Biol. Chem.* 271: 18017-18023.

Kramer, W., D. Corsiero, M. Friedrich, F. Girbig, S. Stengelin, *et al.* (1998). Intestinal absorption of bile acids: paradoxical behavior of the 14 kDa ileal lipid-binding protein in differential photoaffinity labeling. *Biochem. J.* 333: 335-341.

Kramer, W., F. Girbig, U. Gutjahr and S. Kowalewski (1995). Radiation-inactivation analysis of the Na+/bile acid co-transport system from rabbit ileum. *Biochem. J.* 306: 241-246.

Kramer, W., F. Girbig, U. Gutjahr, S. Kowlewski, K. Jouvenal, *et al.* (1993). Intestinal bile acid absorption. *J. Biol. Chem.* 268: 18035-18046.

Kramer, W., G. Wess, U. Bewersdorf, D. Corsiero, F. Girbig, *et al.* (1997). Topological photaffinity labeling of the rabbit ileal Na+/bile-salt-cotransport system. *Eur. J. Biochem.* 249: 456-464.

Lazaridis, K.N., P. Tietz, T. Wu, S. Kip, P. A. Dawson, and N. F. Larusso. Alternative splicing of the rat sodium bile acid transporter changes its cellular localization and transport properties. *Proc. Natl. Acad. Sci. USA* 97: 11092-11097

Love, M.W. and P.A. Dawson (1998). New insights into bile acid transport. *Curr. Opin. Lipidol.* 9: 225-229.

Nagy, A., J. Rossant, R. Nagy, W. Abramow-Newerly and J.C. Roder (1993). Derivation of completely cell culture-derived mice from early-passage embryonic stem cells. *Proc. Natl. Acad. Sci. USA* 90: 8424-8428.

Oelkers, P., L.C. Kirby, J.E. Heubi and P.A. Dawson (1997). Primary bile acid malabsorption caused by mutation in the ileal sodium-dependent bile acid transporter gene (SLC10A2). *J. Clin. Invest.* (99): 1880-1887.

Payoust, M.R., L. Lack and I.M. Weiner (1965). Effect of intestinal resection on bile salt absorption in dogs. *Am. J. Physiol.* 208(2): 363-369.

Robb, T.A. and G.P. Davidson (1984). Analysis of individual bile acids and their glycine/taurine conjugates by high-performances thin-layer chromatography and densitometry. *Ann. Clin. Biochem* 21: 137-140.

Sacchettini, J.C., S.M. Hauft, S.L. Van Camp, D.P. Cistola and J.I. Gordon (1990). Developmental and structural studies of an intracellular lipid binding protein expressed in the ileal epithelium. *J. Biol. Chem.* 265: 19199-19207.

Schwarz, M., E.G. Lund, K.D.R. Setchell, H.J. Kayden, J.E. Zerwekh, *et al.* (1996). Disruption of cholesterol 7 alpha-hydroxylase gene in mice: ii bile acid deficiency is overcome by induction of oxysterol 7 alpha-hydroxylase. *J. Biol. Chem.* 271: 18024-18031.

Shneider, B.L., K.D.R. Setchell and M. Crossman (1997). Fetal and Neonatal expression of the apical sodium-dependent bile acid transporter in the rat ileum and Kidney. *Pediatric Res.* 42: 189-194.

Shearman, D.J.C. and N.D.C. Finlayson (1989). Diseases of the gastrointestinal tract and liver, Edinburgh; New York : Churchill Livingstone, 1989 : 459-466.

Stewart, C.L. (1993). Production of chimera between embryonic stem cells and embryos. *Methods Enzymol.* 225: 823-855.

Storch, J. and A.E.A. Thumser (2000). The fatty acid transport function of fatty acid-binding proteins. *Bioch. Biophys. Acta* 1486: 28-44.

Sundaram, G.S. and H.S. Sodhi (1971). Color detection of bile acids in thin-layer chromatography. *J. Chromatogr* 61: 370-372.

Thomas, K.R. and M.R. Capecchi (1987). Site-directed mutagenesis by gene targeting in mouse embryo-derived stem cells. *Cell* 51(3): 503-12.

Torchia, E.C., S.K. Cheema and L.B. Agellon (1996). Co-ordinate regulation of bile acid biosynthetic and recovery pathways. *Bioch. Biophys. Res. Com.* 225: 128-133.

Tsuzuki, T. and D.E. Rancourt (1998). Embryonic stem cell gene targeting using bacteriophage lamda vectors generated by phage-plasmid recombination. *Nucleic Acids Res.* 26(4): 988-993.

Turley, S., M. Schwarz, D.K. Spady and J.M. Dietschy (1998). Gender-related differences in bile acid and sterol metabolism in outbred CD-1 mice fed low- and high cholesterol diets. *Hepatology 1998* 28: 1088-1094.

Vassileva, G., L. Huwyler, K. Poirier, L.B. Agellon and M.J. Toth (2000). The intestinal fatty acid binding protein is not essential for dietary fat absorption in mice. *Faseb J.* in press.

Weinberg, S.L., G. Burckhardt and F.A. Wilson (1986). Taurocholate transport by rat intestinal basolateral membrane vesicles. *J. Clin. Invest.* 78: 44-50.

Chapter 7: Summary and Conclusion

Through a series of chemical modifications in the liver, highly insoluble molecules of cholesterol are converted into the more soluble and amphipathic compounds known as bile acids. These natural detergents are an indispensable component of the digestive system, and their levels are highly conserved in the body (e.g. EHC) to ensure that an optimal concentration is present in the gut for the digestion and absorption of lipophilic nutrients. Because bile acids are also the end product of cholesterol catabolism, their metabolism has important consequences for whole body cholesterol homeostasis. To illustrate, the administration of a bile acid sequestrant can ameliorate severe hypercholesterolemic conditions. Therefore, understanding of ileal and hepatic bile acid metabolism can provide important insights into how sterols and their derivatives affect whole body physiology.

The molecular cloning of putative bile acid binding and transporting proteins has opened a new era in the study of the mechanisms that govern the movement of bile acids within the EHC. We now have a better understanding of how hepatocytes and ileocytes take up and secrete bile acids. Nevertheless, the molecular events that govern the cellular movement and interactions of bile acids once they are taken up by cells remain a virtual black box. Intracellular bile acid binding proteins may play a role in the translocation of bile acids from the cellular sites of uptake to the sites of efflux. These proteins may also sequester bile acids and protect against bile acid-mediated cytotoxicity. The paucity of adequate cellular models has hindered progress in this area.

One of the objectives of this thesis was to construct a model system to define the function of putative bile acid binding proteins. As detailed in Chapter 3, McNtcp cells were established by the stable expression of recombinant ntcp in the hepatoma cell line, McArdle RH-7777. McNtcp cells displayed saturable TCA uptake kinetics and other conjugated bile acids competed with TCA for uptake. The expression of ntcp in these cells was sufficient to mimic TCA uptake observed in primary cultures of hepatocytes. These findings are consistent with the notion that ntcp is an important determinant of conjugated bile acid recovery in the liver (Hagenbuch 1997).

Another objective of this thesis was to characterize the response of McNtcp cells to bile acids. Because of their detergent properties, bile acids are thought to mediate hepatocyte damage in cholestatic liver disease (Hofmann 1999). However, taurine-conjugated bile acids were well tolerated in McNtcp.24 cells (Chapter 4), a cell line that expressed a high level of bile acid uptake activity in comparison to primary hepatocytes (Chapter 3). Nevertheless, McNtcp.24 cells did form intracellular inclusions with TCA that were reminiscent of structures observed in cholestatic hepatocytes. In stark contrast, glycine-conjugated bile acids were extremely cytotoxic to McNtcp.24 cells (Chapter 5). Treatment of McNtcp.24 cells with glycine-conjugated bile acids induced cellular changes typical of apoptosis concomitant with the activation of the caspase proteases. The differential response to conjugated bile acids observed in this cell line suggested that liver-derived cells possess a mechanism to distinguish different species of bile acids. This notion was corroborated in a non-liver derived cell line that stably expressed asbt (Chapter 5). CHO.asbt.35 cells accumulated bile acids to similar levels as McNtcp.24 cells, but did not show differential sensitivity to different bile acids. Both taurine and glycine-conjugated bile acids induced apoptosis and the activation of caspase proteases in CHO.asbt.35 cells, indicating that most species of bile acids have the capacity to be cytotoxic. The basis of the differential response to amidated bile acids observed between these cell lines appears to depend on the activation of survival pathways in McNtcp.24 cells by taurine-conjugated bile acids, but not in CHO.asbt.35 cells. In addition, these findings suggest that endogenously bile acid transporting cell types may possess similar survival mechanisms to protect against bile acid-mediated cytotoxicity.

Having characterized the cytotoxic response of McNtcp.24 cells to bile acids, I was able to test the hypothesis that expression of a high affinity bile acid binding protein could rescue these cells from bile acid induced cytotoxicity. I established the BN cells by the stable expression of the human bile acid binder (HBAB) in McNtcp.24 cells (Chapter 5). Expression of HBAB did not overtly affect the capacity of BN cells to internalize or secrete bile acids. More importantly, expression of HBAB in McNtcp.24 cells was unable to protect these cells from apoptosis induced by glycine conjugated bile acids. These finding suggest that HBAB cannot prevent bile acids from interacting with elements of the apoptotic machinery once they have been internalized by BN cells. Moreover, the class of proteins represented by HBAB may not function in the sequestration and cytoprotection from the cytotoxic effects of bile acids, but may have another role to play in hepatic bile acid metabolism (e.g. regulation of the substrate pool for FXR).

McNtcp cells have already proven a useful model system in the study of cyp7a mRNA stability (Agellon *et al.* 1997) and the mechanisms of GCDCA-induced apoptosis (Roberts *et al.* 1997; Faubion *et al.* 1999). Because McArdle RH-7777 cells have been extensively used to study lipoprotein assembly and secretion, McNtcp cells should prove an ideal model in the study of bile acids in lipoprotein metabolism. Bile acid transport competent cell lines such as BN, McNtcp and CHO.asbt may prove invaluable in the study of FXR-mediated gene regulation.

The last goal of this thesis was to determine if expression of the ileal lipid binding protein (ilbp) was crucial for the conservation of bile acid in the EHC. I constructed a strain of mice that harbored a mutation in the *ilbp locus*. Deletions of portions of the *ilbp* gene disrupted both ilbp mRNA and protein expression in *ilbp*$^{-/-}$ mice. *Ilbp*$^{-/-}$ mice were viable, and indistinguishable from wild type or heterozygous littermates. The size and spectrum of bile acids in the EHC of *ilbp*$^{-/-}$ mice were similar in comparison to wild type mice, demonstrating that ilbp expression is not vital for the conservation of bile acids in the EHC. In addition, these findings suggest that ilbp is not a crucial component of the ileal bile acid reclamation system. The role of ilbp in ileal recovery may be subtle, and increased hepatic bile acid biosynthesis may compensate for decreased efficiency of intestinal bile acid conservation.

Ilbp null mice will prove to be an important tool to address relevant questions about hepatic and intestinal bile acid metabolism. As discussed in Chapter 1, asbt has been reported to form large protein complexes with ilbp (Kramer *et al.* 1995). Are these complexes still formed in the absence of ilbp gene expression? How is the formation of such complexes related to asbt function and its role ileal bile acid recovery? Is asbt expression perturbed in *ilbp* null mice? What are major cellular bile acid binding proteins in the *ilbp*$^{-/-}$ mice? Are there changes in ileum morphology? Is the bile acid biosynthetic pathway upregulated to compensate for ilbp protein deficiency? What is the role of ilbp in FXR-mediated gene regulation? Future studies should address these issues.

In conclusion, the role of cytosolic bile acid binding proteins with respect to intracellular bile acid trafficking and cytoprotection appears to be subtle. The challenge of future studies will be to determine how their function affects bile acid metabolism in the liver and intestine. In addition, cells that endogenously transport bile acids may have evolved mechanisms to differentiate different species of bile acids and elaborate the various biological activities of these bile acids. Fig. 7-1 summarizes the molecular events following entry of bile acids into cells. Internalized bile acids most likely interact with membrane-bound and cytosolic proteins such as HBAB. Through these proteins, bile acids may regulate cellular functions such as the expression of FXR-dependent genes. Interactions of bile acids with components of the survival or apoptotic machinery decide whether the cell lives or dies. The ultimate fate of internalized bile acids is to be secreted by membrane-bound transporters.

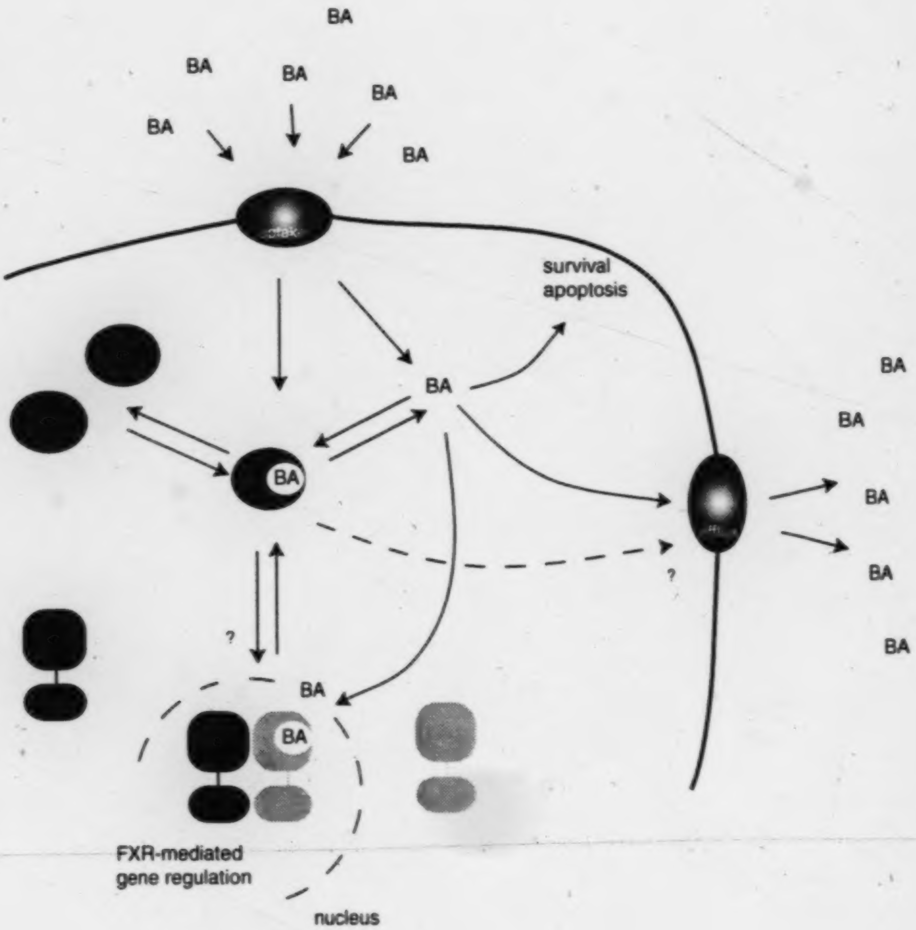

Fig. 7-1 Schema depicting the molecular events that occur once bile acid are internalized by cells. Bile acids are transported from the cellular sites of uptake and are secreted at the sites of efflux (oval circles). In transit to the sites of efflux, bile acids are in equilibrium with intracellular bile acid binding proteins (black circles) and may interact with proteins in the plasma membrane and other organelles that determine cellular survival or death. Intracellular bile acid binding proteins may play a subtle role in intracellular trafficking of bile acids leading to efflux or interaction with other cellular proteins such as FXR (connected circles) to modulate cellular function.

REFERENCES

Agellon, L. and S. Cheema (1997). The 3'-untranslated region of the mouse cholesterol 7alpha-hydroxylase mRNA contains elements responsive to post-transcriptional regulation by bile acids. *Biochem. J.* 328: 393-399.

Faubion, W.A., G.M. E, H. Miyoshi, S.F. Bronk, P.J. Roberts, *et al.* (1999). Toxic bile salts induce rodent hepatocyte apoptosis via direct activation of Fas. *J. Clin. Invest.* 103: 137-145.

Hagenbuch, B. (1997). Molecular properties of hepatic uptake systems for bile acids and organic anions. *J. Membrane Biol.* 160: 1-8.

Hofmann, A.F. (1999). The continuing importance of bile acids in liver and intestinal disease. *Arch. Intern. Med.* 159(2647-2658).

Kramer, W., F. Girbig, U. Gutjahr and S. Kowalewski (1995). Radiation-inactivation analysis of the Na+/bile acid co-transport system from rabbit ileum. *Biochem. J.* 306: 241-246.

Roberts, L.R., H. Kurosawa, S.F. Bronk, P.J. Fesmier, L.B. Agellon, *et al.* (1997). Cathepsin B contributes to bile salt-induced apoptosis of rat hepatocytes. *Gastroenterology.* 113: 1714-1726.

Appendix I: Composition of commonly used buffers

1. PBS: phosphate buffered saline = 2.6 mM KCl, 1.5 mM KH_2PO_4, 137 mM NaCl, 8 mM Na_2HPO_4.

2. TBS: Tris buffered saline = 25 mM Tris-HCl (pH 7.4), 137 mM NaCl, 10 mM EDTA.

3. 1 X SSC = 0.15 M NaCl, 15 mM sodium citrate.

4. TE = 10 mM Tris-HCl, pH 7.5, 1 mM EDTA.

Appendix II : Additional data for Chapter 6

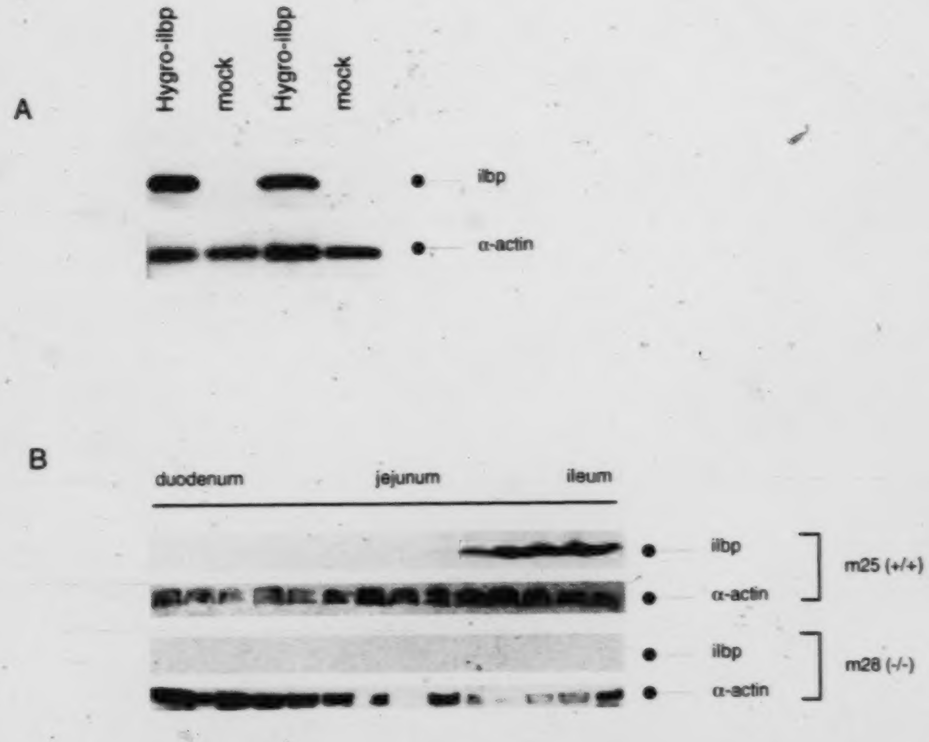

Fig. 1 Detection of ilbp expression in protein extracts from transfected cells and mouse intestinal sections. **A**. CHO cells were transiently transfected with salmon sperm DNA (Mock) and a plasmid encoding the mouse ilbp cDNA (Hygro-ilbp) using the lipofectamine reagent. Cellular extracts were prepared after 24 h post-transfection as detailed in Section 5.2.2. Twenty μg of total cellular protein was subjected to immunoblot analysis with ilbp or α-actin antiserum as detailed in Chapter 2. Only cells transfected with the Hygro-ilbp plasmid expressed an immuno-reactive band of 14 kD using ilbp antiserum, demonstrating the specificity of this antiserum for ilbp. **B**. Protein extracts were prepared from intestinal sections from ilbp$^{-/-}$ and ilbp$^{+/+}$ mice. Immunoblot analysis was performed as detailed in Chapter 2 using the Ilbp antiserum from (**A**). Ilbp can be detected in terminal sections of small intestine of wildtype mice, but more importantly, ilbp expression is absent in intestinal sections from ilbp$^{-/-}$ mice. The immunoblots in (**B**) were done by Mr. Eric Labonte, a graduate student in the laboratory of Dr. L B Agellon.